Transport and Dispersion of Fluorescent Tracer Particles for the Flat-Bed Condition, Rio Grande Conveyance Channel, Near Bernardo, New Mexico

GEOLOGICAL SURVEY PROFESSIONAL PAPER 562–I

Transport and Dispersion of Fluorescent Tracer Particles for the Flat-Bed Condition, Rio Grande Conveyance Channel, Near Bernardo, New Mexico

By R. E. RATHBUN, V. C. KENNEDY, *and* J. K. CULBERTSON

SEDIMENT TRANSPORT IN ALLUVIAL CHANNELS

GEOLOGICAL SURVEY PROFESSIONAL PAPER 562-I

UNITED STATES GOVERNMENT PRINTING OFFICE, WASHINGTON : 1971

UNITED STATES DEPARTMENT OF THE INTERIOR

GEOLOGICAL SURVEY

William T. Pecora, *Director*

Library of Congress catalog-card No. 76-609684

For sale by the Superintendent of Documents, U.S. Government Printing Office, Washington, D.C. 20402 - Price 65 cents (paper cover)

CONTENTS

ILLUSTRATIONS

TABLES

SYMBOLS

$A(z)$ Area under the experimental concentration as a function of time curve at lateral position z, in gram-hours per gram.

$A_r(z)$ Relative area, equal to $A(z)$ divided by the total area under the $A(z)$ as a function of z curve.

A' Area under the concentration as a function of time curve for the depth-integrated samples at the weir, in particle-hours per gram.

A_i' Area under the concentration as a function of time curve for size class i of the depth-integrated samples at the weir, in particle-hours per gram.

B Width of the channel, in feet.

$C(t)$ Concentration of fluorescent tracer in a size split of a "dust-pan" sample, expressed as grams of fluorescent tracer per gram of total material in the size split.

$C_r(t)$ Relative concentration of fluorescent tracer, equal to the concentration divided by the area under the concentration as a function of time curve.

$\bar{C}(t)$ Mean concentration of fluorescent tracer across the channel width, in grams per gram.

$\bar{C}_r(t)$ Relative mean concentration of fluorescent tracer, equal to the mean concentration divided by the area under the mean concentration as a function of time curve.

$C(z)$ Concentration of fluorescent tracer at lateral position z, in grams per gram. (May also refer to the concentration of fluorescent dye at lateral position z in the dye-dispersion test, milligrams per liter.)

$C^*(z)$ Concentration of sediment at lateral position z, determined from a depth-integrated sample at z, milligrams per liter.

$C'(t)$ Concentration of fluorescent tracer in a depth-integrated sample, expressed as number of fluorescent particles of a specific color per gram of total sediment in the sample, in particles per gram.

$C_r'(t)$ Relative mean concentration of fluorescent tracer in a depth-integrated sample, equal to the concentration divided by the area under the concentration as a function of time curve.

$\bar{C}'(t)$ Mean concentration of fluorescent tracer in a depth-integrated sample, determined from a composite of depth-integrated samples taken across the weir at equally spaced intervals, in particles per gram.

d_{16} Particle diameter for which 16 percent by weight are smaller, in millimeters.

d_{50} Median particle diameter, in millimeters.

d_{84} Particle diameter for which 84 percent by weight are smaller, in millimeters.

K_x, K_z Dispersion coefficients in the x, z directions, in square feet per second.

N Total number of fluorescent particles of all sizes of a specific color injected at the beginning of the experiment.

N_i Total number of fluorescent particles of size class i of a specific color injected at the beginning of the experiment.

$n(t)$ Total number of fluorescent particles of a specific color in a depth-integrated sample at time t.

p_i Percent of the total weight of a depth-integrated sample that is in sieve class i, in percent.

Q Total water discharge, in cubic feet per second.

$q(z)$ Water discharge per unit of width at lateral position z, in cubic feet per second per foot.

Q_s Total sediment-transport rate, in tons per day.

Q_{si} Total sediment-transport rate for size class i, in tons per day.

$q_s(z)$ Sediment-transport rate per unit of width at lateral position z, in tons per day per foot.

$\bar{q}_s$ Mean sediment-transport rate per unit of width, in tons per day per foot.

T_z Fraction of the total water discharge in the width increment Δz centered at lateral position z.

t Time, in hours.

$\bar{t}$ Time required for the centroid of the tracer mass to reach the measurement section, in hours.

$t_{0.01}$ Time required for the mean concentration at the measurement section to decrease to 1.0 percent of the maximum mean concentration, in hours.

Δt Time correction for the finite time interval required for injection of the fluorescent materials, in hours.

$\bar{V}$ Velocity of the centroid of the tracer mass, in feet per second.

W Weight of fluorescent material injected at the beginning of the experiment, in pounds.

$W(t)$ Total weight of sediment in a depth-integrated sample at time t, in grams.

$w(z)$ Weighting factor relating the unit sediment-transport rate at lateral position z with the mean unit sediment-transport rate for the cross section.

z Lateral distance, measured from the right bank of the channel, in feet.

Δz Increment of width, in feet.

$\bar{z}$ Mean lateral position of the tracer mass at the measurement section, measured from the right bank, in feet.

γ Specific weight of the water-sediment mixture, in pounds per cubic foot.

σ A measure of the gradation, equals $\frac{1}{2}(d_{84}/d_{50} + d_{50}/d_{16})$

σ_t^2 Variance of the mean concentration as a function of time curves, in hours^2.

σ_z^2 Variance of the lateral distributions of the tracer materials at the measurement section, in feet^2.

ENGLISH-METRIC CONVERSIONS

Principal item	*English unit*	*Factor*	*Metric unit*
Length	feet	0.3048	meter
		30.48	centimeter
		304.8	millimeter
Area	square feet	929.0	square centimeters
		.09290	square meters
Weight	pounds	453.6	grams
		.4536	kilograms
Velocity	feet per second	0.3048	meters per second
		30.48	centimeters per second
Water discharge	cubic feet per second	0.02832	cubic meters per second
		2.832×10^{4}	cubic centimeters per second
Sediment-transport rate	tons per day	0.9072	metric tons per day
Specific weight	pounds per cubic feet	0.01602	grams per cubic centimeter

TRANSPORT AND DISPERSION OF FLUORESCENT TRACER PARTICLES FOR THE FLAT-BED CONDITION, RIO GRANDE CONVEYANCE CHANNEL, NEAR BERNARDO, NEW MEXICO

By R. E. RATHBUN, V. C. KENNEDY, and J. K. CULBERTSON

ABSTRACT

A fluorescent tracer technique was applied to a study of the rates of transport and dispersion of sediment particles of various diameters and specific gravities for the high-velocity flat-bed condition of alluvial-channel flow. Two runs were conducted in the Rio Grande conveyance channel near Bernardo, N. Mex., on December 13 and 14, 1966. An instantaneous point source of fluorescent material was used in each run. Samples of the bed material moving on or near the bed surface were obtained throughout the passage of the tracer masses with the "dustpan" sampler especially designed for this study.

The mean lateral positions of the distributions of tracer materials tended to follow the thalweg of the channel and shifted toward the right bank in moving from the injection point to the measurement section. The amount of shift increased with increasing particle fall diameter.

The lateral dispersion of the tracer masses as represented by σ_z^2, the variance of the lateral distribution of fluorescent material at the measurement section, decreased with increasing fall diameter.

The sediment-transport rates calculated from the fluorescent tracer experiments were about 57 and 14 percent larger than the sediment-transport rates measured at the weir in runs 1 and 2, respectively. The agreement in run 2 was good because positive and negative errors for the different sieve classes were compensating.

The variation of the centroid velocities of the quartz tracer masses with fall diameter was approximately U-shaped; the minimum velocity occurred for tracer particles having fall diameters comparable to or slightly larger than the median fall diameter of the bed material in transport. The maximum centroid velocities observed were for the 0.125- to 0.177-millimeter sieve class of quartz tracer, and these were approximately 26 and 16 percent of the mean water velocity in runs 1 and 2, respectively.

The centroid velocities of the garnet and monazite tracer masses were about an order of magnitude less than the centroid velocities for quartz tracer particles of comparable fall diameter.

The longitudinal dispersion of quartz tracer particles as represented by σ_t^2, the variance of the curves of mean concentration as a function of time at the measurement section, varied with fall diameter approximately inversely to the manner in which the centroid velocities varied with fall diameter. The σ_t^2 values for the garnet and monazite tracer particles showed relatively little variation with fall diameter but were about an order of magnitude larger than the σ_t^2 values for quartz particles of comparable fall diameter.

The fluorescent tracer technique is a simple and sensitive experimental method for the study of the transport and dispersion of groups of particles in a natural or laboratory alluvial channel. However, considerable improvement in technique is still needed.

INTRODUCTION

Problems associated with rates of transport of sediment by natural and artificial waterways are many, both in number and in type. Among the problems are those involving river management, design and operation of canals and reservoirs, and degradation around bridge piers and below dams.

A problem closely related to the rate of sediment transport is the rate of dispersion of the sediment. Development of nuclear energy industries and the increasing use of agricultural chemicals have resulted in the undesirable presence of radioisotopes, pesticides, and herbicides in the environment. Furthermore, there is considerable evidence that these substances are adsorbed by sediment particles. Thus, in the event that toxic material is discharged or accidentally spilled into a stream, the sediment may remove most of it from solution. Thereafter, the rate of transport and of lateral and longitudinal dispersion of the sediment will control the movement and the concentration level of the toxic substance.

An understanding of the laws governing transport of sediments of differing size and specific gravity is also important in geomorphology, in stratigraphic studies, and in the search for concentrations of valuable heavy minerals.

Fluorescent tracers have been used extensively in the study of sediment transport and dispersion, but these investigations have been limited almost exclusively to research on beach erosion. Exceptions are the laboratory work of De Vries (1966) and Lean and Crickmore (1966) and the field study of Crickmore (1967). The

application of the fluorescent tracer technique to a study of the transport of sand-size particles in a gravel-bed stream by Kennedy (1968) and Kennedy and Kouba (1970) served as the foundation for the present research and suggested the possibility of a large-scale field study of the transport and dispersion of sand-size particles in a sand-channel stream.

This report describes a field study of the transport and dispersion of sediment particles of various sizes and specific gravities coated with fluorescent dye. Two experiments were conducted in the Rio Grande conveyance channel near Bernardo, N. Mex., on December 13 and 14, 1966. A high-velocity flat-bed condition existed for both experiments. In the preliminary experiment, run 1, three size ranges of quartz, each coated with a different color of fluorescent dye, were used. In the second experiment, run 2, four materials of different specific gravity were each coated with a different color of fluorescent dye. These materials were quartz, garnet, monazite, and lead, and each material contained a range of particle sizes.

This study was the joint effort of Water Resources Division personnel from Denver, Colo., Albuquerque, N. Mex., and Fort Collins, Colo. V. C. Kennedy originated and coordinated the project with the assistance of F. C. Ames. The Albuquerque Field Research Unit (J. K. Culbertson and C. H. Scott) provided extensive logistic support for the fieldwork. Fort Collins personnel conducted preliminary laboratory experiments with the "dustpan" sampler, and C. F. Nordin, Jr., and W. W. Sayre helped in the supervision of the experiments and contributed many ideas and suggestions during the analysis of the data and the preparation of the report.

Personnel from the New Mexico District who assisted with the fieldwork included J. P. Borland, B. M. Delaney, J. D. Dewey, Trancito Diaz, N.D. Haffield, V. W. Norman, David Ortiz, and J. W. Shomaker. Graduate students from Colorado State University who assisted with the fieldwork included J. P. Bennett, W. E. Gaskill, and J. N. Loyacano. Graduate students assisting with the analysis of the samples included N. S. Grigg, Ziad Mughrabi, C. H. Neuhauser, and C. A. Ramirez.

Norman Prime of Menlo Park, Calif., prepared the photomicrographs of the fluorescent materials.

DESIGN OF THE EXPERIMENT

The experiment was designed to permit a study of the longitudinal- and lateral-dispersion characteristics of particles of various diameters and specific gravities in the sand-size range and also to permit an evaluation of the fluorescent tracer technique as a means of measuring the total sediment-transport rate of the bed material.

SELECTION OF SITE

The site chosen for the study was the Rio Grande conveyance channel near Bernardo, N. Mex. The channel contained a weir at which total sediment concentrations could be sampled. Figure 1 is a photograph of the channel and the weir. A series of baffles on the weir upstream of

FIGURE 1.—Rio Grande conveyance channel and the weir used for total sediment concentration sampling.

the crest created sufficient turbulence to suspend all of the sediment in transport as it passed over the weir. The sediment suspended by the action of the baffles was sampled with the standard US DH–48 depth-integrating hand sampler (Guy and Norman, 1970). Figure 2 is a photograph of the baffles and the weir. Details of the

FIGURE 2.—Weir and baffles in the Rio Grande conveyance channel.

design, construction, and operation of the weir have been presented by Harris and Richardson (1964) and Gonzalez, Scott, and Culbertson (1969).

The 800-foot straight reach immediately upstream of the weir was selected as the study reach so that the total sediment-transport rates computed at the weir could be used to check the sediment-transport rates computed from the fluorescent tracer experiments. Figure 3 is a photograph of the study reach as viewed in an upstream direction from the weir.

FIGURE 3.—Study reach, viewed in an upstream direction from the weir.

TYPE OF INJECTION

Possible types of injection procedures are the instantaneous line source, the continuous line source, the instantaneous point source, and the continuous point source. The mechanical requirements for a line source are more demanding than for a point source, and information on the lateral-dispersion characteristics of the channel cannot be obtained. The continuous source has the advantage that only a few samples are necessary after equilibrium has been attained at the measurement section. However, the continuous source must be maintained until equilibrium is obtained, and continuous feeding is demanding of both manpower and fluorescent materials. On the basis of these considerations, the instantaneous point-source method of injection was chosen for the study.

QUANTITY OF FLUORESCENT MATERIAL

One of the requirements of any tracer procedure is that the quantity of material introduced be small enough so that the natural sediment-transport process is not disturbed. At the same time, sufficient tracer material must be injected so that statistically significant numbers of particles are obtained in the samples. The quantity of fluorescent material required was estimated in the following way.

It was assumed that the injected tracer material was instantaneously and uniformly mixed throughout the length of the study reach. This assumption was obviously conservative and resulted in estimated peak fluorescent tracer concentrations that were smaller than the actual experimental values. Concentration of fluorescent material in a sample as used in this report is defined as the ratio of the weight of tracer material in a specific size range of the sample to the total weight of all sediment in that size range of the sample. For the flat-bed condition, most of the material in transport is concentrated in a thin layer near the bed surface. Opinions differ as to the thickness of this moving layer. However, for the purpose of illustration, assume that the moving layer is 0.1 foot thick and that the water-sediment mixture in the moving layer is 50 percent sediment by volume. The study reach was 800 feet long from the injection point to the weir, and the mean channel width was about 70 feet. Thus, the total dry weight of sand participating in the transport process and present in the study reach at any instant is estimated as $800 \times 70 \times 0.50 \times 2.65 \times 62.4 = 463{,}000$ pounds. For the flat-bed condition in the Rio Grande conveyance channel, approximately 50 percent of the material in transport is in the size range from 0.125 to 0.250 mm (millimeter). Therefore, about 231,000 pounds of sediment in active storage in the 0.125- to 0.250-mm size range is present in the study reach at any instant. Fluorescent tracer concentrations of the order of 10^{-3} to 10^{-4} are adequate for purposes of analysis; and if the mean fluorescent tracer concentration in the reach is of this order, then the quantity of tracer material in the 0.125- to 0.250-mm size range should be between about 23 and 231 pounds.

THE "DUSTPAN" SAMPLER

The application of the fluorescent tracer technique to the study of the transport and dispersion rates of sediments for the high-velocity flat-bed condition required a different type of sampler from those usually used in sediment-transport studies. Because the concentrations of fluorescent tracer could not be determined in situ, it was necessary to obtain samples from the channel for laboratory analysis. These samples had to contain all sizes of the bed material in transport, and the sample time was necessarily as short as possible so that several samples could be obtained as the tracers moved through the measurement section. Thus, the sampling position best suited to meet these requirements was on or just above the bed surface.

Sampling the moving bed material for a fluorescent tracer experiment, however, has one major advantage over sampling the bed-material discharge with any of the bedload samplers described by Hubbell (1964). This advantage is that the efficiency of the sampler is unimportant in fluorescent tracer experiments, provided that the fluorescent tracer particles of any specific size behave identically with nontagged particles of the same size. Efficiency was defined by Hubbell (1964) as "the ratio of the weight of bedload collected during any single sampling time to the weight of bedload that would have passed through the sampler width in the same time had the sampler not been there." The significant factor in the "dustpan" sample is the ratio of the number of fluorescent particles of a given size to the number of nonfluorescent particles of the same size.

A rear view of the "dustpan" sampler designed for this study and used in the experiments is shown in figure 4.

FIGURE 4.—"Dustpan" sampler; rear view.

The flow expansion in both the horizontal and vertical directions resulted in a decrease in flow velocity and deposition of sediment in the sampler. The sampler was constructed from galvanized sheet metal, and a 6-foot length of ¾-inch pipe was used as the handle. The fin on the top of the sampler served to stabilize the sampler in high-velocity flows. A small wooden baffle was positioned across the inside of the sampler on the bottom about 6 inches from the inlet. Dimensions of the sampler and the position of the baffle are shown in figure 5.

SAMPLING ARRANGEMENT

A plan-view sketch of the study reach is shown in figure 6. The injection point was 800 feet upstream of the weir. The injection point was not positioned nearer the highway bridge because of possible effects from the slight bend just upstream of the bridge. Measurement sections *A*, *B*, *C*, and *D* were 100, 300, 500, and 700 feet, respectively, downstream from the injection point. The position of the thalweg, or line of maximum depth, for the study reach is shown also in figure 6.

Because information concerning the rates of movement of sediment particles for the high-velocity flat-bed condition was nonexistent, sampling was concentrated initially at cross section *D* so as to insure that the fluorescent particles did not pass completely through the study reach before they could be sampled. Subsequent adjustments to the sampling arrangement were dependent on the qualitative examination of the samples from cross section *D*.

EXPERIMENTAL PROCEDURE

PREPARATION OF THE FLUORESCENT MATERIALS

The fluorescent materials used in the preliminary experiment, run 1, were some of the materials prepared by Kennedy and Kouba, and the preparation procedure used for this material has been described previously (Kennedy and Kouba, 1970). This material was prepared from a natural river sand that contained minerals other than quartz; hence, it should correctly be called quartzose sand. However, for brevity, it will be referred to as quartz in this report. The amounts available were 281 pounds of green quartz (approximately 0.15 to 0.30 mm), 252 pounds of yellow quartz (approximately 0.30 to 0.52 mm), and 295 pounds of red quartz (approximately 0.52 to 1.29 mm).

The fluorescent materials for run 2 were prepared by a procedure similar to that of Kennedy and Kouba (1970). The fluorescent dyes used were the A series of Day-Glo pigments (Switzer Brothers, Inc., Cleveland, Ohio).[1] The rocket red (A–13), arc yellow (A–16), signal green (A–18), and horizon blue (A–19) dyes were chosen for use because they were the most easily distinguishable from each other by the human eye. A vinyl plastic VAGH, blend 1508 (Union Carbide Corp., South Charleston, W. Va.) was also used with the dye to produce an abrasion-resistant coating.

[1] Use of company names is for identification purposes only and does not imply official endorsement of any product.

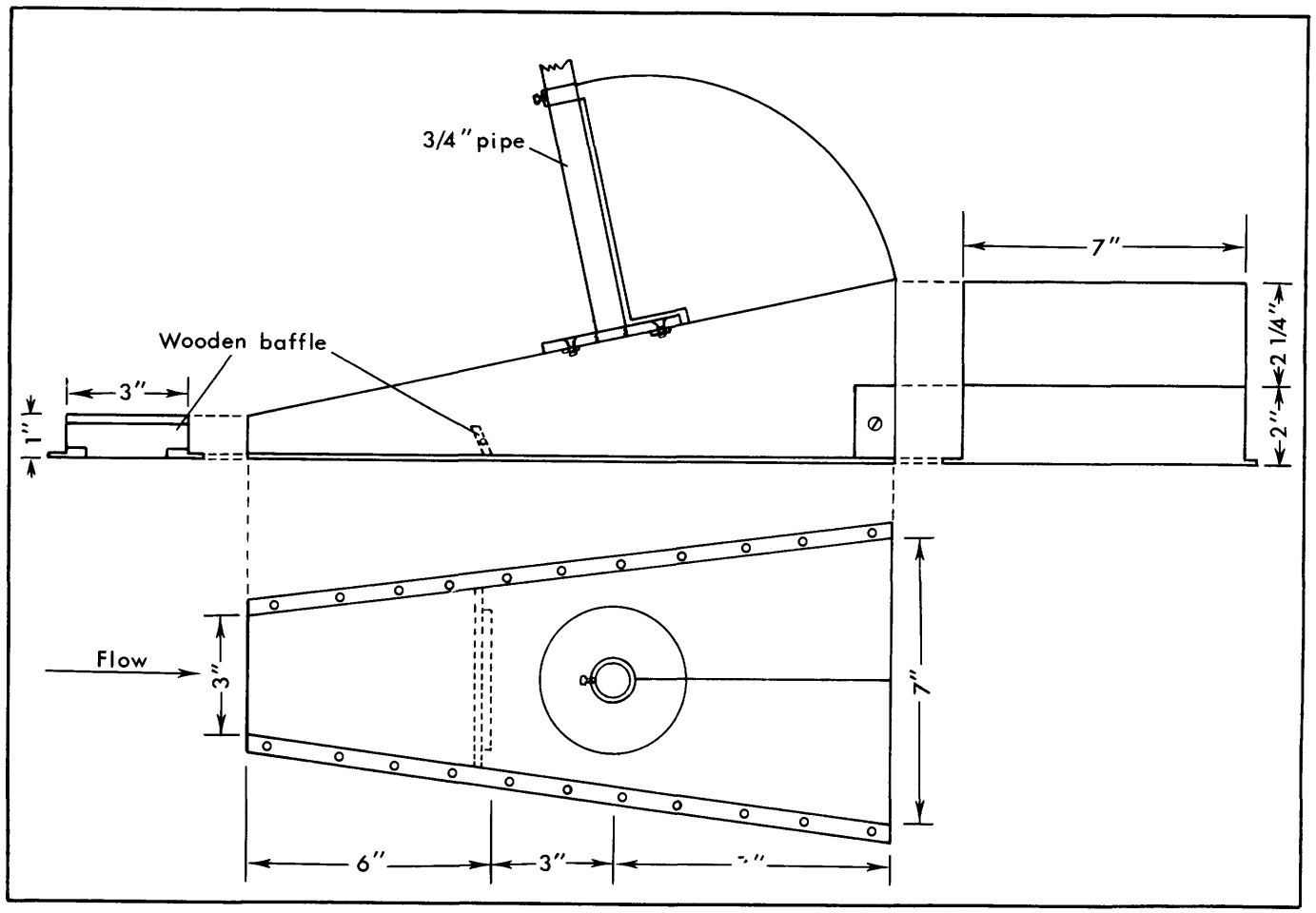

FIGURE 5.—Detailed sketch of the "dustpan" sampler.

Commercial grade acetone was used as the solvent. A quantity of acetone was saturated with the vinyl plastic by adding the vinyl powder slowly to the acetone with constant stirring. The vinyl-acetone solution was then saturated with the appropriate dye. About 100 pounds of the material to be coated was placed in a small motor-driven cement mixer. As the material tumbled, a small quantity of the solution was mixed into the material and the acetone allowed to evaporate. When the coating was completely dry, more of the dye solution was added. This process was continued until fluorescence of the material under an ultraviolet light indicated that an adequate coating had been obtained.

If no loosely cemented aggregates of particles existed in the dry material, the material was placed in canvas bags. If aggregates of particles existed, the material was passed between rubber rollers to break the aggregates into single particles.

TABLE 1.—*Summary of the median fall diameters of the various sieve classes of fluorescent tracers from runs 1 and 2 and the bed material from the Rio Grande conveyance channel*

Sieve class (mm)	Median fall diameter (mm)							
	Bed material	Run 1			Run 2			
		Green quartz	Yellow quartz	Red quartz	Quartz	Garnet	Monazite	Lead
(1) 0.125–0.177	0.156	0.150	.....	.....	0.152	0.232	0.235	.....
(2) 0.177–0.250	.201	.189	.....	.....	.204	.300	.305	0.715
(3) 0.250–0.350	.270	.231	0.271	.....	.289	.405	.484	1.12
(4) 0.350–0.500	.446	.....	.358	.....	.420	.578	.721	1.36
(5) 0.500–0.707	.630	.....	.452	0.539	.541	.690	.....	.....
(6) 0.707–1.00	.....	.....	.....	.613	.694	.....	.....	.....
(7) > 1.00	.....	.....	.....	.839	.....	.....	.....	.....
Specific gravity	.....	.....	.....	.....	2.65	4.08	4.79	11.3

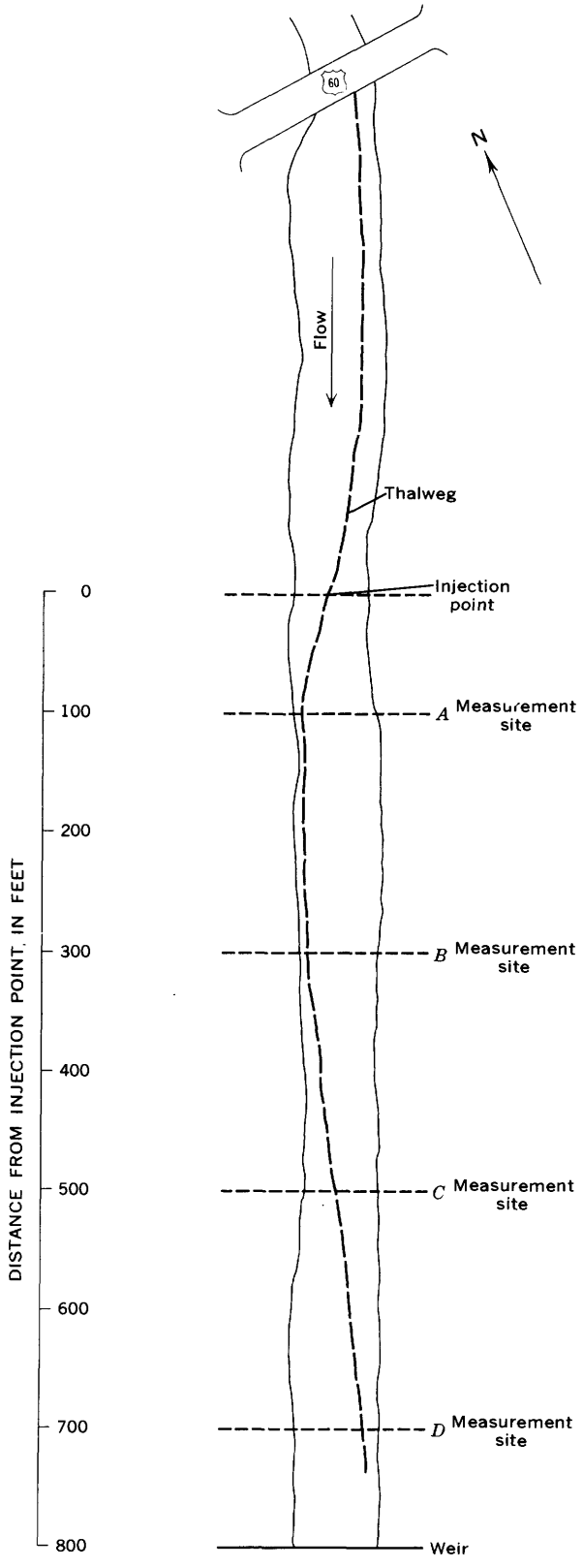

FIGURE 6.—Plan-view sketch of the study reach.

One disadvantage of the fluorescent coatings prepared by this procedure was that the coatings were nonwetting. Therefore, when the fluorescent materials were placed in water, the particles had a tendency to cluster together in groups. This clustering was avoided by adding detergent to the fluorescent material before injection.

The fluorescent materials prepared in this manner for run 2 consisted of 199 pounds of Ottawa flint quartz and 194 pounds of Ottawa crystal quartz (Ottawa Silica Co., Ottawa, Ill.), 232 pounds of garnet, 288 pounds of monazite, and 83 pounds of lead shot. The specific gravities of the coated materials were 2.65, 4.08, 4.79, and 11.3 for the quartz, garnet, monazite, and lead, respectively.

Median fall diameters were determined for each $\sqrt{2}$ sieve class of the fluorescent materials used in runs 1 and 2, as well as for samples of the bed material from the Rio Grande conveyance channel. Fall diameters were determined either by dropping single particles in a column of quiescent distilled water or by the visual-accumulation tube method (U.S. Inter-Agency Committee on Water Resources, 1957a). The visual-accumulation tube was used to analyze the materials smaller than 0.350 mm, and the single-particle method was used for materials larger than 0.350 mm. Fall velocities obtained from the single-particle method were converted to median fall diameters by means of table 2 of U.S. Inter-Agency Committee on Water Resources (1957b). The median fall diameters are summarized in table 1.

Photomicrographs of the material from two sieve classes of bed material from the Rio Grande conveyance channel, one sieve class of each of the three colors of fluorescent quartz used in run 1, and one sieve class of each of the four minerals used as tracers in run 2 are presented in figures 7, 8, and 9, respectively.

The photomicrographs show that the tracer materials used in run 1 were angular. Hence, the particles would tend to have a shape factor less than the 0.7 usually attributed to naturally worn quartz particles. This shape effect explains why the fall diameters for some sieve classes of tracer materials from run 1 were smaller than the lower limit of the sieve class. (See U.S. Inter-Agency Committee on Water Resources, 1957b, fig. 7.) The effect of shape on the difference between sieve diameter and fall diameter increases with fall diameter.

The fall diameters for the garnet, monazite, and lead tracer particles used in run 2 are larger than the sieve diameters because of the specific gravity effect.

INJECTION OF THE FLUORESCENT MATERIALS

The instantaneous point-source method of injection was used for both runs 1 and 2. Initially, the intent was to use a 4-inch inside diameter steel tube as an injection tube. However, the tube clogged when the material was poured rapidly into it; so in both runs 1 and 2 the fluorescent material was poured from the back of the boat as rapidly

A

B

FIGURE 7.—Two sieve classes of bed material from the Rio Grande conveyance channel. *A*, 0.177–0.250 mm. *B*, 0.250–0.350 mm.

A

B

C

FIGURE 8.—Three sieve classes of fluorescent materials, run 1. *A*, Green quartz, 0.177–0.250 mm. *B*, Yellow quartz, 0.350–0.500 mm. *C*, Red quartz, 0.707–1.00 mm.

as possible. Figure 10 is a photograph of the injection process for run 1. The injection point for run 1 was the centerline of the channel 800 feet upstream from the weir. The green fluorescent material was injected first, then the yellow fluorescent material, and then the red fluorescent material. The green, yellow, and red fluorescent materials required 2 minutes and 45 seconds, 2 minutes, and 2 minutes, respectively, for injection.

A tendency for the large particles to migrate toward the right bank (facing downstream) was observed in run 1, and therefore the injection point for run 2 was moved 7 feet to the left of the centerline. As in run 1, the fluorescent material was dumped from the back of the boat as rapidly as possible. The crystal quartz was injected first, followed by the flint quartz, garnet, monazite, and lead; the materials required 1 minute, 1 minute, 1 minute and 10 seconds, 1 minute, and 35 seconds, respectively, for injection. The amounts of fluorescent material injected for each sieve class for runs 1 and 2 are summarized in table 2. The quantities shown for quartz in run 2 include both the crystal quartz and the flint quartz.

The totals given in table 2 are slightly less than the total amounts of fluorescent materials prepared because of the presence of small quantities of material in the ends of the size distributions. The only significant difference is

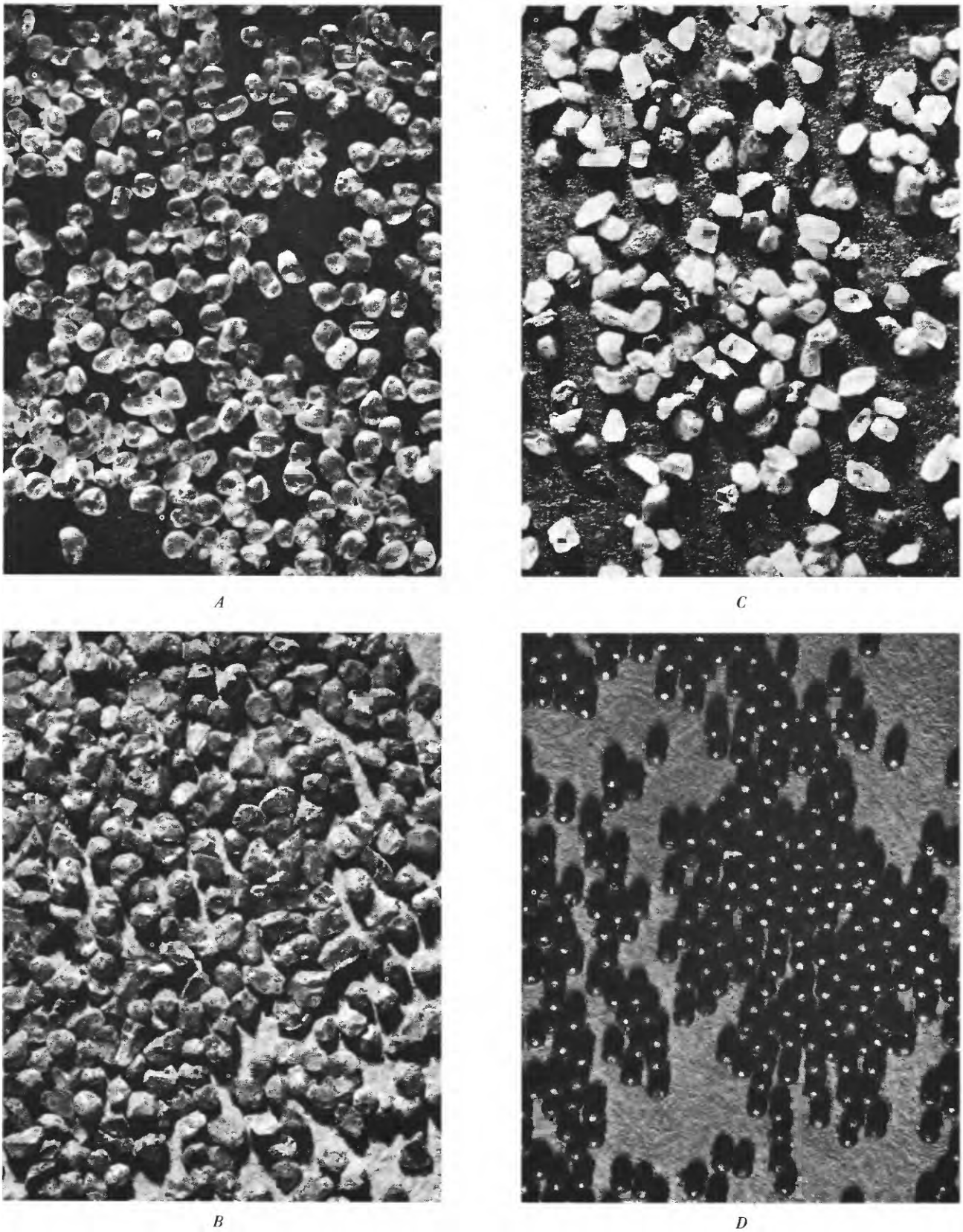

FIGURE 9.—Four sieve classes of fluorescent materials, run 2. *A*, Ottawa quartz. 0.250–0.350 mm. *B*, Garnet, 0.250–0.350 mm. *C*, Monazite, 0.250–0.350 mm. *D*, Lead, 0.177–0.250 mm.

FIGURE 10.—Injection of the fluorescent materials, run 1.

for the monazite where there was considerable material in the 0.088- to 0.125-mm sieve class. However, particles smaller than 0.125 mm were not considered in the analysis of the samples because of the difficulty of distinguishing between actual fluorescent particles and chips or flakes of dye from large particles.

TABLE 2.—*Summary of the amounts of fluorescent material injected for each sieve class, runs 1 and 2, in pounds*

Sieve class (mm)	Quantity injected						
	Run 1			Run 2			
	Green quartz	Yellow quartz	Red quartz	Quartz	Garnet	Monazite	Lead
0.125–0.177	39.6	.....	.....	4.4	8.1	83.7	.....
0.177–0.250	125.5	.....	.....	16.7	40.2	46.6	1.8
0.250–0.350	111.8	69.3	.....	53.0	94.7	30.9	46.8
0.350–0.500		130.5	.....	126.0	77.0	56.5	33.2
0.500–0.707		49.2	65.3	177.1	9.5	30.4	.....
0.707–1.00			131.3	14.5	.....	.....	.....
> 1.00			93.6	.....	.....	.....	.....
Total.....	276.9	249.0	290.2	391.7	229.5	248.1	81.8

HYDRAULIC AND SEDIMENT-CONCENTRATION MEASUREMENTS

Prior to and during both experimental runs, measurements of the hydraulic parameters water discharge, water-surface slope, and cross-section measurements were obtained. Depth-integrated samples of suspended sediment were obtained at the weir at 5-foot intervals for lateral positions from 5 feet to 70 feet from the right bank throughout both runs. About 5 minutes and 8 minutes in runs 1 and 2, respectively, were required to obtain one complete set of samples across the weir. The 5-minute schedule was maintained for about 1 hour in run 1, and the 8-minute schedule for about 2 hours in run 2. Thereafter, the time interval between samples was increased gradually in both runs.

The results of the hydraulic measurements are summarized in table 3, and the total-sediment-concentration measurements at the weir are summarized in tables 4 and 5 for runs 1 and 2, respectively. For run 1, the mean total-sediment-transport rate between the hours of 1313 and 1504, December 13, when most of the fluorescent tracer material passed through the study reach, was 5,490 tons per day of material larger than 0.062 mm. For run 2, the mean total-sediment-transport rate between the hours of 1006 and 1151, December 14, when most of the quartz tracer material passed through the study reach, was 4,220 tons per day of material larger than 0.062 mm.

The water discharge was not as constant as desired but decreased at an approximately uniform rate throughout both runs. Figure 11 is a discharge hydrograph based on the record from the gaging station just upstream of the

TABLE 3.—*Summary of the hydraulic data for the study reach*

[cfs, cubic feet per second; fps, feet per second; ft/ft, feet per foot]

Date (Dec. 1966)	Time	Discharge (cfs)	Mean width (ft)	Mean depth (ft)	Mean velocity (fps)	Water-surface slope × 10^4 (ft/ft)	Water temperature (° C)
13	0845	920	72.9	2.76	4.66	7.1	2.0
14	0840	750	72.9	2.48	4.05	7.0	.....
14	1500	720	72.9	2.48	4.05	7.0	.....
15	0815	590	72.9	2.27	3.63	7.0	.....

TABLE 4.—*Total-sediment-concentration measurements at the weir, run 1, December 13, 1966*

[mg/l, milligrams per liter]

Time	Water discharge (cfs)	Concentration > 0.062 mm (mg/l)	Concentration < 0.062 mm (mg/l)
1313	905	2,280	2,920
1320		2,060	2,900
1326		2,290	2,930
1331		2,350	2,920
1337		2,310	2,910
1341		2,280	2,880
1346		2,470	2,800
1350		.....	.....
1354		2,280	2,860
1358		2,150	2,880
1404	900	2,260	2,860
1408		2,590	2,660
1422		2,390	2,820
1434		2,120	2,810
1444		2,180	2,780
1453		2,330	2,780
1504	900	1,860	2,080
1524		1,940	2,730
1542		1,960	2,590
1604	890	2,150	2,670
1624		2,500	2,640
1713		1,900	2,580
1737		2,440	2,590
1806	845	2,000	2,490
1838		1,920	2,470
1906		2,260	2,500
1930		2,010	2,420
2005		2,410	2,430

TABLE 5.—*Total-sediment-concentration measurements at the weir, run 2, December 14, 1966*

Time	Water discharge (cfs)	Concentration > 0.062 mm (mg/l)	Concentration < 0.062 mm (mg/l)
1006	740	2,120	2,270
1015		2,180	2,200
1023		2,000	2,210
1030		2,080	2,220
1038		2,170	2,210
1046		2,260	2,230
1054		2,150	2,230
1100		2,160	2,210
1109		2,040	2,210
1117		2,180	2,200
1125		2,130	2,200
1134		1,960	2,180
1142		2,150	2,180
1151	735	2,000	2,180
1218		1,950	2,160
1414		1,690	1,940
1435		1,860	2,070
1503		2,460	2,040
1534		2,300	2,020
1604		2,090	2,020
1634		2,010	2,010
1703		1,830	1,980
1738		2,040	1,960
1904		1,820	1,950
2013		2,150	1,960
2108		2,030	1,950
2205		2,060	1,930
2305		2,160	1,890

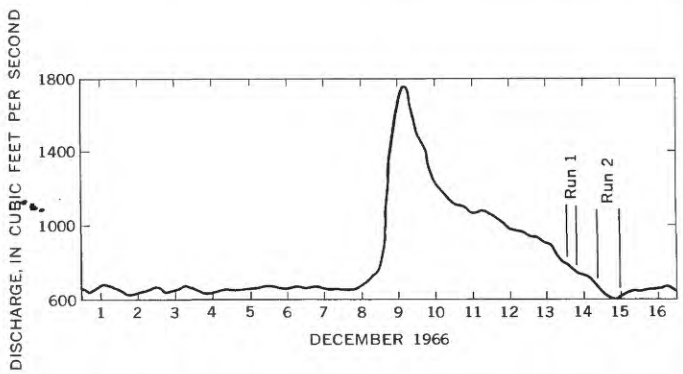

FIGURE 11.—Discharge hydrograph, from the gaging station just upstream from the weir, for the period December 1–16, 1966.

weir for the period December 1 to December 16. Run 1 was completed in the period between 1310 and 1800 hours on December 13, and run 2 was completed in the period between 1000 and 2400 hours on December 14.

The cross-section measurements obtained on December 14 at 0815 hours are shown in figure 12. These measurements show that the thalweg is near the right bank at cross section *A* and near the left bank at cross section *D*.

A dispersion test for a water-soluble fluorescent dye was completed just prior to the start of run 1 to permit a determination of the limits of lateral dispersion for particles of essentially zero diameter. A Rhodamine WT dye solution was injected continuously from a constant-head tank at the same injection point that was used for the fluorescent sediment tracers in run 1. Sampling was begun after sufficient time had elapsed to insure a steady-state concentration distribution at each of the cross sections. A complete set of samples across the width of the channel was obtained at cross sections *A*, *B*, and *C*, and two sets spaced about 7 minutes apart were obtained at cross section *D*. A nylon cord to which 24-ml (milliliter) screwcap vials were attached at 2-foot intervals was stretched across the channel. The cross-section samples were obtained simultaneously by dipping the vials into the channel. After the bottles filled, the cord was raised and the vials were removed from the line, capped, and labeled. The dye concentration of each sample was determined with a G..K. Turner fluorometer.

SAMPLING PROCEDURE

Sampling was begun by three 3-man boatcrews at cross section *D* just prior to the start of the injection of the fluorescent materials so that background samples could be obtained. These samples were used to check the bed material in the reach for naturally fluorescent materials which might be mistaken for the fluorescent tracer materials.

Two men in each crew sampled while the third marked sample bags and assisted in emptying the samplers. With the exception of positions near the banks, sampling for approximately 30 seconds was sufficient to obtain 500- to 800-gram samples. Small canvas bags were used for sample storage. Figure 13 is a photograph of the three boatcrews in the process of sampling at cross section *D*.

In run 1, samples were collected at lateral positions 17, 23, 37, 43, 55, and 63 feet from the right bank. Unfortunately, no samples were obtained at position 30 until late in the experiment. Inspection of the samples indicated that the large red particles were moving toward the right bank; therefore, the crews were shifted toward the right bank, and samples were obtained at lateral positions 3, 7, and 12 feet from the right bank as well as at the other positions. The inspection of the samples also indicated that the tracer materials were moving through the study reach very rapidly; therefore, all three crews remained at cross section *D* for the entire experiment. After 5 hours, sampling was discontinued because inspection of the samples indicated that essentially all the fluorescent material had passed through the study reach.

In run 2, samples were collected at lateral positions 18, 24, 30, 36, 42, 48, 54, and 60 feet from the right bank at cross section *D*. Samples were collected as rapidly as possible for about 3 hours; then at the rate of three to four samples at each position per hour for another 4 hours;

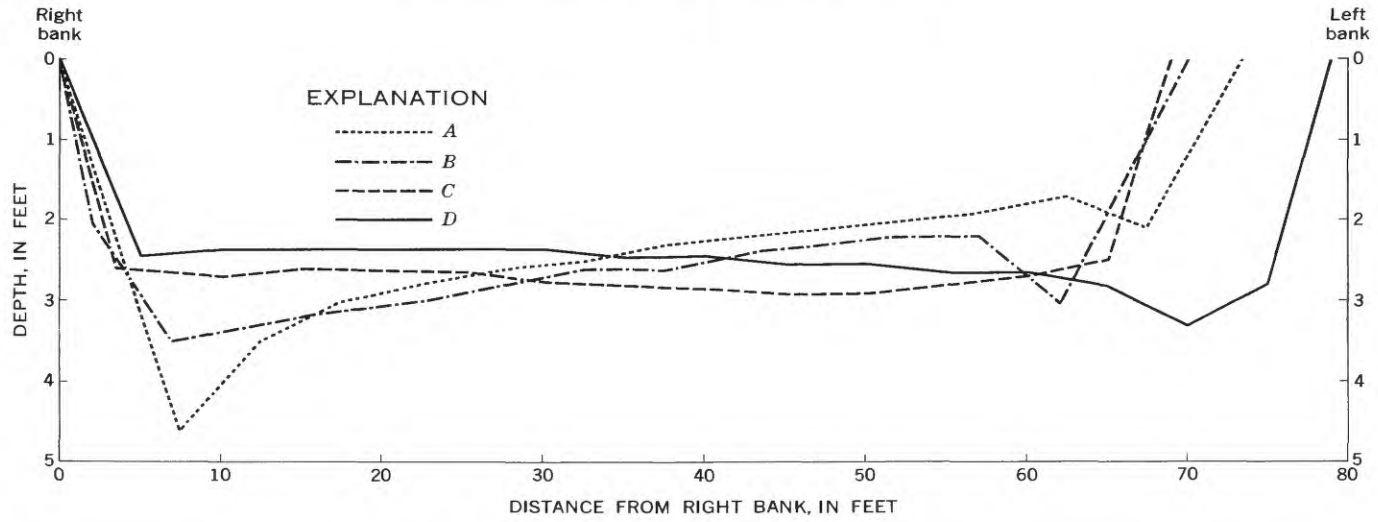

FIGURE 12.—Cross-section measurements obtained at 0815 hours, December 14, 1966.

then two samples at each position per hour for the next 3 hours; and, finally, hourly samples at each position for 4 more hours. Major sampling was discontinued about 14 hours after injection of the fluorescent materials.

FIGURE 13.—Three boatcrews "dustpan" sampling at cross section *D*.

In addition to the "dustpan" samples, a number of 6-inch core samples were obtained at various positions in the study reach about 22 hours after injection of the fluorescent materials.

ANALYSIS OF THE SAMPLES

Analysis of the samples consisted of sieving the samples into the various size classes, counting the number of fluorescent particles of each color in each sieve class, and converting the number of fluorescent particles to concentrations. The concentration of a fluorescent tracer is the ratio of the weight of tracer material in a given size range of the sample to the total weight of all material in that size range of the sample.

All the samples were dried at room temperature. A $\sqrt{2}$ series of 8-inch stainless steel sieves was used for the sieving, and samples were sieved on a Ro-Tap shaker for 10 minutes. After completing the sieving of each sample, the sieves were inspected under an ultraviolet light to insure that no fluorescent particles remained which might contaminate the next sample.

The number of fluorescent particles of each color in each size class was determined by counting with the equipment shown in figure 14. The equipment consisted of an ultraviolet light source, a vibratory sand feeder, a

FIGURE 14.—Equipment used for determining the number of fluorescent particles in the samples.

variac for controlling the voltage to the sand feeder, and a hand tabulator for keeping a running count of the number of fluorescent particles of each color. The procedure consisted of placing a split of a size fraction in the sand feeder, adjusting the voltage on the variac to give the desired feed rate, and counting the fluorescent particles of each color as they fell from the end of the sand feeder into the glass dish. Sizes smaller than the 0.125 mm were not counted because of the difficulty of differentiating between actual fluorescent particles and chips or flakes of dye from the large fluorescent particles.

A statistical analysis of the counting process (C. F. Nordin, Jr., written commun., 1968) has shown for tracer concentrations less than about 0.1 that the probability that the measured tracer concentration is between 0.9 and 1.1 of the true tracer concentration is 95 percent if about 400 tracer particles are counted. Thus, it was necessary only to count until 400 fluorescent particles were obtained and then weigh that part of the particular size split associated with the 400 fluorescent particles. If the size split contained large numbers of particles of several colors, then the counting process was continued until 400 fluorescent particles of the lesser of the predominant colors in the size split were obtained. The entire size split was counted if the sample contained less than 400 fluorescent particles of any color.

The numbers of fluorescent particles of each color in each size split were converted to concentrations with the numbers of fluorescent particles per gram of fluorescent material. These numbers were determined for the different sieve classes of each fluorescent material. A specific number of fluorescent particles (usually 1,000) of a specific sieve class was counted and weighed. This counting and weighing process was continued until a subsequent measurement did not change the overall mean by more than 2.0 percent. The numbers of fluorescent particles per gram of fluorescent material for the fluorescent materials used in runs 1 and 2 are given in table 6.

TABLE 6.—*Numbers of fluorescent particles per gram of fluorescent material for the sieve classes of fluorescent tracer materials used in runs 1 and 2*

Sieve class (mm)	Particles per gram						
	Run 1			Run 2			
	Green quartz	Yellow quartz	Red quartz	Quartz	Garnet	Monazite	Lead
0.125–0.177	128,000	.....	.....	101,000	74,100	87,000	.....
0.177–0.250	48,500	.....	.....	45,800	33,200	38,800	13,600
0.250–0.350	23,600	15,500	.....	15,800	12,600	7,520	4,910
0.350–0.500	.....	6,360	.....	5,510	5,380	3,210	3,250
0.500–0.707	.....	3,220	1,990	2,540	2,760	.....	.....
0.707–1.00	.....	.....	810	1,170	.....	.....	.....
> 1.00	.....	.....	293	.....	.....	.....	.....

PRESENTATION AND DISCUSSION OF RESULTS

The basic experimental data obtained in this study consisted of $C(t)$, the fluorescent tracer concentration as a function of time from the "dustpan" samples obtained at the various lateral positions at cross section D; $C'(t)$, the fluorescent tracer concentration as a function of time from the depth-integrated samples obtained at the weir; and the hydraulic and sediment-concentration measurements for the study reach at the time of the experiments.

A large number of graphs of fluorescent tracer concentration as a function of time for the different sieve classes and specific gravities were obtained for the two runs (54 for run 1 and 105 for run 2). The $C(t)$ data were obtained for all sieve classes of the quartz in run 1 and of the quartz, garnet, and monazite in run 2. None of the lead tracer particles in run 2 were found. The data for the 0.500- to 0.707-mm sieve class of monazite in run 2 were discarded because of the possibility of contamination from the large red quartz particles from run 1 that apparently were temporarily trapped along the right bank. Background samples collected prior to the start of run 2 contained no fluorescent particles; however, samples obtained at lateral positions 18 and 24 feet about 4 hours after the start of run 2 contained some of the large red quartz particles from run 1.

A small number of the graphs representative of all of the data of fluorescent tracer concentration as a function of time were selected to be included as examples. For run 1, one set of graphs of concentration as a function of time at lateral positions, z, of 7, 17, 23, 37, 43, and 55 feet from the right bank for one sieve class of each of the three colors was selected. These sieve classes were the 0.177–0.250 mm for the green quartz, the 0.350–0.500 mm for the yellow quartz, and the 0.707–1.00 mm for the red quartz. The graphs are presented in figures 15, 16, and 17 for the green, yellow, and red quartz, respectively.

For run 2, graphs of the concentration as a function of time at lateral positions, z, of 18, 24, 30, 36, 42, 48, and 54 feet for the 0.250- to 0.350-mm sieve class of quartz and the 0.177- to 0.250-mm sieve class of monazite were selected. These graphs are presented in figures 18 and 19. The concentrations plotted in figures 18 and 19 are relative concentrations; that is, each concentration value has been divided by the total area under the curve of concentration as a function of time. The relative concentrations are given by

$$C_r(t) = \frac{C(t)}{\int_0^\infty C(t)\,dt}. \qquad (1)$$

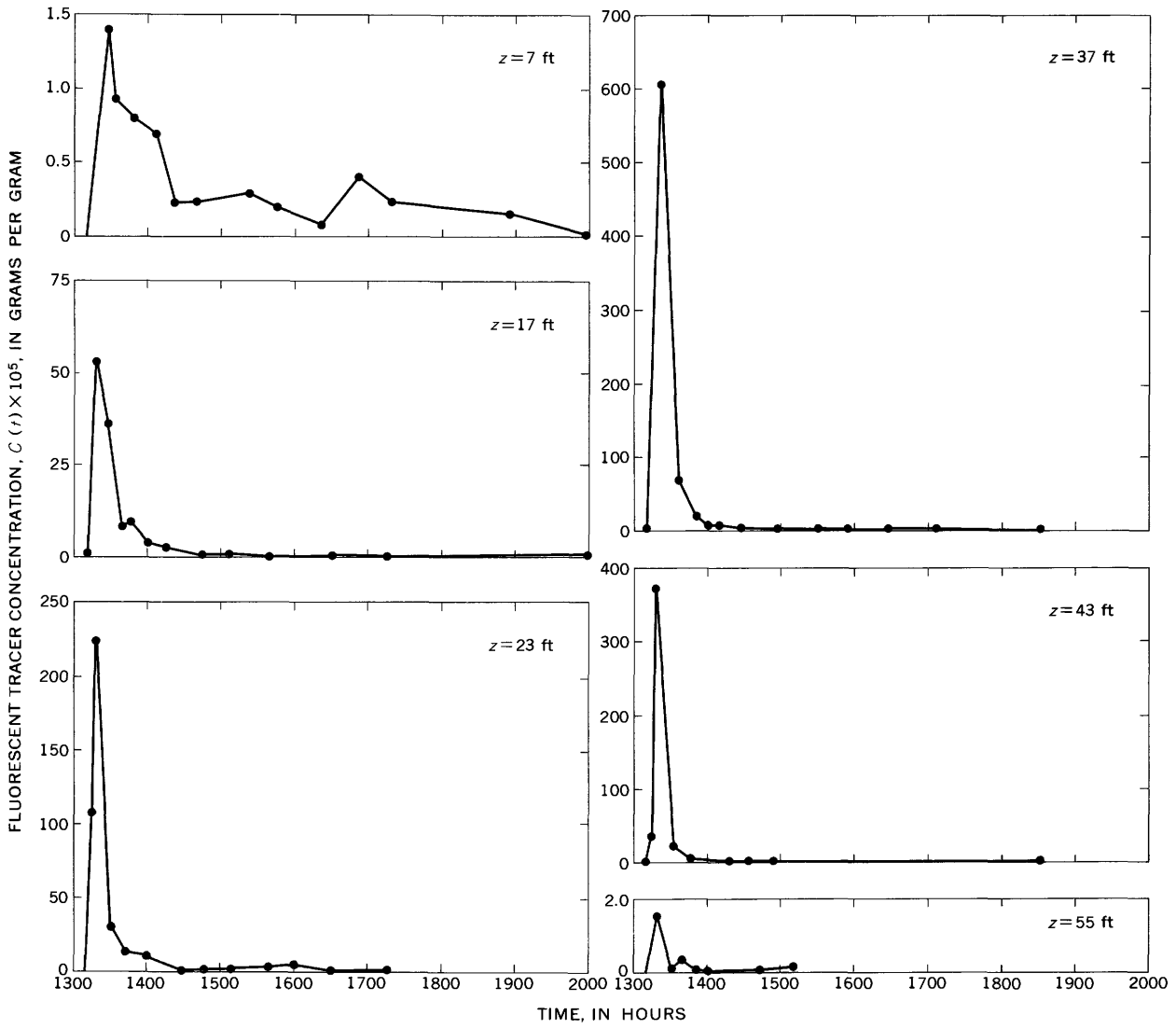

FIGURE 15.—Variation with time of the concentration of the 0.177- to 0.250-mm sieve class of green quartz at lateral positions of 7, 17, 23, 37, 43, and 55 feet; cross section *D*, run 1.

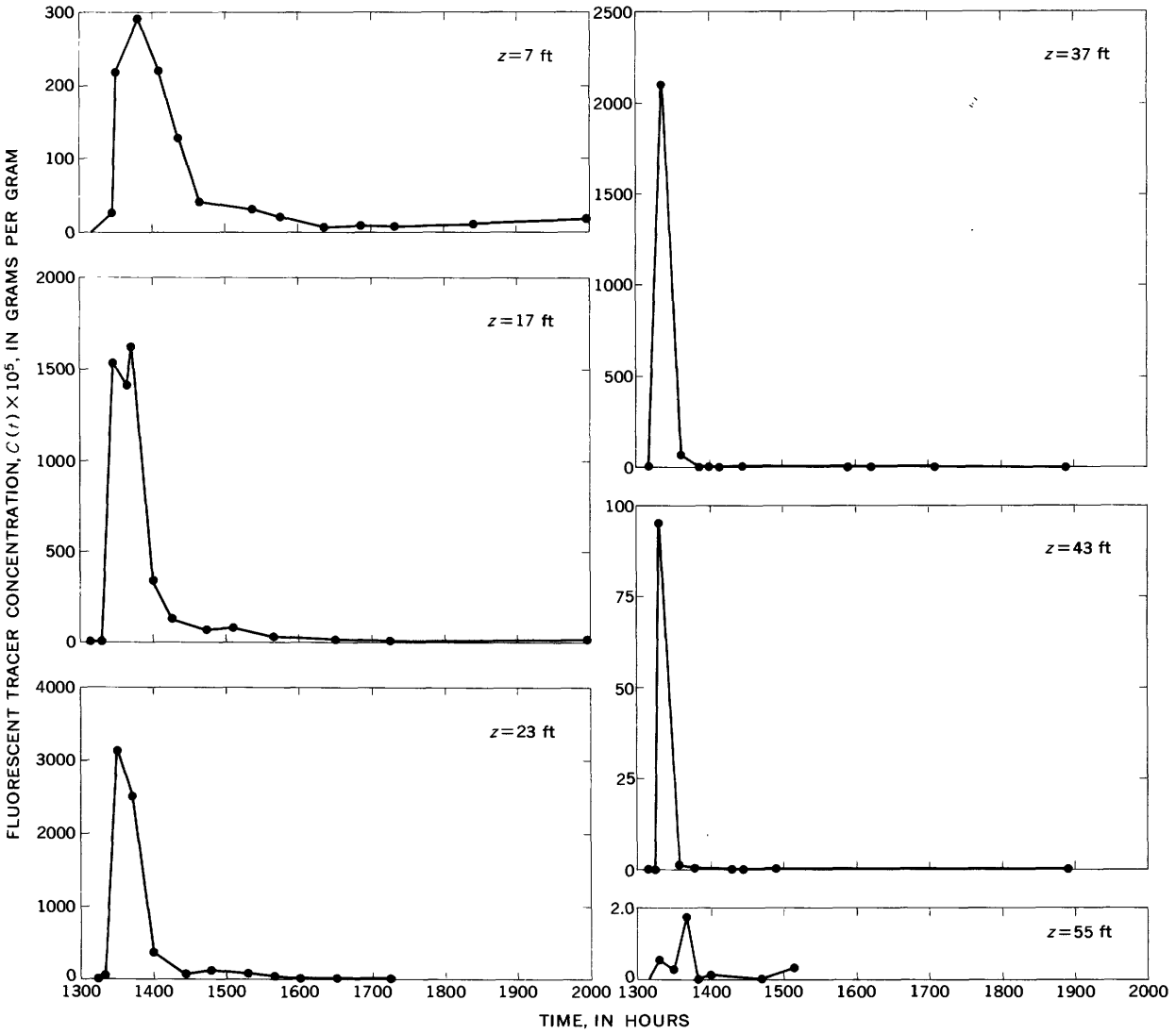

FIGURE 16.—Variation with time of the concentration of the 0.350- to 0.500-mm sieve class of yellow quartz at lateral positions of 7, 17, 23, 37, 43, and 55 feet; cross section *D*, run 1.

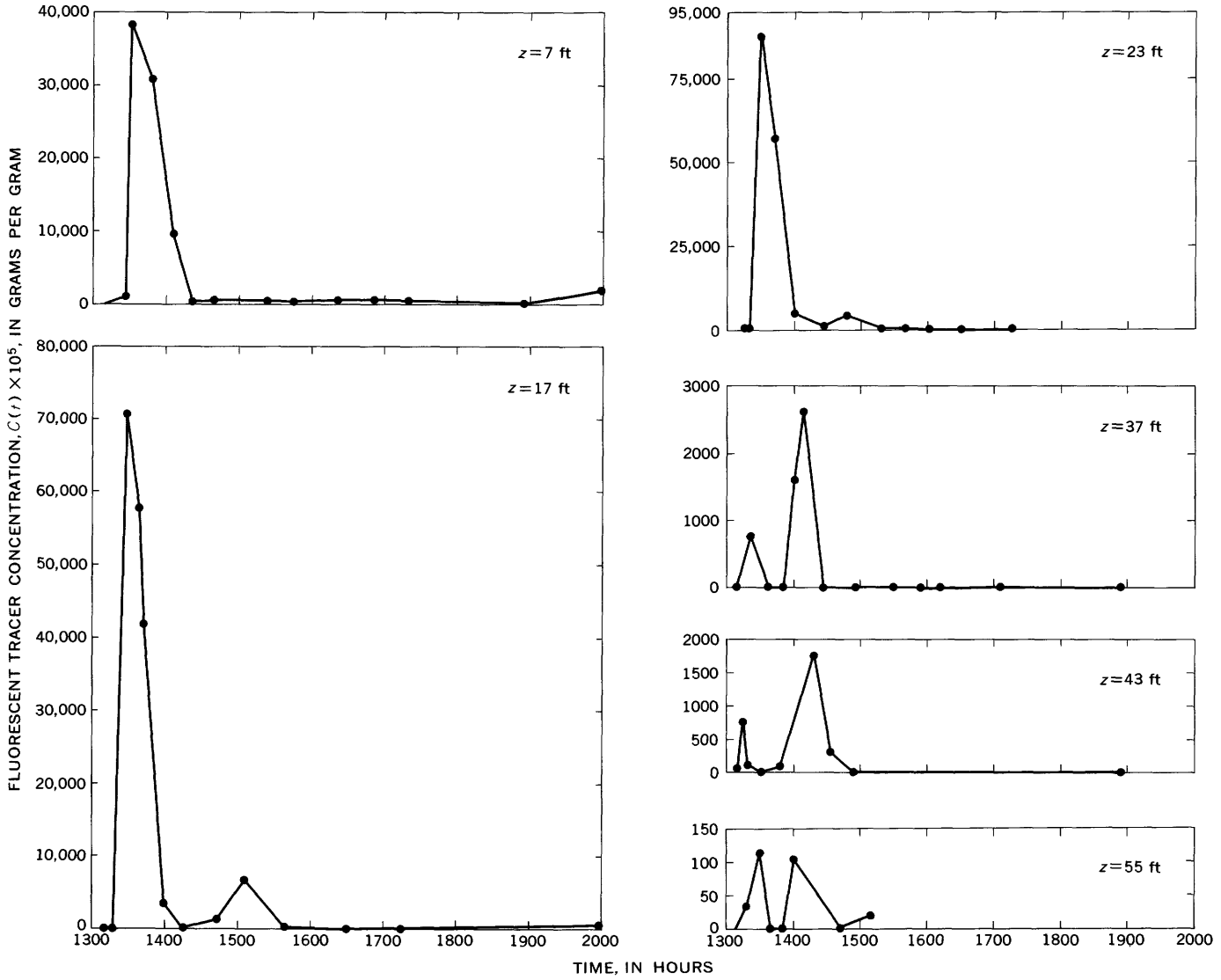

FIGURE 17.—Variation with time of the concentration of the 0.707- to 1.00-mm sieve class of red quartz at lateral positions of 7, 17, 23, 37, 43, and 55 feet; cross section *D*, run 1.

The quantity $C(t)$ is the fluorescent tracer concentration of a specific sieve class at a specific lateral position at time t. The quantity $C_r(t)$ is the normalized, or relative, concentration obtained by dividing $C(t)$ by the total area under the concentration versus time curve. The normalization procedure indicated by equation 1 corrects for the differences in the quantities of the quartz and monazite injected and facilitates presenting the results for the two minerals on the same graphs. These particular sieve classes were chosen for presentation because they have approximately the same median fall diameters (0.289 mm for the quartz and 0.305 mm for the monazite; see table 1).

Most of the results of this study depend upon the concentrations of fluorescent tracer material in the "dustpan" samples. Concentration of fluorescent material in a sieve class of a sample is defined as the grams of fluorescent tracer per gram of total material in that sieve class. If the tracer particles of a specific sieve diameter behave exactly as the nontagged particles of the same diameter, then the efficiency of the "dustpan" sampler is not important. This should be true for the quartz tracer particles if no significant shape differences exist between the tracer particles and the bed-material particles because the bed material is predominately quartz.

The efficiency of the "dustpan" sampler is of concern, however, when minerals with a specific gravity different from that of quartz are used as tracers, as in run 2. Concentrations for the garnet and monazite were expressed as the grams of garnet or monazite in the sieve class per gram of total material in that sieve class. The total material, however, was essentially all quartz; and because of the specific gravity difference between the minerals, the quartz associated with the garnet or monazite in a sieve class would have a smaller median fall diameter than the median fall diameter of the garnet or monazite. Therefore, if there were any washing of the sample during the sampling period or when the sampler was raised to the water surface, and if the effect of the washing were related to fall diameter, then the concentrations of the garnet and monazite would be affected.

An analysis of the size distributions of various "dustpan," core, and depth-integrated samples obtained during the two runs suggested that washing of the fines from the "dustpan" samples may have occurred. On the other hand, the analysis suggested that, if washing did occur, the effect was essentially uniform with respect to time and position at cross section D. If the washing effect is uniform with respect to time and position at cross section D, then the results should not be affected significantly because the data analysis involves ratios of concentration integrals. Details of the analysis of the washing effect are presented in appendix A.

The experimental data from the two runs were used to determine (a) the lateral-dispersion characteristics of the tracer materials between the injection point and cross section D; (b) the feasibility of applying the fluorescent tracer technique to sediment-transport-rate determinations; (c) the velocities of the centroids of the tracer materials between the injection point and cross section D; and (d) the longitudinal-dispersion characteristics of the tracer materials between the injection point and cross section D. Each of these items is discussed in detail in the following sections.

LATERAL-DISPERSION CHARACTERISTICS OF THE TRACER MATERIALS

The lateral-dispersion coefficient, K_z, can be calculated from the rate of change of the variance of the lateral distribution of the tracer material with distance downstream (Sayre and Chang, 1968). In the fluorescent tracer experiments, however, meaningful data were obtained only at cross section D because of the rapid rate at which the tracer material moved through the study reach. Therefore, a true lateral dispersion coefficient could not be calculated. However, the variance, σ_z^2, of the area under the curves of fluorescent tracer concentration as a function of time versus lateral position at cross section D can be used as a measure of lateral dispersion between the injection point and cross section D. For a valid comparison, this procedure assumes that the initial period required for the establishment of the linear variation of the variance with distance is the same for all size classes and specific gravities of tracer materials.

The lateral distributions of the fluorescent tracer materials at cross section D were represented by plots of the areas under the curves of concentration versus time as a function of lateral position, z, in the cross section—that is, $A(z)$ versus z, where $A(z)=\int_0^\infty C(t)dt$. The $A(z)$ data were normalized by dividing by the area under the $A(z)$ versus z curves, or $\int_0^B A(z)dz$ where B is the channel width. Normalization facilitated the comparison of the lateral distributions for the different sieve classes and specific gravities of tracer materials. The graphs of the normalized, or relative, area, $A_r(z)$, as a function of z for the various sieve classes of fluorescent materials used in run 1 are presented in figure 20; and the graphs of $A_r(z)$ versus z for the different sieve classes of quartz, garnet, and monazite tracers used in run 2 are presented in figures 21, 22, and 23, respectively. Figures 20 through 23 show, in effect, the relative amounts of each fluorescent tracer that passed through each sampling position at cross section D during the runs, if it is assumed that the sediment-transport rate was constant during the run.

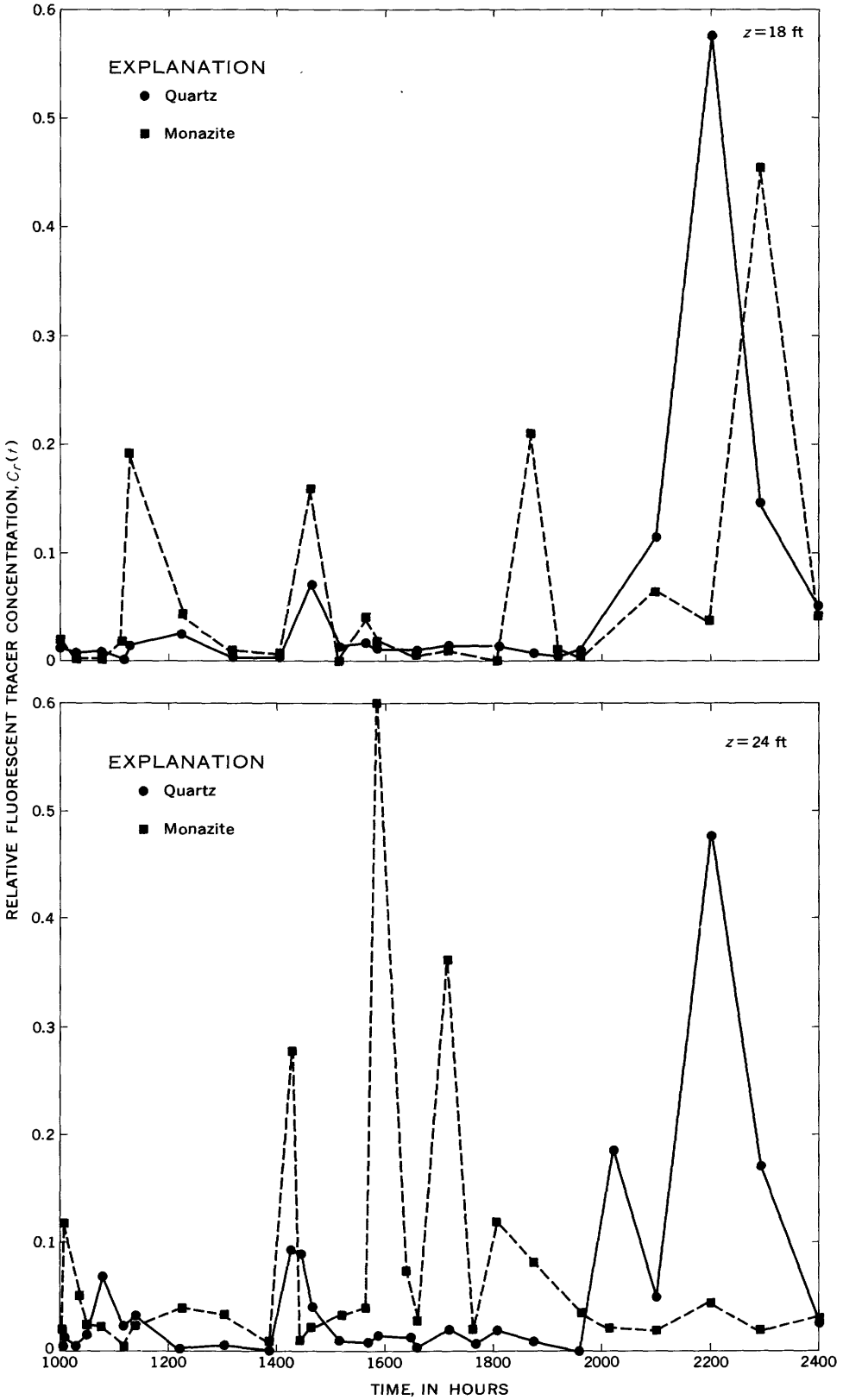

FIGURE 18.—Variation with time of the relative concentrations of the 0.250- to 0.350-mm sieve class of quartz and

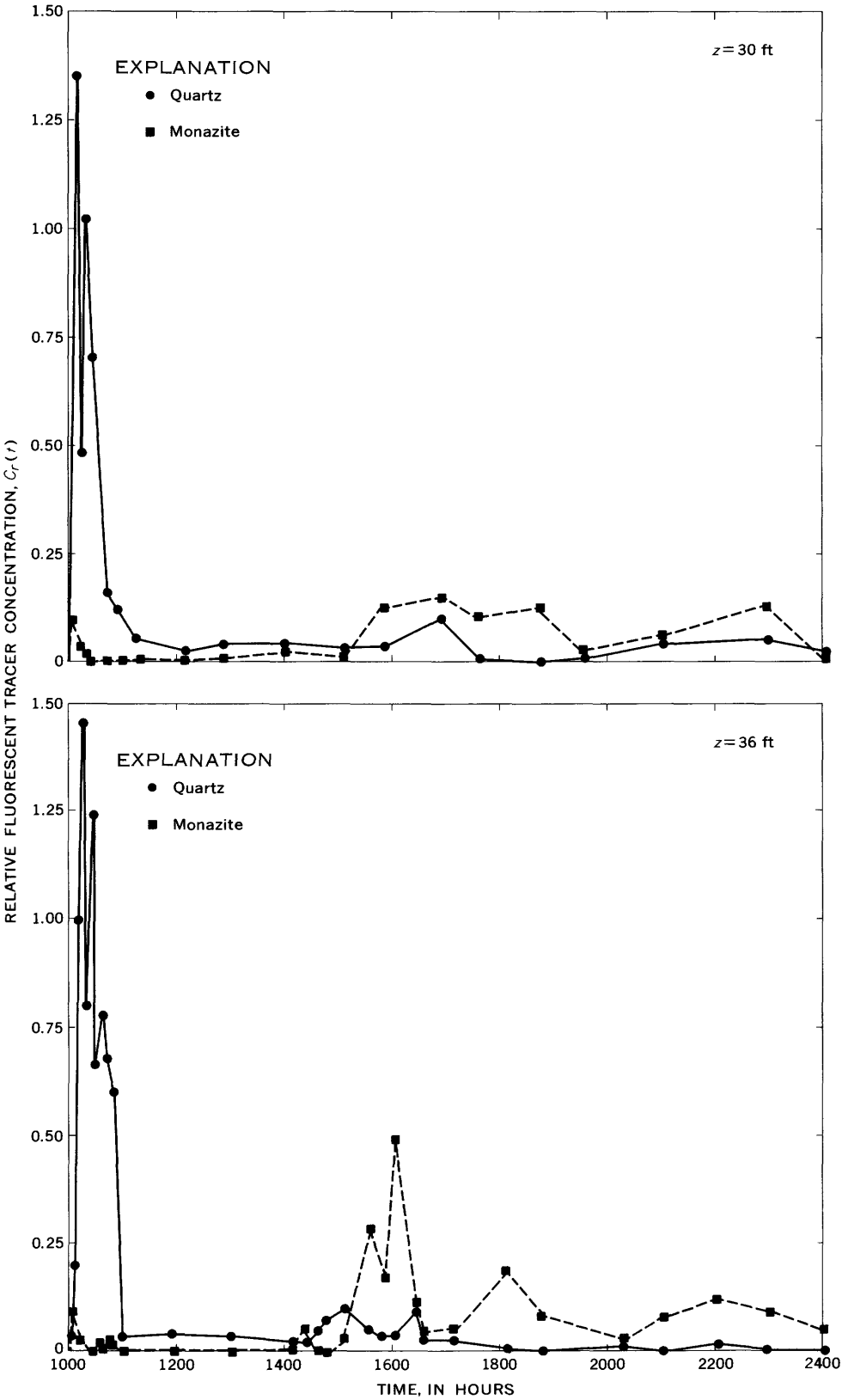

the 0.177- to 0.250-mm sieve class of monazite at lateral positions of $z = 18$, 24, 30, and 36 feet; cross section *D*, run 2.

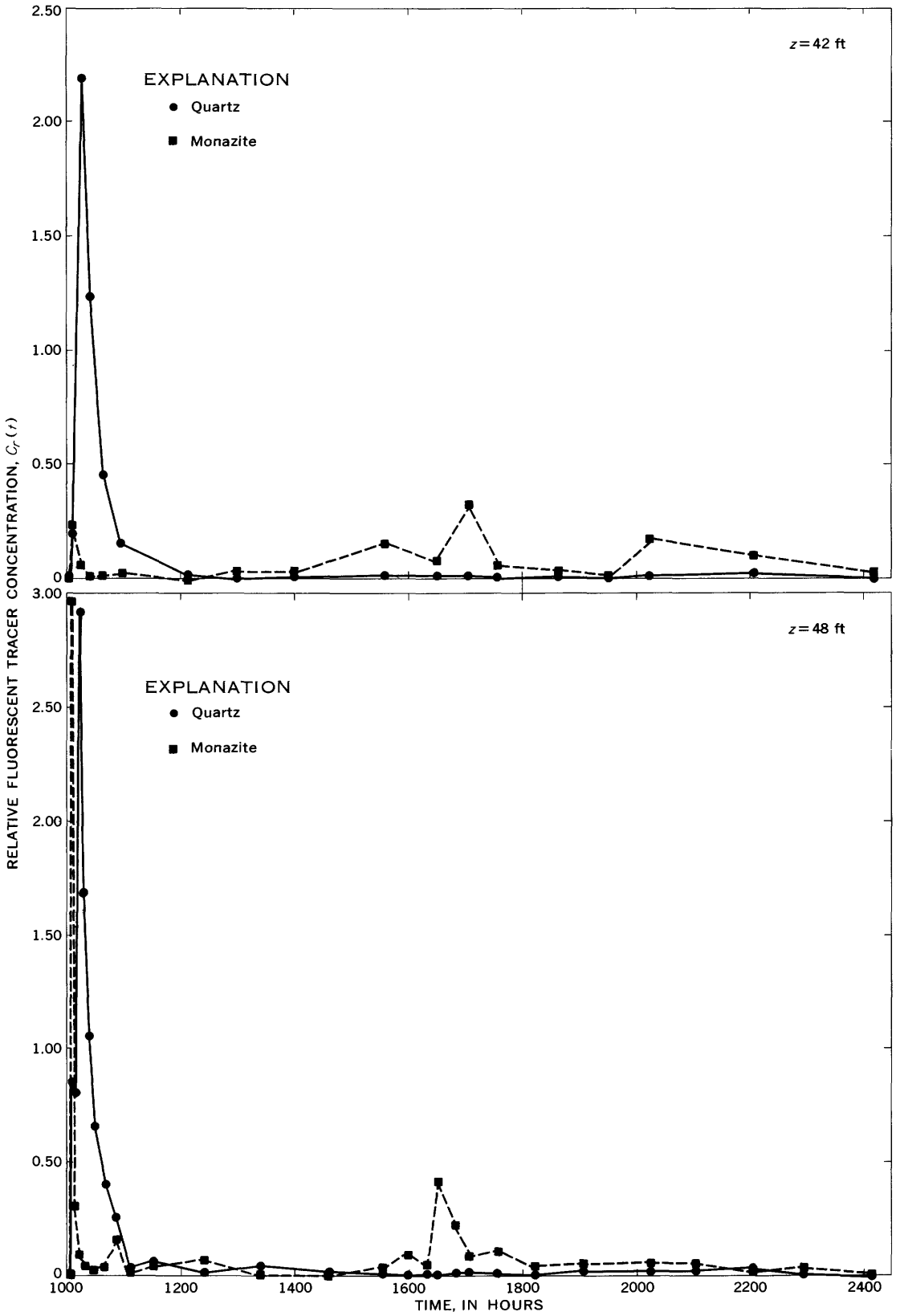

FIGURE 19.—Variation with time of the relative concentrations of the 0.250- to 0.350-mm sieve class of quartz and the 0.177- to 0.250-mm sieve class of monazite at lateral positions of $z=42$, 48, and 54 feet; cross section D, run 2.

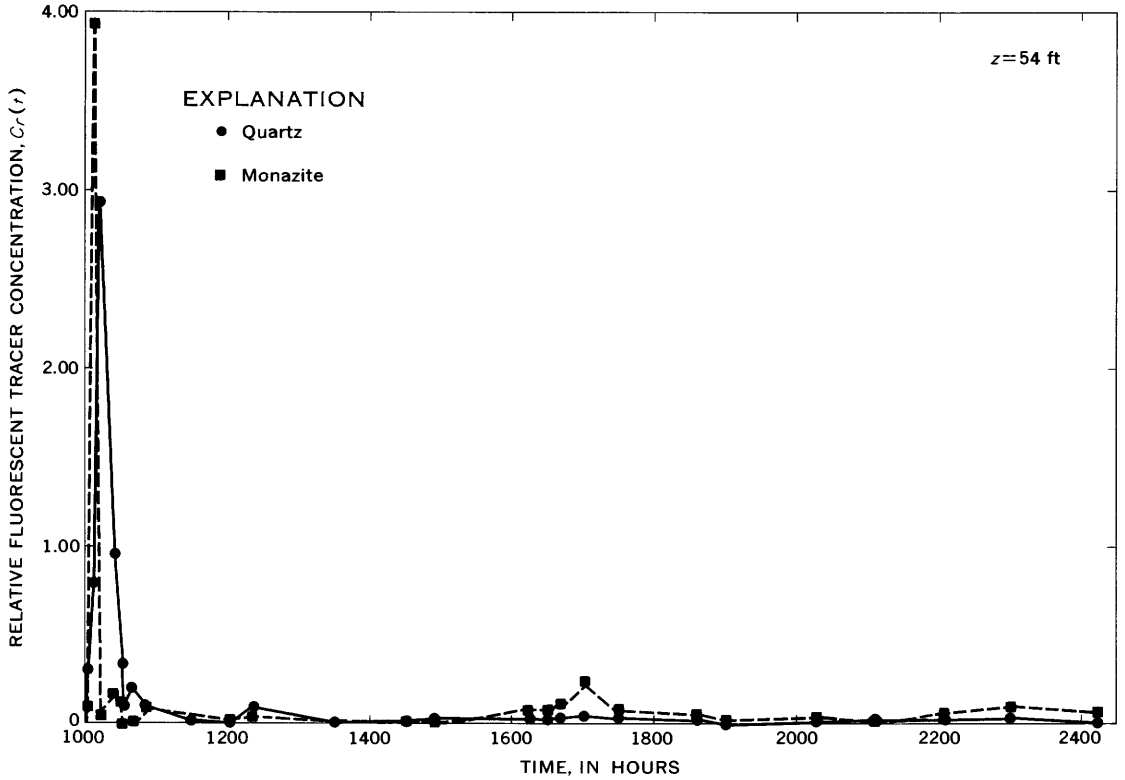

The variance of the lateral distribution at cross section D, σ_z^2, is given by

$$\sigma_z^2 = \frac{\int_0^B z^2 A(z)\,dz}{\int_0^B A(z)\,dz} - \bar{z}^2, \tag{2}$$

where z is the lateral position measured from the right bank of the channel, B is the channel width, $A(z)$ is the area under the curve of concentration versus time at lateral position z and is given by

$$A(z) = \int_0^\infty C(t)\,dt \Big|_{z=z}, \tag{3}$$

and $\bar{z}$ is the mean lateral position of the distribution, defined as

$$\bar{z} = \frac{\int_0^B zA(z)\,dz}{\int_0^B A(z)\,dz}. \tag{4}$$

The integrals in equations 2 and 4 were determined by measuring with a planimeter the areas under the appropriate curves. The $A(z)$ values at the ends of the distribution were assumed to be zero at lateral positions displaced toward the banks from the outside sampling positions a distance equal to one-half of the interval over which the outside sampling position was assumed to apply. The distributions presented in figures 20 through 23 suggest that this assumption is valid, except perhaps for the red quartz particles in run 1. Because of the tendency for the large particles to move toward the right bank, the areas for the red quartz at $z=7$ feet were large. However, an insufficient number of samples was obtained at positions between $z=7$ feet and the right bank, and thus it was necessary to assume that these areas decreased linearly from the values at $z=7$ feet to zero at $z=2$ feet.

The mean lateral position values, $\bar{z}$, and the variances, σ_z^2, of the lateral distributions at cross section D are summarized in tables 7 and 8 for runs 1 and 2, respectively. The mean lateral position values are plotted as a function of the median fall diameters of the sieve classes in figures 24 and 25 for runs 1 and 2, respectively. The variances, σ_z^2, are plotted as a function of the median fall diameters of the sieve classes in figures 26 and 27 for runs 1 and 2, respectively. The numbers next to each point indicate the sieve-class numbers given in tables 7 and 8.

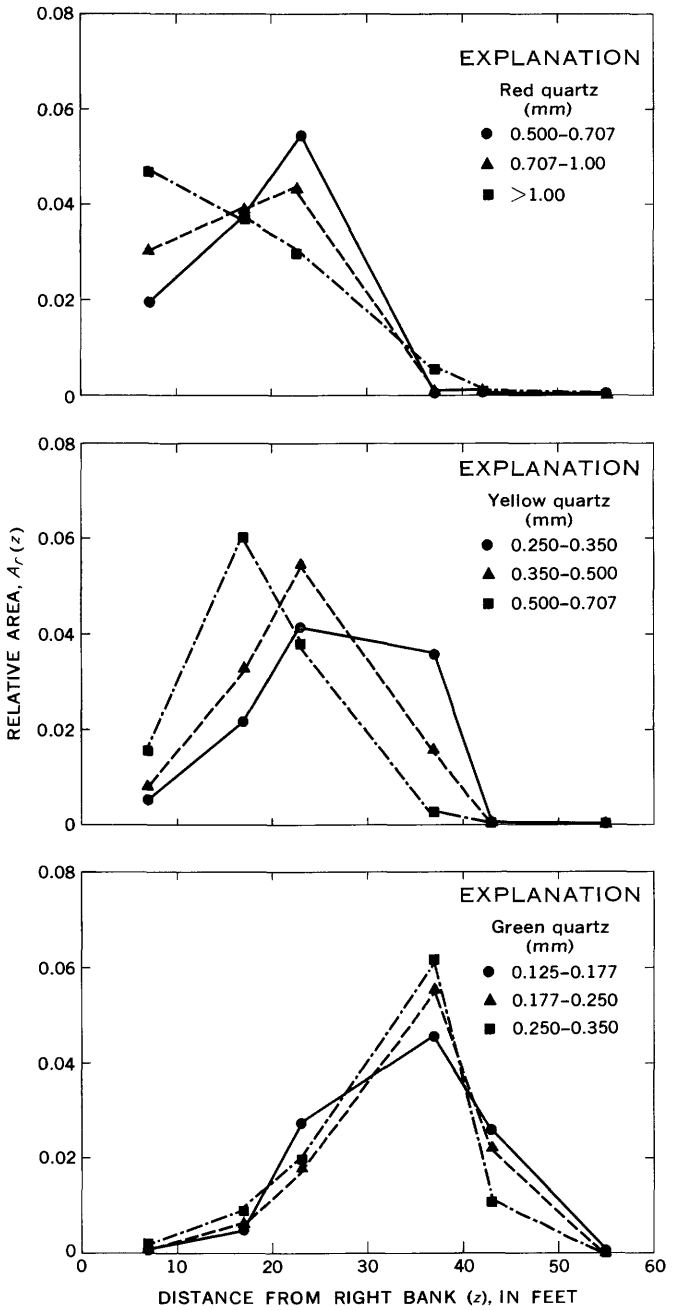

FIGURE 20.—Variation of the area under the curve of concentration versus time with lateral position, z, at cross section D for the different sieve classes of the three colors of quartz tracer, run 1.

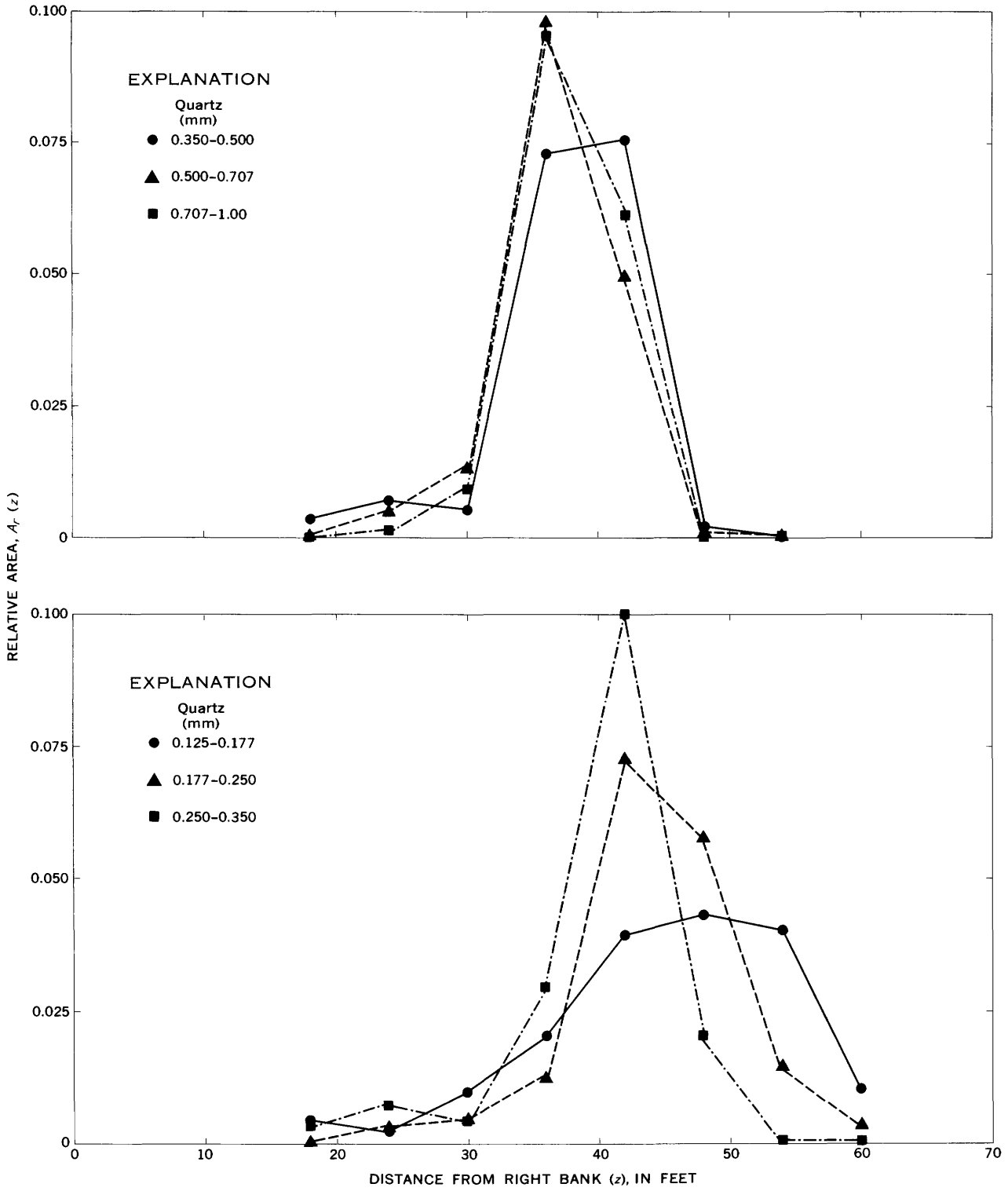

FIGURE 21.—Variation of the area under the curve of concentration versus time with lateral position, z, at cross section D for the different sieve classes of quartz tracer, run 2.

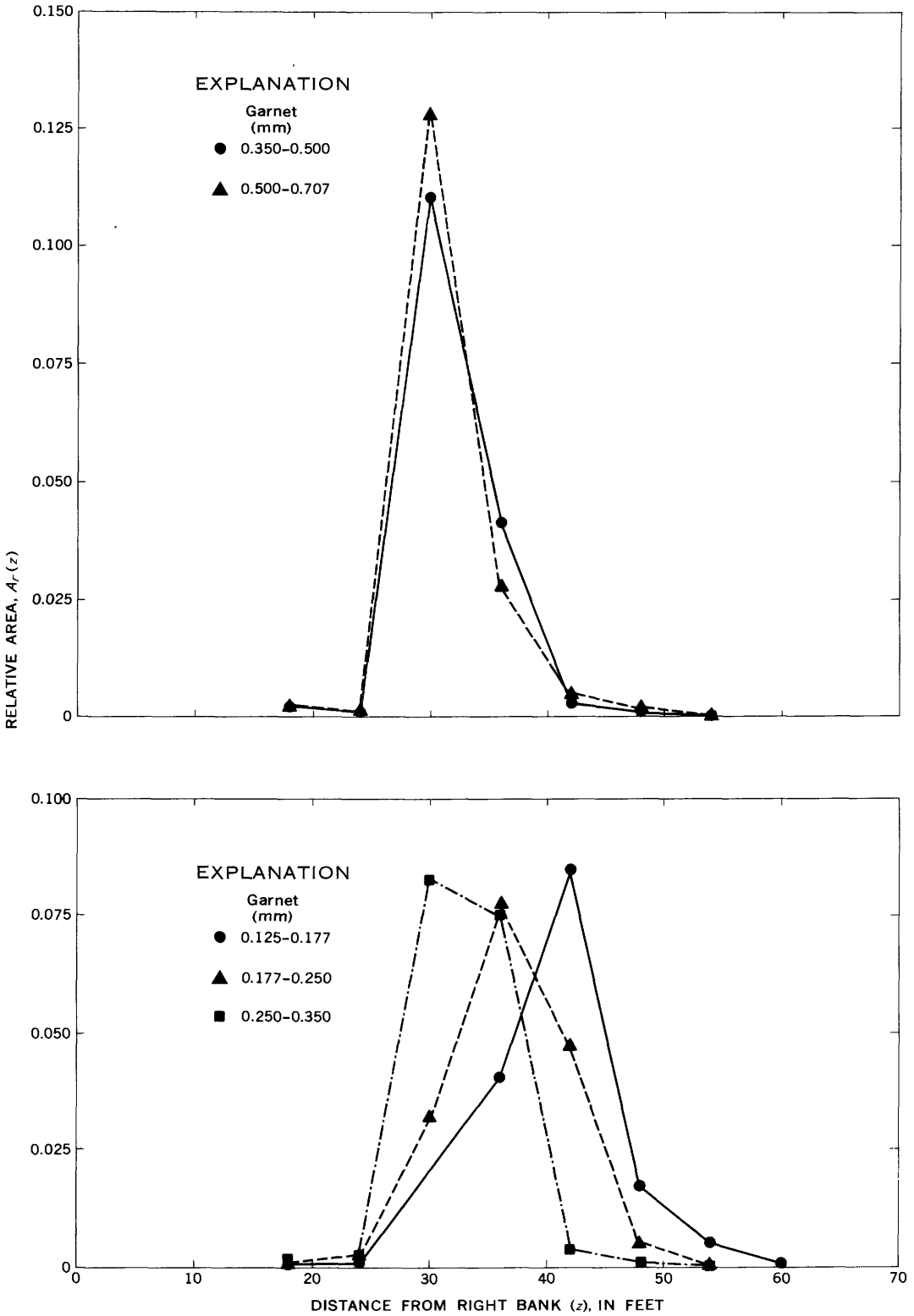

FIGURE 22.—Variation of the area under the curve of concentration versus time with lateral position, z, at cross section D for the different sieve classes of garnet tracer, run 2.

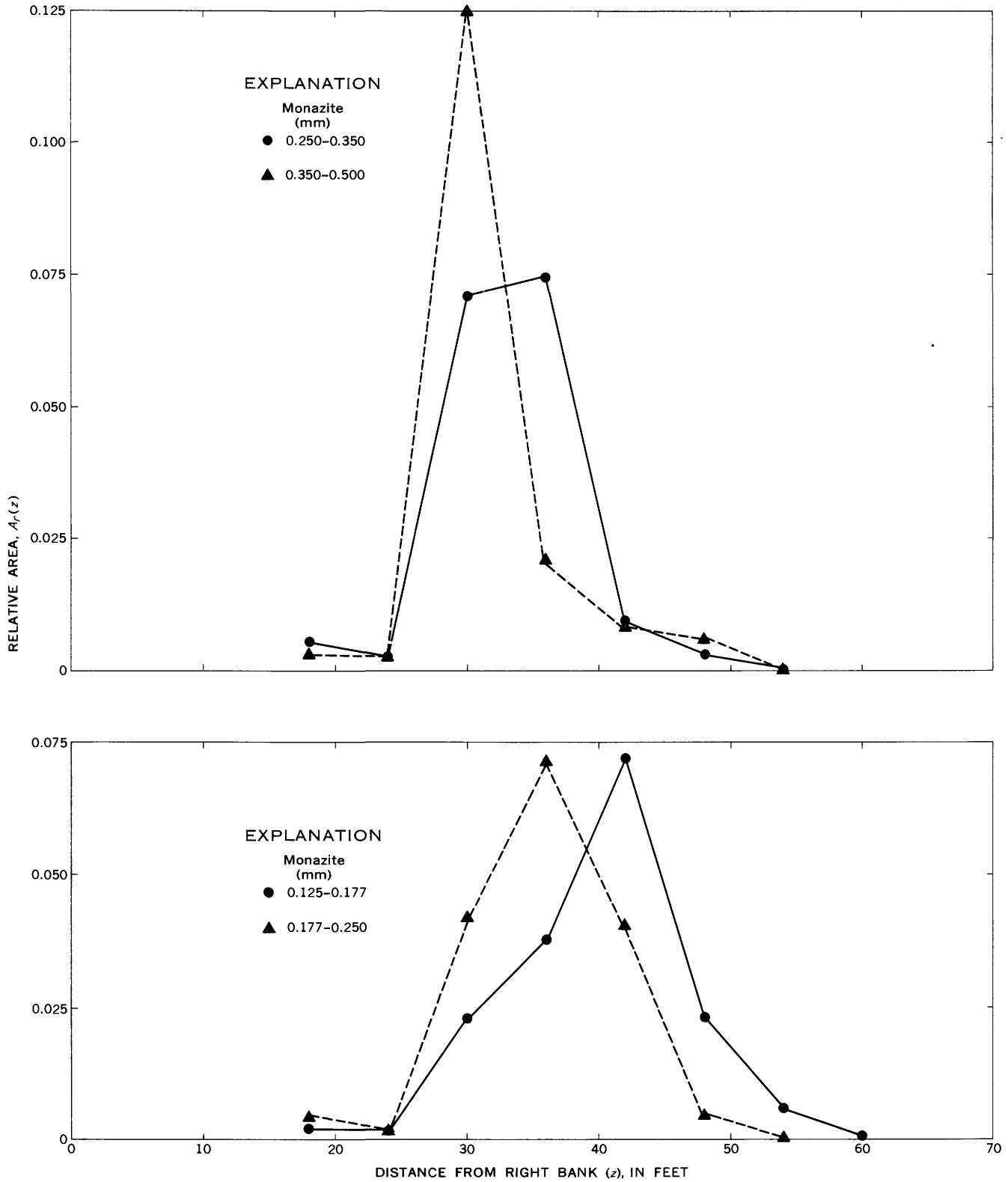

FIGURE 23.—Variation of the area under the curve of concentration versus time with lateral position, z, at cross section D for the different sieve classes of monazite tracer, run 2.

The vertical dashed lines in figures 24 to 27 represent the size limits of the sieve classes used in the analysis of the samples. In several instances, the median fall diameters for some sieve classes of tracer material are smaller than the lower size limit of the sieve class. As discussed previously, shape effects probably contributed to this anomaly. The photomicrographs of the fluorescent materials used in run 1 (see fig. 8) indicate that this material was angular and thus had a shape factor less than the 0.7 usually attributed to naturally worn quartz particles. The median fall diameters for the different sieve classes of garnet and monazite are in general displaced to the next larger sieve class because of the effect of specific gravity.

TABLE 7.—*Summary of the* $\bar{z}$ *and* σ_z^2 *values for the lateral distributions at cross section* D, *run 1*

Color of quartz	Sieve class (mm)	$\bar{z}$ (ft)	σ_z^2 (ft²)
Green	(1) 0.125–0.177	33.7	69.8
	(2) 0.177–0.250	34.4	63.1
	(3) 0.250–0.350	33.2	62.7
Yellow	(3) 0.250–0.350	26.7	82.3
	(4) 0.350–0.500	22.7	61.0
	(5) 0.500–0.707	18.7	34.2
Red	(5) 0.500–0.707	19.0	33.2
	(6) 0.707–1.00	17.9	50.5
	(7) > 1.00	16.5	71.4

TABLE 8.—*Summary of the* $\bar{z}$ *and* σ_z^2 *values for the lateral distributions at cross section* D, *run 2*

Mineral	Sieve class (mm)	$\bar{z}$ (ft)	σ_z^2 (ft²)
Quartz	(1) 0.125–0.177	45.1	78.6
	(2) 0.177–0.250	44.2	38.7
	(3) 0.250–0.350	40.3	36.6
	(4) 0.350–0.500	37.9	26.9
	(5) 0.500–0.707	37.0	17.9
	(6) 0.707–1.00	37.8	14.4
Garnet	(1) 0.125–0.177	40.1	32.9
	(2) 0.177–0.250	36.7	26.2
	(3) 0.250–0.350	33.0	14.5
	(4) 0.350–0.500	31.7	12.5
	(5) 0.500–0.707	31.4	14.4
Monazite	(1) 0.125–0.177	39.9	44.6
	(2) 0.177–0.250	35.9	30.7
	(3) 0.250–0.350	33.4	25.0
	(4) 0.350–0.500	31.9	25.3

The mean lateral positions and the variances for the dye-dispersion test were calculated from summation approximations of equations 4 and 2, respectively. These approximations are

$$\bar{z}=\frac{\sum_{z=0}^{z=B} zC(z)\Delta z}{\sum_{z=0}^{z=B} C(z)\Delta z} \tag{5}$$

and

$$\sigma_z^2=\frac{\sum_{z=0}^{z=B} z^2C(z)\Delta z}{\sum_{z=0}^{z=B} C(z)\Delta z}-\bar{z}^2. \tag{6}$$

The approximations were assumed valid for the dye-dispersion test because samples were obtained every 2 feet across the channel width.

The results of the dye-dispersion test are summarized in table 9. The variances at the different cross sections were corrected for the effect of width by the method of Fischer (1967), and the corrected variances are given in table 9. A plot of the variance as a function of longitudinal distance from the source suggested that the second measurement, $D(2)$, at cross section D was the more correct of the two. The $D(2)$ values of $\bar{z}$ and σ_z^2 for the dye-dispersion test are shown near the ordinates of figures 24 and 26, respectively.

TABLE 9.—*Summary of the* $\bar{z}$, σ_z^2, *and* $\sigma_{\bar{z}}^2$ *(corrected) values for the dye-dispersion test*

Cross section	Width (ft)	$\bar{z}$ (ft)	$\sigma_{\bar{z}}^2$ (ft²)	$\sigma_{\bar{z}}^2$ (corrected) (ft²)
A	73.5	26.8	7.88	7.74
B	70	22.6	19.5	21.2
C	69	30.7	32.8	36.5
D(1)	79	35.2	103	87.7
D(2)	79	34.2	68.5	58.4

The mean lateral positions for the quartz tracer particles ranged from 34.4 feet from the right bank for the 0.177- to 0.250-mm sieve class of green quartz to 16.5 feet for the > 1.00-mm sieve class of red quartz in run 1 and from 45.1 feet from the right bank for the 0.125- to 0.177-mm sieve class to 37.0 feet for the 0.500- to 0.707-mm sieve class of quartz tracer in run 2. The tendency for the large tracer particles to move toward the right bank is evident from the results presented in figures 24 and 25. The difference in the magnitude of the effect for runs 1 and 2 may be attributed to the fact that the injection point for run 2 was moved 7 feet to the left of the channel centerline after the behavior of the tracer particles in run 1 was observed. There was little difference in the $\bar{z}$ values of the garnet and monazite for particles of comparable fall diameter. However, the garnet and monazite $\bar{z}$ values were displaced 2 to 6 feet toward the right bank from the $\bar{z}$ values for quartz particles of comparable fall diameter.

A possible explanation for the movement of the large particles toward the right bank may be based on a consideration of the cross-section measurements obtained prior to the start of run 2. (See figs. 12 and 6.) The thalweg, or line of maximum depth, shifted from approximately

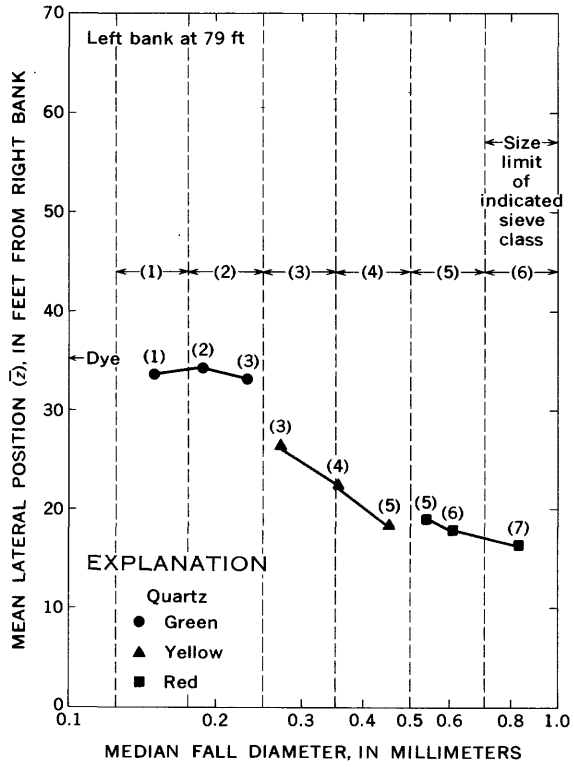

FIGURE 24.—Variation with fall diameter of the mean lateral positions of the tracer distributions at cross section *D*, run 1. Numbers in parentheses are sieve class numbers; see tables 7 and 8.

the centerline at the injection point to the right bank at cross section *A* and then back to the left bank at cross section *D*; the maximum depth was greatest at cross section *A*. The results of the fluorescent tracer experiments suggest that the large tracer particles, particularly in run 1, tended to follow the thalweg from the injection point to the right bank and then to move down the reach along the bank.

Figures 26 and 27 show a distinct difference in the variation of σ_z^2 with fall diameter for the large quartz tracer particles in runs 1 and 2, and there are at least two factors that contribute to this difference. These factors are the movement of the red quartz particles toward the right bank and the indication that some of these particles were trapped temporarily along the right bank. The lateral distributions for the three sieve classes of red quartz, and in particular the > 1.00-mm sieve class, are skewed toward the right bank (fig. 20). Temporary entrapment of some of the red quartz was indicated by the appearance of red quartz particles in samples obtained during the middle part of run 2 for positions near the right bank at cross section *D*, even though background samples obtained at cross section *D* prior to the start of run 2 indicated that all of the fluorescent material used in run 1 had passed through the study reach. Both of these factors, the temporary entrapment and the displacement toward the right bank region where water velocities were less than the mean water velocity, would tend to increase σ_z^2 over the values that might be expected if the red quartz particles had moved down the center of the channel without interference.

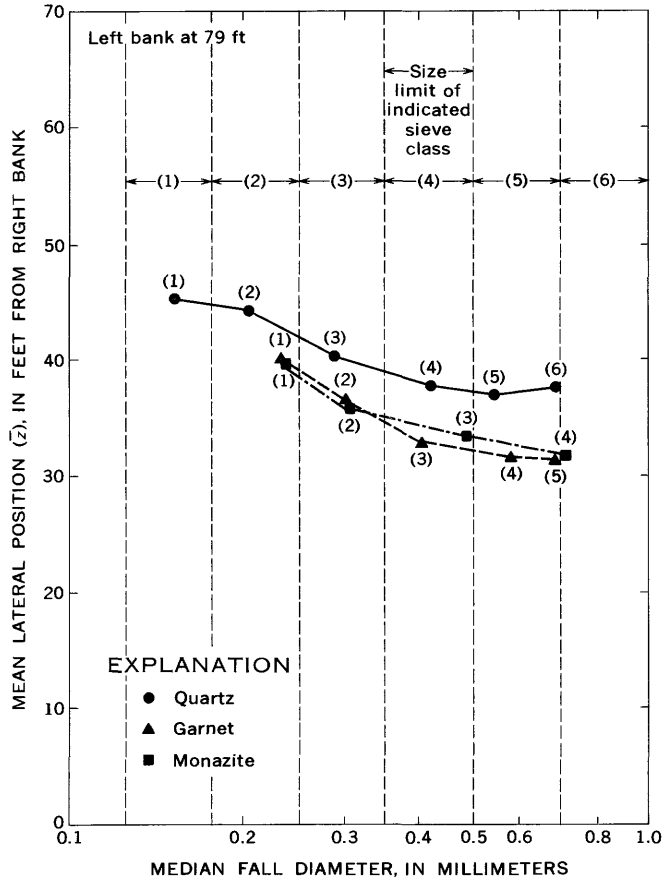

FIGURE 25.—Variation with fall diameter of the mean lateral positions of the tracer distributions at cross section *D*, run 2. Numbers in parentheses are sieve class numbers; see tables 7 and 8.

The σ_z^2 values for the three sieve classes of green quartz in run 1 were approximately the same as the σ_z^2 value for the dye cloud in the dye-dispersion test. The σ_z^2 value for the 0.250- to 0.350-mm sieve class of yellow quartz exceeded the σ_z^2 value for the dye; however, the difference was small.

The σ_z^2 values for garnet in general were less than the σ_z^2 values for quartz particles of comparable fall diameter. The σ_z^2 values for monazite, however, fall in line with the quartz values, with the exception of the value for the 0.350- to 0.500-mm sieve class of monazite. Thus, the lateral dispersion of the heavy minerals as represented by the variance of the lateral distribution at cross section *D* generally decreases with increasing particle diameter, as it does for the quartz, with the exception, however,

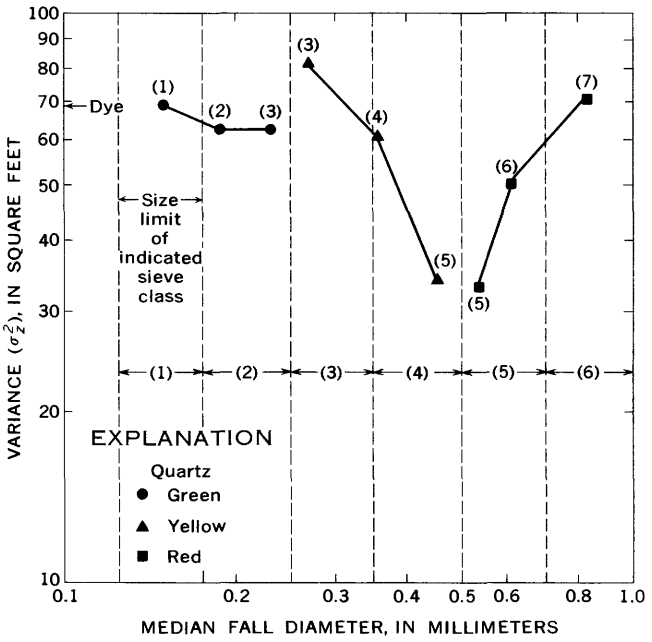

FIGURE 26.—Variation with fall diameter of the variances of the lateral distributions of the tracer masses at cross section *D*, run 1. Number in parentheses are sieve class numbers; see tables 7 and 8.

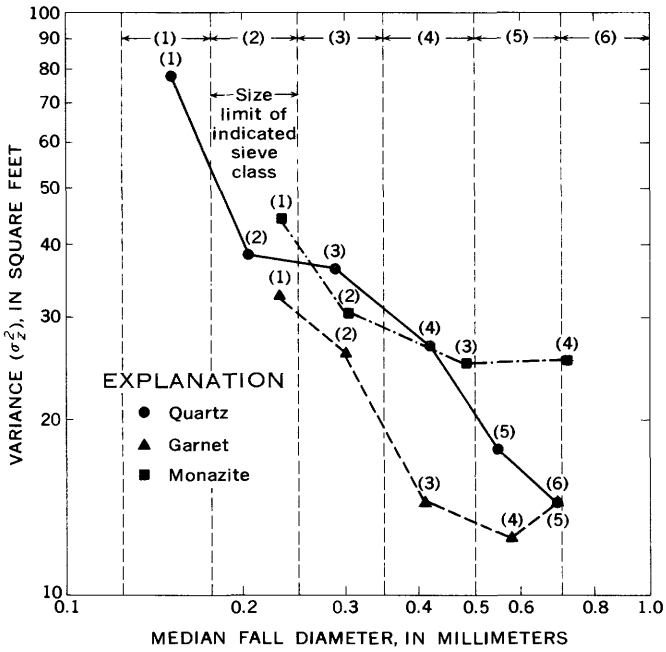

FIGURE 27.—Variation with fall diameter of the variances of the lateral distributions of the tracer masses at cross section *D*, run 2. Numbers in parentheses are sieve class numbers; see tables 7 and 8.

that there is a slight increase in the variance for the large sizes of garnet and monazite.

The results of the two fluorescent tracer experiments suggest that at least two factors may be important in causing lateral mixing of sediment particles. These are the turbulence in the flow and the thalweg. In run 1, the injection point apparently was on the thalweg and the large particles tended to follow the thalweg to the right bank whereas the small particles were mixed in the lateral direction to about the same extent as the dye cloud. Thus, in run 1 the lateral mixing of the small particles was caused primarily by the turbulence in the flow, and the lateral mixing of the coarse particles was caused primarily by the thalweg. Particles with a fall diameter of about 0.5 mm were affected least by the two factors. (See fig. 26.) In run 2, the shift of the injection point apparently was sufficient to remove the fluorescent tracers from most of the influence of the thalweg and lateral mixing as indicated by σ_z^2 decreased with increasing fall diameter. The large and heavy particles mixed the least because they spent a greater proportion of the time resting on or rolling along the bed surface than did the small particles.

APPLICATION OF FLUORESCENT TRACERS TO THE MEASUREMENT OF THE SEDIMENT-TRANSPORT RATE

The use of fluorescent tracers for the determination of the sediment-transport rate assumes that the tracer particles and the natural sediment particles behave identically. Also, the quantity of tracer material injected must be small in comparison with the natural sediment-transport rate. Sediment-transport rate as used in this report refers to the rate of movement of the channel bed material and includes the suspended bed-material load and the bedload but does not include the fine material or "wash load."

"DUSTPAN" SAMPLES AT CROSS SECTION *D*

The time-integration method was used to calculate the sediment-transport rate from the fluorescent tracer concentrations of the "dustpan" samples obtained at cross section *D*. The time-integration equation is based on the conservation of the tracer material as expressed by

$$W = \int_0^B \int_0^\infty q_s(t, z) C(t, z)\, dt\, dz, \tag{7}$$

where W is the weight of tracer material injected, q_s is the sediment-transport rate per unit of channel width, C is the fluorescent tracer concentration, and B is the channel width. The quantities q_s and C are functions of lateral position, z, and time, t. If q_s, the sediment-transport rate, is steady, it is independent of time, and equation 7 becomes

$$W = \int_0^B q_s(z) \int_0^\infty C(t, z)\, dt\, dz. \tag{8}$$

Because samples were obtained at various positions across the channel at cross section *D* throughout the pas-

sage of the tracer mass, the variation of the quantity $\int_0^\infty C(t)\,dt$ with z was determined. However, it is necessary also to know how q_s varies with z. It was assumed that

$$q_s(z) = \bar{q}_s w(z), \tag{9}$$

where $q_s(z)$ is the unit sediment-transport rate at z, $\bar{q}_s$ is the mean unit sediment-transport rate for the cross section, and $w(z)$ is the weighting factor at z. Substitution of equation 9 into equation 8 yields, after rearrangement,

$$\bar{q}_s = \frac{W}{\int_0^B w(z)A(z)\,dz}, \tag{10}$$

where $A(z)$ is defined by equation 3. In general, the overall size distribution of the bed material in transport will not match exactly the size distribution of the tracer material. Therefore, equation 10 must be applied to each size class and the results summed to obtain the total sediment-transport rate. The weighting factors were determined from a set of depth-integrated samples obtained at the weir. Details of the procedure are given in appendix B.

The mean unit sediment-transport rates, $\bar{q}_s$, for the various sieve classes of quartz tracer were calculated from equation 10. The denominators of equation 10 were determined by plotting the product $w(z)A(z)$ as a function of z and measuring the areas under the curves with a planimeter. These $\bar{q}_s$ values were converted to the total sediment-transport rates, Q_s, by multiplying by the channel width at cross section D. The Q_s values for the various sieve classes calculated from the fluorescent tracer concentrations of the "dustpan" samples at cross section D are summarized in tables 10 and 11 for runs 1 and 2, respectively. The measured Q_s values determined from the depth-integrated samples obtained at the weir are presented also in tables 10 and 11. The calculations of the sediment-transport rates were limited to sieve sizes larger than 0.125 mm. For sizes smaller than 0.125 mm, it was difficult to distinguish between chips of dye from large particles and actual fluorescent particles.

TABLE 10.—*Summary of the calculation of the sediment-transport rate, "dustpan" samples at cross section* D, *run 1*

Color of quartz	Sieve class (mm)	Q_s (calculated) (tons per day)	Q_s (measured) (tons per day)	$\frac{Q_s \text{ (calculated)}}{Q_s \text{ (measured)}}$
Green	0.125–0.177	2,109	1,515	1.39
	0.177–0.250	2,336	1,191	1.96
	0.250–0.350	1,670	922	1.81
Yellow	0.250–0.350	1,277	922	1.38
	0.350–0.500	323	357	.88
	0.500–0.707	55	33	1.67
Red	0.500–0.707	39	33	1.18
	0.707–1.00	16	0	.....
	>1.00	14	0	.....
Total (maximum)		6,523	4,018	1.62
(minimum)		6,114	4,018	1.52

TABLE 11.—*Summary of the calculation of the sediment-transport rate, "dustpan" samples at cross section* D, *run 2*

Quartz sieve class (mm)	Q_s (calculated) (tons per day)	Q_s (measured) (tons per day)	$\frac{Q_s \text{ (calculated)}}{Q_s \text{ (measured)}}$
0.125–0.177	859	1,194	0.72
0.177–0.250	1,724	937	1.84
0.250–0.350	747	713	1.05
0.350–0.500	118	203	.58
0.500–0.707	36	25	1.44
0.707–1.00	6.9	0	.....
Total.....	3,491	3,072	1.14

In run 1, two calculations of the sediment-transport rate were possible because of the overlap of the green and yellow 0.250- to 0.350-mm sieve classes and the yellow and red 0.500- to 0.707-mm sieve classes. The maximum value given in table 10 was obtained by using the 0.250- to 0.350-mm sieve class of green quartz and the 0.500- to 0.707-mm sieve class of yellow quartz as tracers for the 0.250- to 0.350-mm and 0.500- to 0.707-mm sieve classes of bed material, respectively. The minimum value was obtained by using the 0.250- to 0.350-mm sieve class of yellow quartz and the 0.500- to 0.707-mm sieve class of red quartz as tracers for the 0.250- to 0.350-mm and 0.500- to 0.707-mm sieve classes of bed material, respectively. The maximum value was about 6.7 percent larger than the minimum value.

The maximum and minimum calculated sediment-transport rates are 62 and 52 percent larger than the sediment-transport rate measured at the weir. The ratios of the calculated sediment-transport rates to the measured sediment-transport rates for the various sieve classes are included in table 10 and each ratio is greater than 1.0 for all size classes with the exception of the 0.350- to 0.500-mm sieve class of yellow quartz.

Several factors could contribute to the fact that the calculated sediment-transport rates were almost all larger than the measured sediment-transport rates. Probably the key factor is the assumption inherent in equation 10 that all of the fluorescent tracer material injected is sampled as it passes through the measurement section. However, sampling at any cross section must be limited to a reasonable number of points with linear interpolation assumed valid between the points. A large quantity of fluorescent material could pass unsampled between two sampling positions or could pass through a sampling position while samples were being obtained at another position. These problems would be most important for high-velocity flows where the fluorescent material is moving very rapidly. In addition, a quantity of the fluorescent material may be trapped within the study reach temporarily, or sampling may be terminated before the fluorescent tracer material has passed completely through a study reach. All these factors would result in

low values of the areas, $A(z)$, under the concentration as a function of time curves and, hence, high values for the calculated sediment-transport rates.

In run 1 the failure to sample at $z=30$ feet may have caused some reduction of the areas under the $A(z)$ as a function of z curves. In the absence of data at $z=30$ feet, the areas were assumed to vary linearly with z between $z=23$ feet and $z=37$ feet. A consideration of figure 20 suggests that the areas at $z=30$ feet could be larger than these interpolated values without resulting in unusual $A(z)$ versus z relations. However, it is believed that these possible errors in the areas would not be large enough to account for all of the difference between the calculated and measured sediment-transport rates in run 1.

An additional factor that must be considered is the accuracy of the sediment-transport rates as measured at the weir. The basis of the weir operation is that all the sediment is suspended by the action of the baffles as the sediment passes over the weir and the sampler nozzle traverses the entire depth of flow at the weir crest. It is essential that all of the sediment be suspended and that the suspended sediment be sampled accurately. Errors in the sediment concentrations determined from the depth-integrated samples may occur if the intake velocity of the sampler differs significantly from the stream velocity. If the transit rate is too slow, overfilled sample bottles will result and the samples must be discarded. If the transit rate is too rapid, then the intake velocities are less than the stream velocities and the measured sediment concentrations are greater than the true sediment concentrations. The effect of an incorrect intake velocity increases with particle diameter (U.S. Inter-Agency Committee on Water Resources, 1941, fig. 14) and is very important for particles in the sand-size range.

In run 2, the calculated sediment-transport rate was about 14 percent larger than the measured rate. The good agreement, however, was fortuitous, as is shown by the ratios of the calculated to the measured sediment-transport rates given in table 11. Two of the ratios were less than 1.0, and this negative deviation balanced the positive deviations for the other three sieve classes. There are no apparent reasons why the ratios for the 0.125- to 0.177-mm and 0.350- to 0.500-mm sieve classes should be less than 1.0. However, when the ratio of the measured sediment-transport rate for run 1 to the measured rate for run 2 was calculated for the different sieve classes, it was found that the ratio values were between 1.27 and 1.32 with the exception of the ratio for the 0.350- to 0.500-mm sieve class. This ratio was 1.76 and the large difference for the 0.350- to 0.500-mm sieve class suggests the possibility of an error in the measured sediment-transport rates for this sieve class. Also note that the Q_s (calculated)/Q_s (measured) ratio for this sieve class was less than 1.0 in both runs.

The mean deviations, regardless of sign, of the calculated sediment-transport rates from the measured sediment-transport rates for the different sieve classes were 51 and 41 percent for runs 1 and 2, respectively.

DEPTH-INTEGRATED SAMPLES AT THE WEIR

The calculation of the sediment-transport rate from the fluorescent tracer concentrations of the depth-integrated samples required a slightly different procedure than was used for the "dustpan" samples from cross section D. Because the amount of sand in the depth-integrated samples was small and, consequently, because the number of fluorescent particles in each size split would have been very small, the depth-integrated samples generally were not sieved into size classes. Because the samples were not sieved, only the total number of fluorescent particles of each color was obtained for each sample. The concentration of fluorescent material for these samples, therefore, was defined as the number of particles of a specific color per gram of sediment in the sample. Generally the 14 samples obtained across the weir for each sample time were composited to give one sample for that particular time.

In addition to requiring the modification of the definition of fluorescent tracer concentration, the small size of the depth-integrated samples necessitated two assumptions. First, it was assumed that the fluorescent particles were sampled at the weir in the same proportion as that at which the particles were injected. Second, it was assumed that the sieve-size distribution of the depth-integrated samples at the weir did not change with time during the run.

With these assumptions, it may be shown that the equation for the calculation of the sediment-transport rate of size class i from the concentrations of fluorescent tracers in the depth-integrated samples has the form

$$Q_{s_i}=\frac{Np_i}{A'}, \tag{11}$$

where

$$A'=\int_0^\infty \bar{C}'\,(t)\,dt. \tag{12}$$

Equation 11 is similar in form to equation 10 but has the following differences. First, the weight of fluorescent tracer injected, W, has been replaced by N, the number of fluorescent particles of a specific color injected, and p_i is the fraction of the total weight of sediment in the sample that is in size class i. Second, $A(z)$ has been replaced by A', which was accomplished by replacing in equation 3 the concentration, C, as grams of fluorescent tracer per gram of sediment by C', the concentration as

number of fluorescent particles per gram of sediment. Third, the integration across the channel width has been accomplished by the averaging effect of compositing a set of samples taken across the weir; hence the transport rate, Q_{si}, is the total transport rate for size class i for the cross section, and the concentration is a mean concentration, indicated by the overbar, for the cross section. Details of the development of equation 11 and a discussion of the two assumptions are presented in appendix C.

The variation with time of $\bar{C}'$ for the three colors of quartz used in run 1 and the quartz, garnet, and monazite tracers used in run 2 are presented in figures 28 and 29, respectively. The concentrations plotted in figures 28 and 29 are relative concentrations, $\bar{C}'_r(t)$; that is, each concentration for a given color or specific gravity has been divided by the area under the curve A'. Thus, $\bar{C}'_r(t)$ is equal to $\bar{C}'(t)/A'$ where A' is defined by equation 12.

The sediment-transport rates for the different sieve classes of fluorescent quartz were calculated from equation 11, and the results are summarized in tables 12 and 13 for runs 1 and 2, respectively. The N values were determined from the quantities of fluorescent materials injected (table 2) and the numbers of fluorescent particles per gram of fluorescent material (table 6). The p_i values were determined from the sieve-size distributions for the depth-integrated samples (fig. 41). The A' values were determined for each color of fluorescent quartz tracer by plotting $\bar{C}'$ as a function of time and measuring the area under the curve with a planimeter (figs. 28 and 29).

TABLE 12.—*Summary of the calculation of the sediment-transport rate, depth-integrated samples at the weir, run 1*

Color of quartz	Sieve class (mm)	Q_s (calculated) (tons per day)	Q_s (measured) (tons per day)
Green	0.125–0.177	2,403	1,515
	0.177–0.250	1,889	1,191
	0.250–0.350	1,463	922
Yellow	0.250–0.350	451	922
	0.350–0.500	174	357
	0.500–0.707	16	33
Red	0.500–0.707	3	33
	0.707–1.00	0	0
	>1.00	0	0
Total (maximum)		5,945	4,018
(minimum)		4,920	.....

TABLE 13.—*Summary of the calculation of the sediment-transport rate, depth-integrated samples at the weir, run 2*

Quartz sieve class (mm)	Q_s (calculated) (tons per day)	Q_s (measured) (tons per day)
0.088–0.125	890	1,013
0.125–0.177	1,050	1,194
0.177–0.250	824	937
0.250–0.350	627	713
0.350–0.500	178	203
0.500–0.707	22	25
0.707–1.00	0	0
Total	3,591	4,085

In run 1, only the three sieve classes of each of the three colors contributed a significant number of fluorescent particles to the total number of particles of each color injected. As with the calculation of the sediment-transport rate from the "dustpan" sample concentrations, two answers were possible because of the overlap of the green and yellow 0.250- to 0.350-mm sieve classes and the yellow and red 0.500- to 0.707-mm sieve classes. The maximum of the two calculated results is about 48 percent larger, and the minimum is about 22 percent larger, than the sediment-transport rate measured at the weir. The big difference between the two calculated values is caused by the large difference between the sediment-transport rates predicted for the 0.250- to 0.350-mm sieve class of green quartz and the 0.250- to 0.350-mm sieve class of yellow quartz.

There is some basis for selecting the minimum of the two results as the more accurate. The results presented in table 1 show that the median fall diameter of the 0.250- to 0.350-mm sieve class of the yellow quartz was essentially identical with that of the natural bed material, whereas the median diameter of the 0.250 to 0.350-mm sieve class of the green quartz was about 17 percent smaller. This suggests that the 0.250- to 0.350-mm sieve class of the yellow quartz is the better of the two "tracers" for the 0.250- to 0.350-mm sieve class of the natural bed material. Large differences exist among the median fall diameters for the 0.500- to 0.707-mm sieve classes of yellow and red quartz and the natural bed material. Of the yellow and red quartz fall diameters, the red quartz median fall diameter is nearest to the median fall diameter of the natural bed material. The contribution of this sieve class to the total sediment-transport rate is less than 1 percent, however.

In run 2, the 0.088- to 0.125-mm sieve class contributed almost 6 percent of the total number of quartz tracer particles injected. Therefore, it was necessary to consider this sieve class in addition to the six sieve classes that were considered in the analysis of the "dustpan" samples. The problem of differentiating between the small particles and chips or flakes of dye from the large particles could not be eliminated but was reduced as much as possible by careful counting of the fluorescent particles in the depth-integrated samples. The calculated sediment-transport rate for particles larger than 0.088 mm was about 12 percent smaller than the sediment-transport rate measured at the weir.

Because of the two assumptions necessary in the analysis of the fluorescent tracer concentrations of the

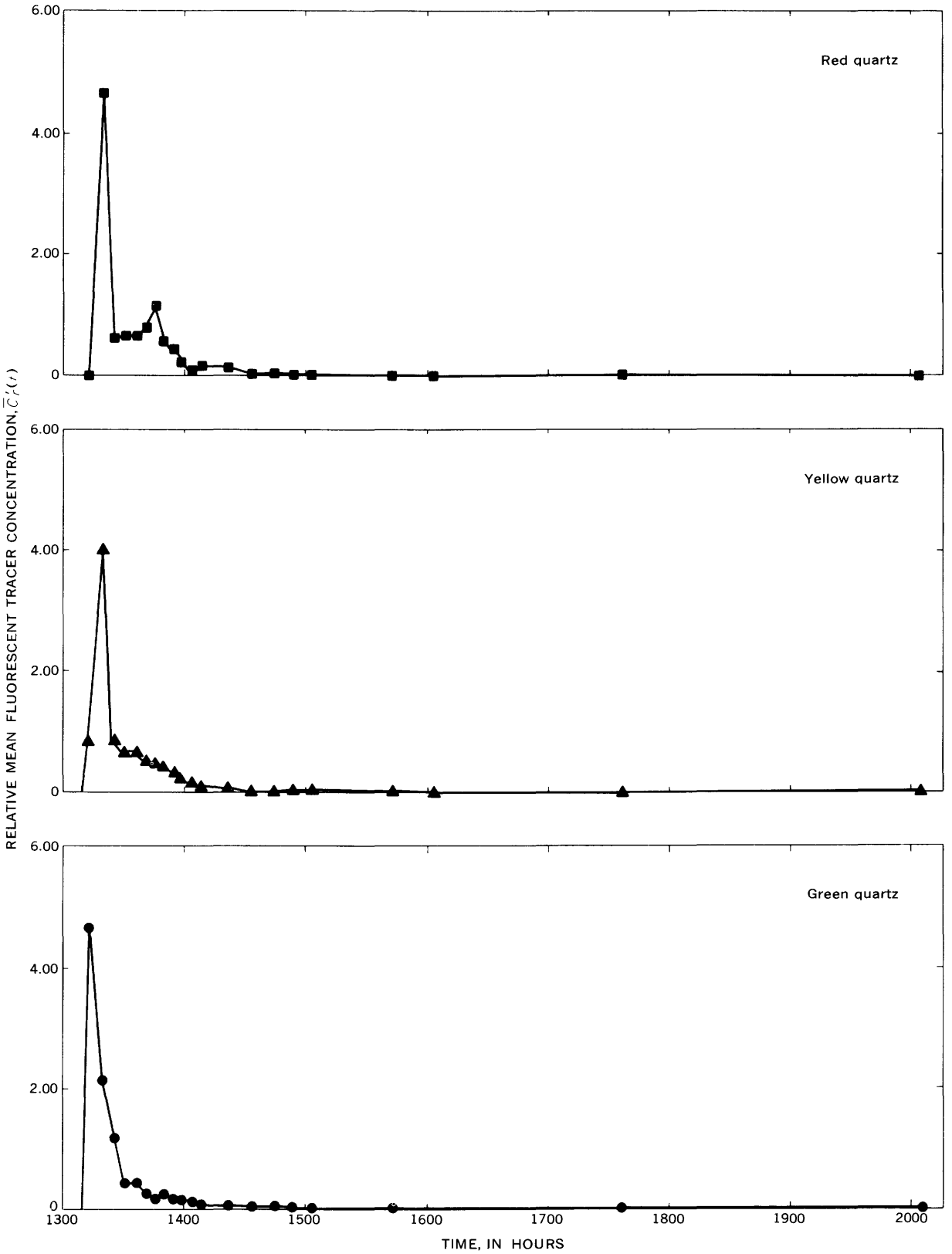

FIGURE 28.—Variation with time of the relative mean fluorescent tracer concentrations of the depth-integrated samples at the weir, run 1.

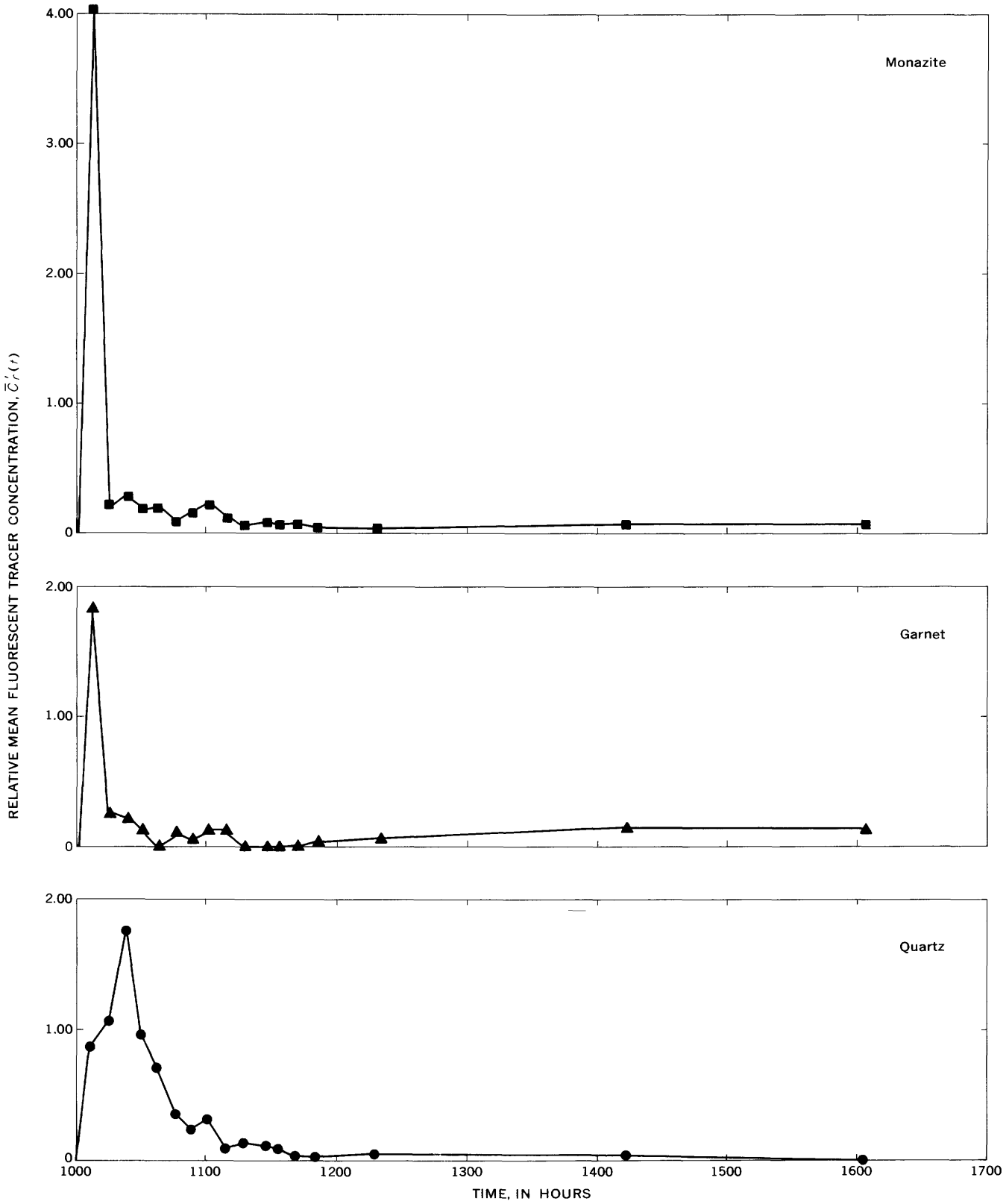

FIGURE 29.—Variation with time of the relative mean fluorescent tracer concentrations of the depth-integrated samples at the weir, run 2.

depth-integrated samples, the ratio of the measured-to-calculated sediment-transport rates for each sieve class of a specific color of tracer was a constant. This can be shown as follows. The measured sediment-transport rate for size class i is

$$Q_{s_i}\,(\text{measured}) = Q_s p_i, \tag{13}$$

where Q_s is the total measured sediment-transport rate. The ratio for size class i is

$$\frac{Q_{s_i}\,(\text{measured})}{Q_{s_i}\,(\text{calculated})} = \frac{Q_s A'}{N}. \tag{14}$$

For a specific color of fluorescent tracer in a specific experiment, all the factors on the right-hand side of equation 14 are constant, and thus the ratio of Q_{s_i} (measured)/Q_{s_i} (calculated) is constant for all size classes.

VELOCITIES OF THE CENTROIDS OF THE TRACER MASSES

The velocities of the centroids of the tracer masses were determined from the data of mean concentration, $\bar{C}$, versus time from cross section D.

The data of fluorescent tracer concentration versus time for each sieve class at the various lateral positions at cross section D were combined to give the mean concentration, $\bar{C}(t)$. The mean concentration for a specific sieve class at time t is given by

$$\bar{C}(t) = \frac{\sum_{z=0}^{z=B} C(z, t)\Delta z}{B}, \tag{15}$$

where $C(z, t)$ is the concentration at time t at lateral position z where z is measured from the right bank, Δz is the width increment over which $C(z, t)$ is assumed to be the concentration, and B is the channel width.

In run 1, the sampling positions were not equally spaced, and one position near the centerline was omitted through an error in sampling procedure. As a result, the sampling position was not always at the center of the Δz increment. The maximum displacement of a sampling position from the center of a width increment was 2 feet for the two center sampling positions. Because the positioning of the samplers at the different sample times was subject to an error of the order of ± 0.5 foot, the 2-foot displacement is not considered significant. Thus, equation 15 for run 1 is

$$\bar{C}(t) = \frac{10C_7(t) + 8C_{17}(t) + 10C_{23}(t) + 10C_{37}(t)}{79} + \frac{9C_{43}(t) + 12C_{55}(t)}{79}, \tag{16}$$

where 79 is the channel width, in feet, at cross section D.

In run 2, the sampling locations were equally spaced at 6-foot intervals and equation 15 for run 2 has the form

$$\bar{C}(t) = \frac{6[C_{18}(t) + C_{24}(t) + C_{30}(t) + C_{36}(t) + C_{42}(t)}{79} + \frac{6[C_{48}(t) + C_{54}(t) + C_{60}(t)]}{79}. \tag{17}$$

The mean concentrations at cross section D for the various sieve classes and specific gravities of tracer materials were calculated from equations 16 and 17 for runs 1 and 2, respectively.

The mean concentration values calculated from equations 16 and 17 were normalized by dividing by the area under the curve of mean concentration versus time to give a relative mean concentration. The relative mean concentration, $\bar{C}_r$, is defined by

$$\bar{C}_r(t) = \frac{\bar{C}(t)}{\int_0^\infty \bar{C}(t)dt}. \tag{18}$$

The relative mean concentration values as a function of time for the various sieve classes of quartz tracers used in run 1 are presented in figures 30, 31, and 32.

The relative mean concentration values as a function of time for the quartz, garnet, and monazite tracers used in run 2 are presented in figures 33, 34, and 35, respectively.

The centroid velocities were calculated from

$$\bar{V} = \frac{700}{(\bar{t} - \Delta t)3600}, \tag{19}$$

where $\bar{V}$ is the velocity of the centroid of the tracer mass, in feet per second; 700 is the distance, in feet, between the injection point and cross section D; $\bar{t}$ is the mean time, in hours, or the time required for the centroid of the tracer mass to move from the injection point to cross section D; and Δt is the time difference, in hours, between the start of the experiment and the mean injection time for a given sieve class or specific gravity of tracer material.

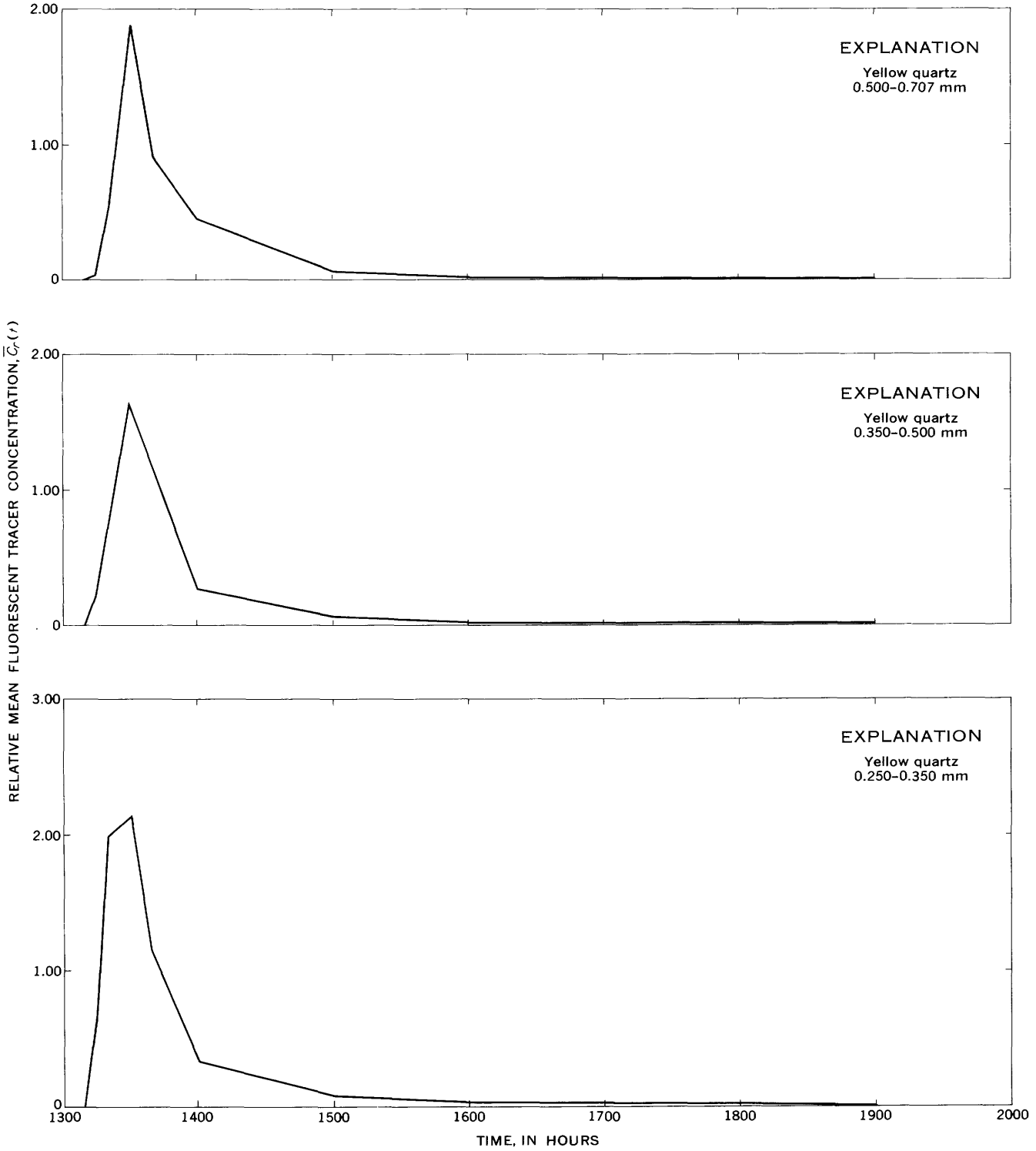

FIGURE 30.--Variation with time of the relative mean concentration at cross section D of the 0.250- to 0.350-mm, 0.350- to 0.500-mm, and 0.500- to 0.707-mm sieve classes of yellow quartz, run 1.

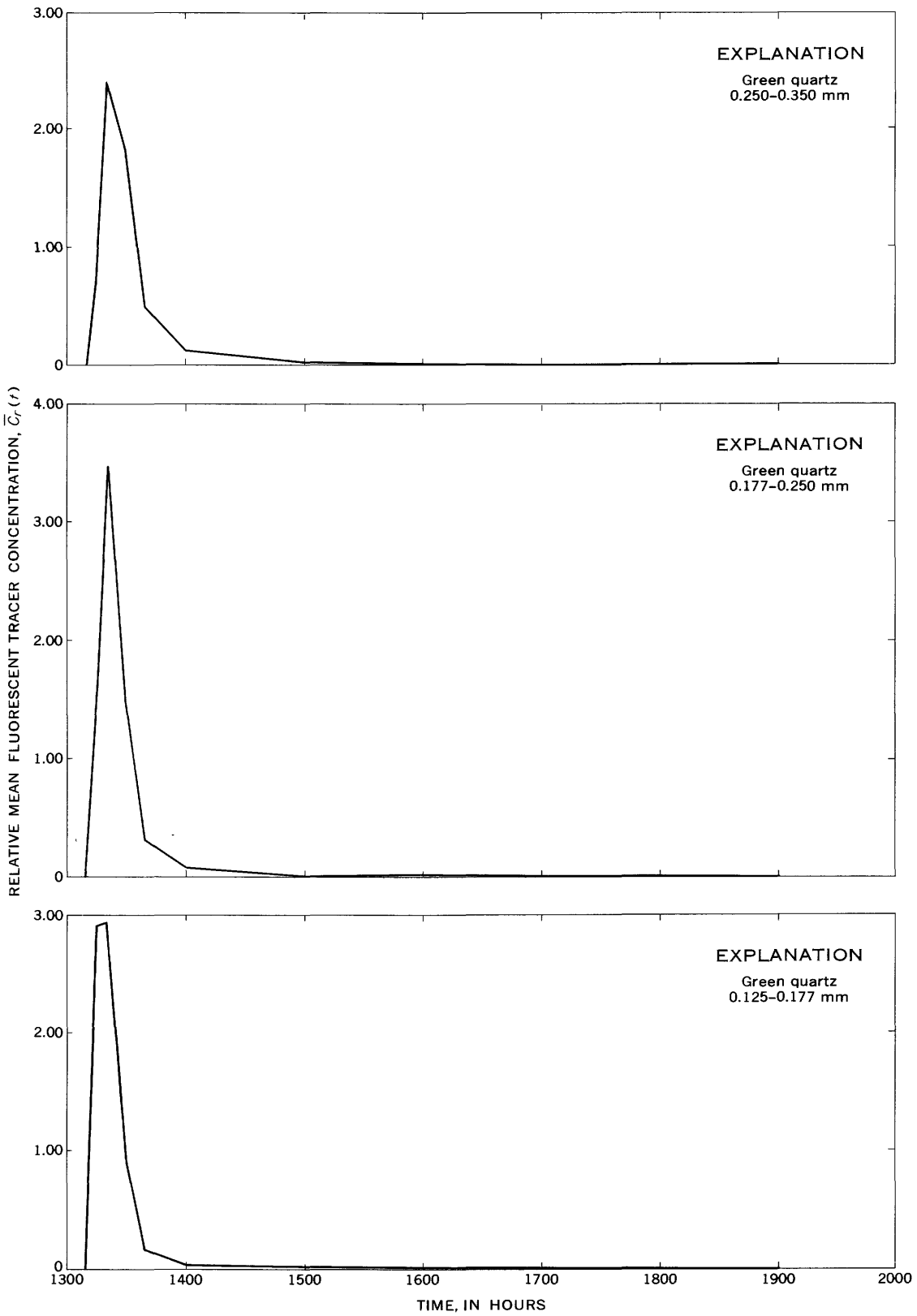

FIGURE 31.—Variation with time of the relative mean concentration at cross section D of the 0.125- to 0.177-mm, 0.177- to 0.250-mm, and 0.250- to 0.350-mm sieve classes of green quartz, run 1.

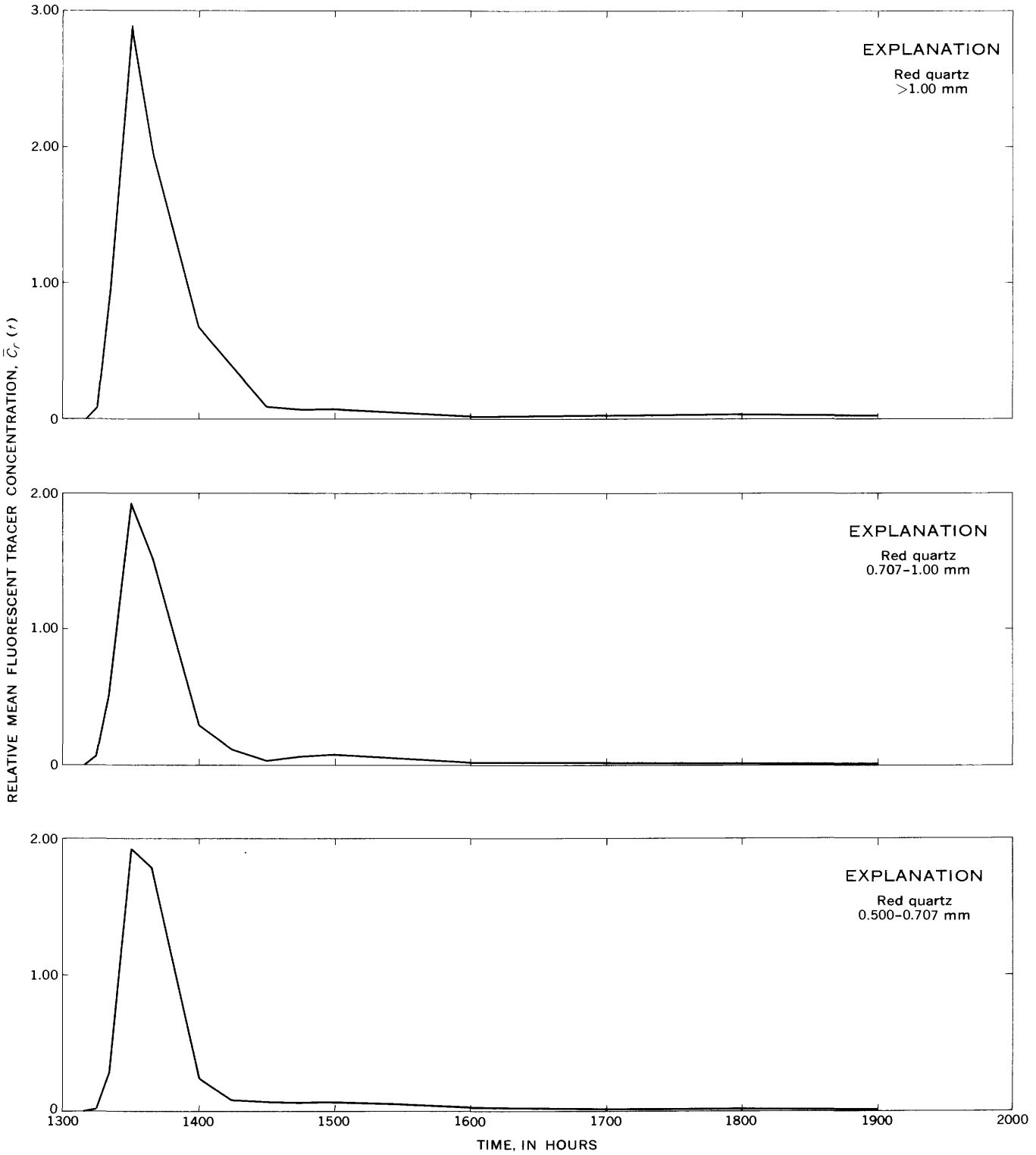

FIGURE 32.—Variation with time of the relative mean concentration at cross section D of the 0.500- to 0.707-mm, 0.707- to 1.00-mm, and > 1.00-mm sieve classes of red quartz, run 1.

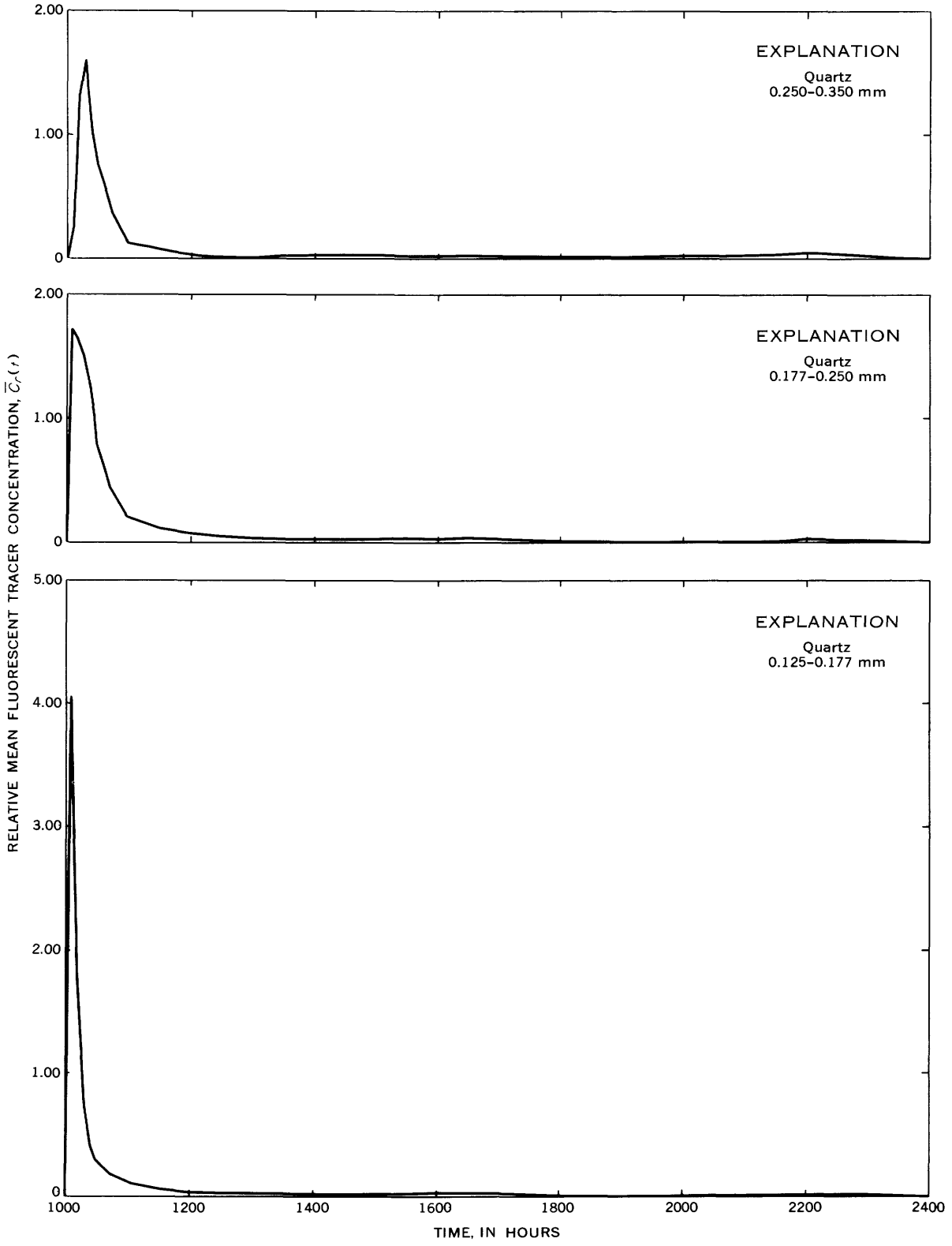

FIGURE 33.—Variation with time of the relative mean concentration

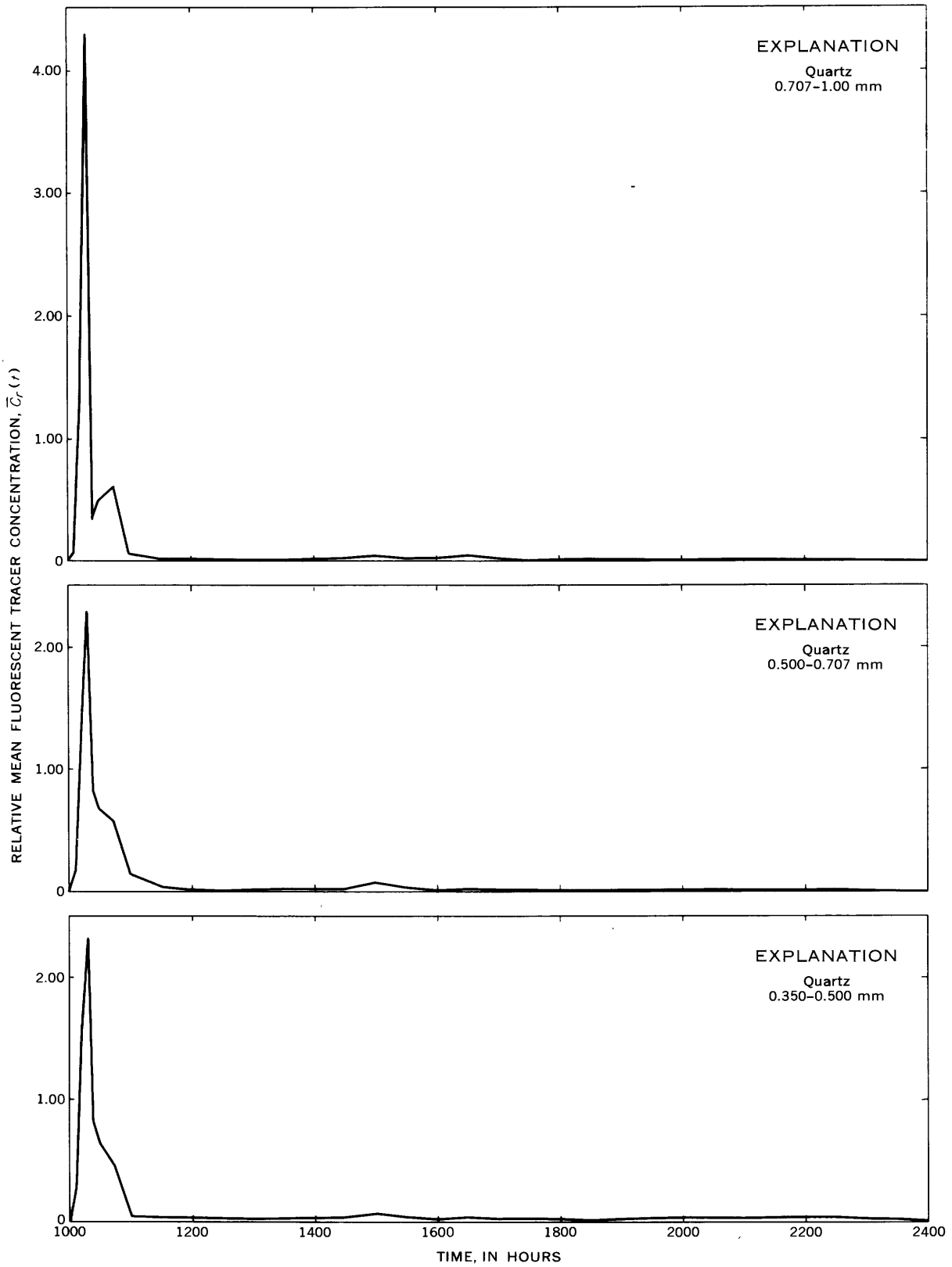

at cross section *D* of the six sieve classes of quartz tracer, run 2.

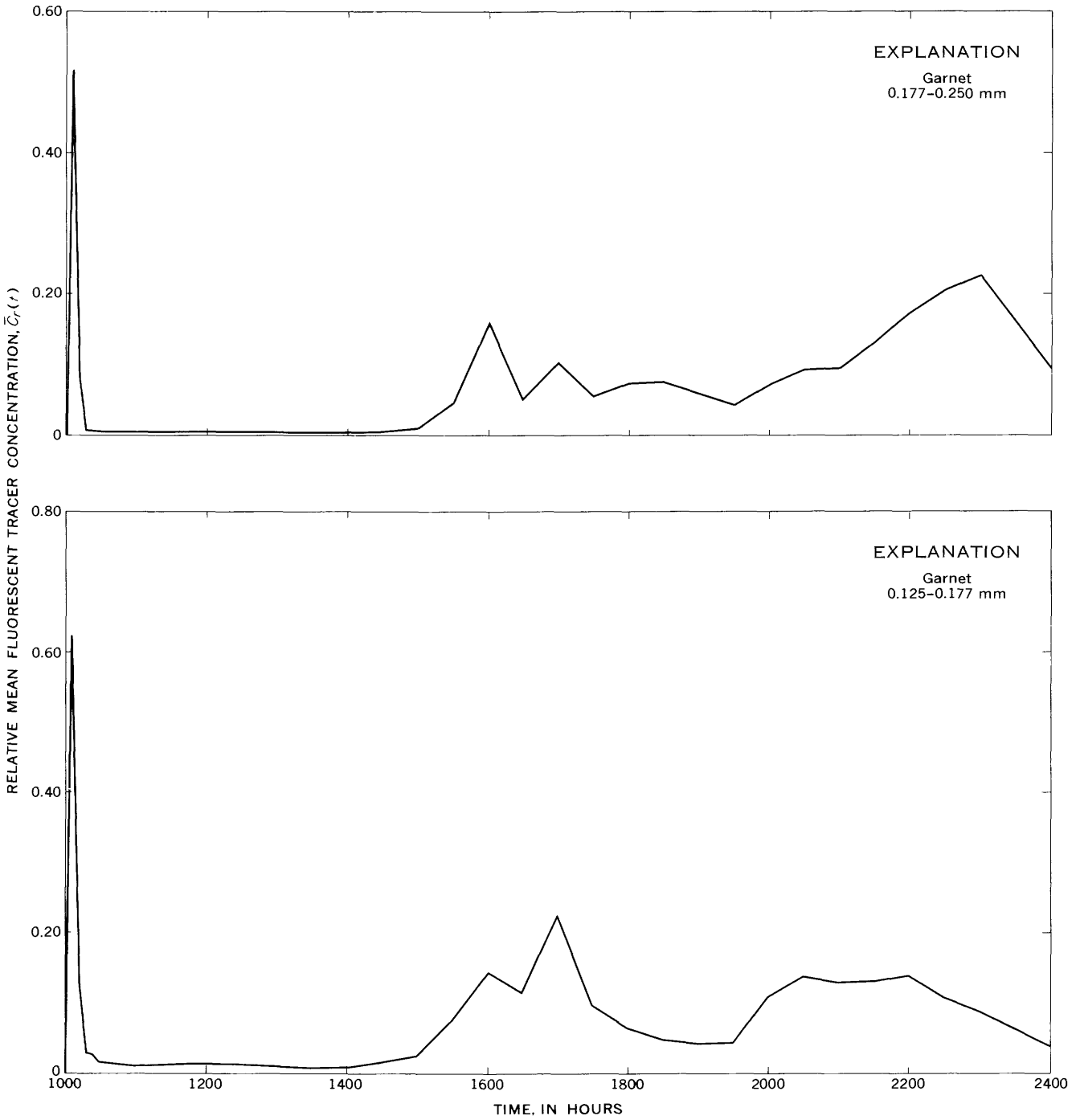

FIGURE 34.—Variation with time of the relative mean concentration at cross section *D* of the five sieve classes of garnet tracer, run 2 (classes 3–5 on opposite page).

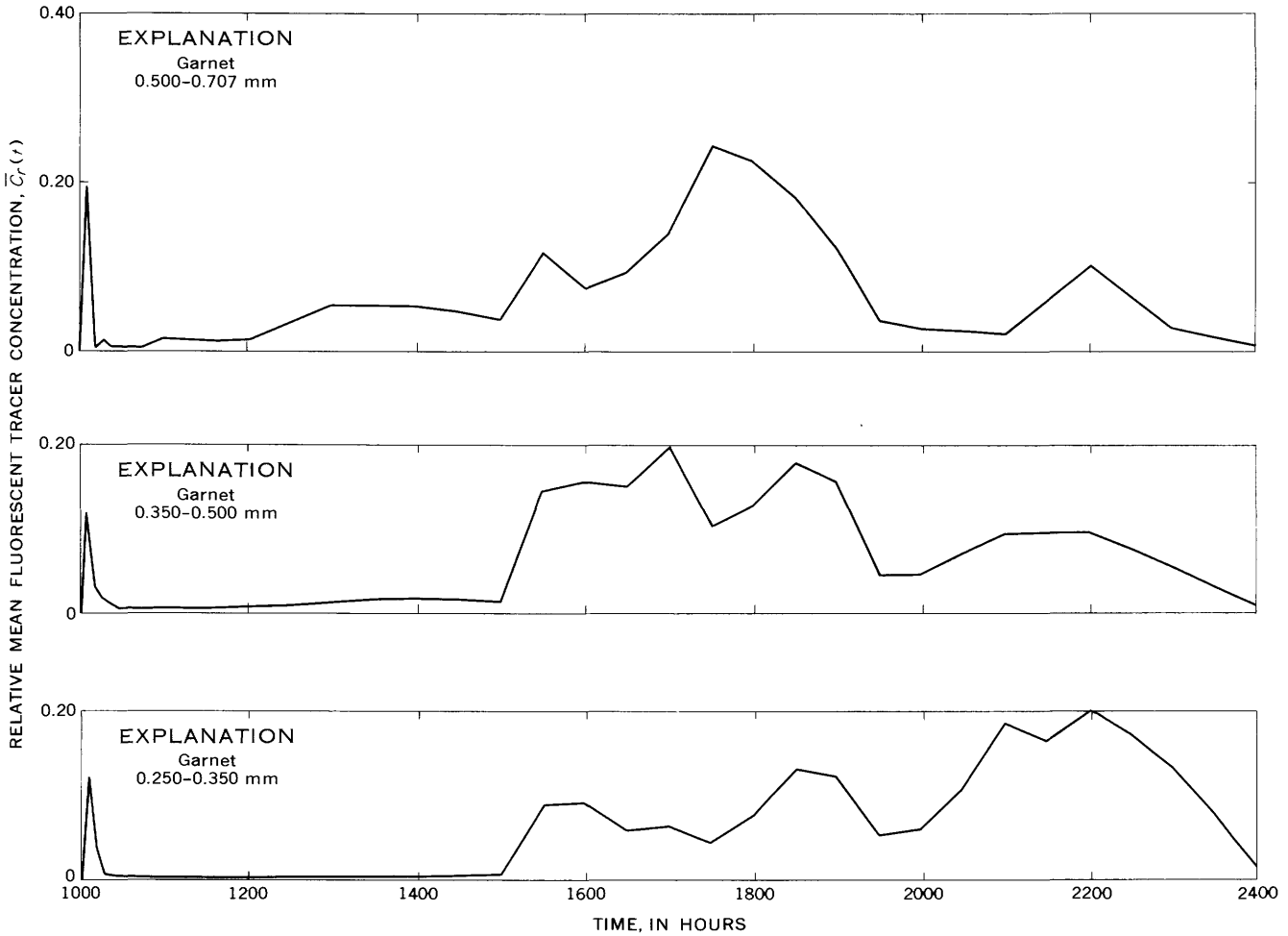

The mean time, or $\bar{t}$ values, were calculated from

$$\bar{t}=\frac{\int_0^\infty t\bar{C}(t)dt}{\int_0^\infty \bar{C}(t)dt}=\int_0^\infty t\bar{C}_r(t)dt, \qquad (20)$$

where $\bar{C}$ is the mean concentration at cross section D as calculated from equation 15. The times, t and $\bar{t}$, are relative to the time at which the experiment was begun.

Mean time values were calculated from equation 20 for each sieve class and specific gravity of tracer material. The integrals were evaluated by measuring the areas under the appropriate curves with a planimeter. For the purpose of standardizing the calculations, the $\bar{C}(t)$ as a function of t curves for the different sieve classes and specific gravities were truncated at the time at which the mean concentration for a particular sieve class decreased to 1.0 percent of the maximum mean concentration for that sieve class. The initial sharp peaks in the garnet and monazite curves (figs. 34 and 35) were disregarded in the determination of the maximum mean concentrations. For the quartz tracers these times occurred within the duration of both of the experimental runs. For the garnet and monazite tracers used in run 2, an extrapolation was required. The maximum extrapolation required was 2.0 hours for the 0.177- to 0.250-mm sieve class of garnet. The mean extrapolation time for the five sieve classes of garnet and the four sieve classes of monazite was 0.67 hour, or about 5 percent of the total time interval of run 2.

The calculation of the centroid velocities from equation 19 requires some justification because this equation assumes that the fluorescent tracer materials were deposited on the bed of the channel at the injection point. However, because the fluorescent tracer materials were dumped at the water surface, they were carried some distance downstream by the flow before deposition on the channel bed. Loyacano (1967) found in some qualitative experiments that the initial fall velocity of groups of particles was four to seven times larger than the fall velocity of the single particles because of the tendency of the particles to fall as a group. Because of the very large injection rates used in the fluorescent tracer experiments and because of the relatively shallow depth of flow in the study reach (less than 3 feet), it was assumed on the basis of Loyacano's work that the tracer

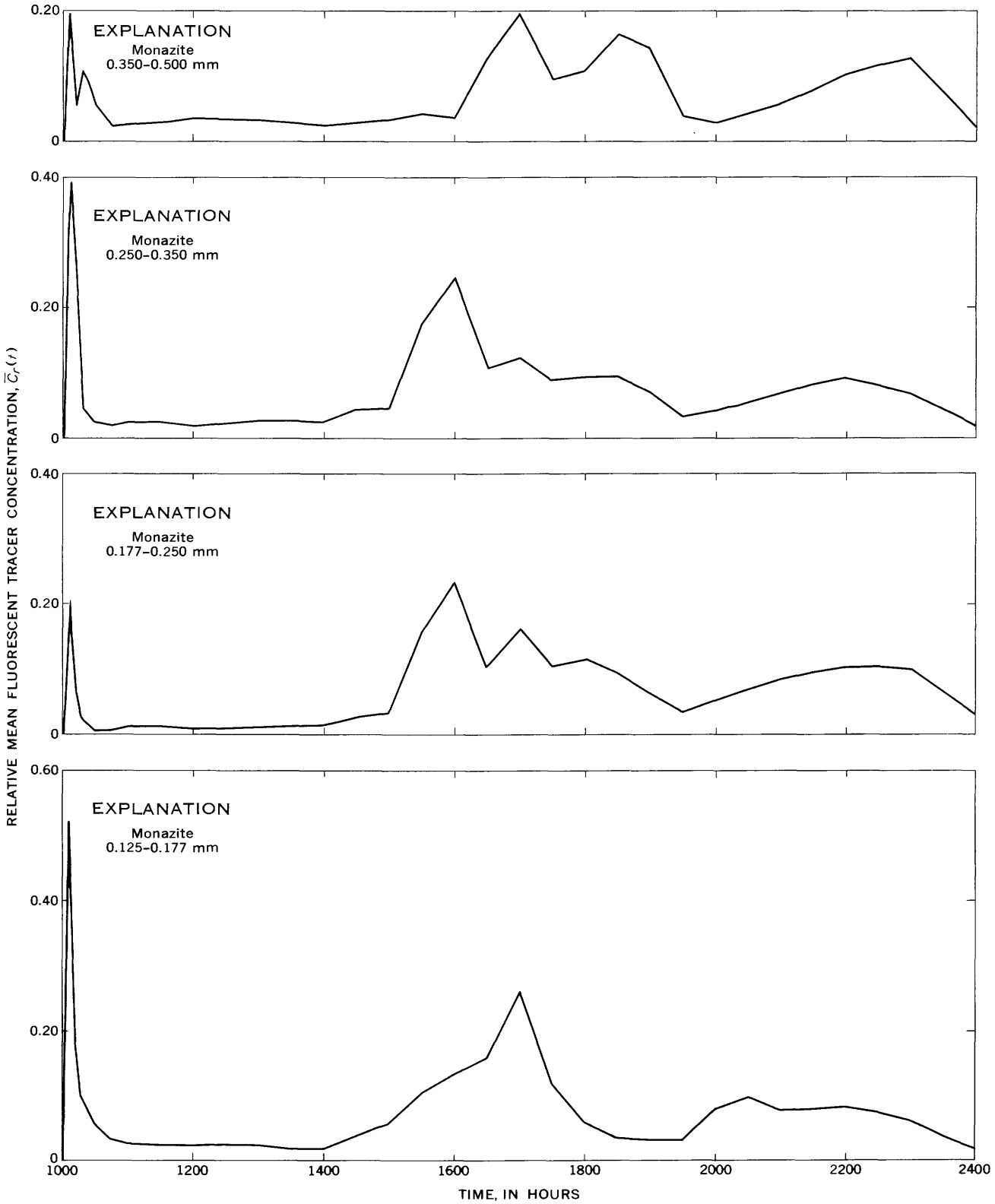

FIGURE 35.—Variation with time of the relative mean concentration at cross section D of the four sieve classes of monazite tracer, run 2.

materials fell rapidly to the bed surface. Hence, the distance traveled by the fluorescent material before deposition on the bed surface was assumed negligible with respect to the 700 feet between the injection point and cross section D.

The centroid velocities calculated from equation 19 and the $\bar{t}$, Δt, and the $t_{0.01}$ values are summarized in tables 14 and 15 for runs 1 and 2, respectively. The $t_{0.01}$ value is the time interval required for the mean concentration at cross section D to decrease to 1.0 percent of the maximum mean concentration.

The centroid velocities for the various sieve classes are plotted as a function of median fall diameters of the sieve classes in figures 36 and 37 for runs 1 and 2, respectively. The vertical dashed lines represent the size limits of the sieve class used in the analysis of the samples, and the numbers correspond to the sieve-class numbers given in the tables.

TABLE 14.—*Summary of the* t, Δt, $t_{0.01}$, *and* $\bar{V}$ *data, run 1*

Color	Sieve class (mm)	Median fall diameter (mm)	$t_{0.01}$ (hours)	$\bar{t}$ (hours)	Δt (hours)	$\bar{V}$ (fps)
Green	(1) 0.125–0.177	0.150	1.33	0.183	0.023	1.22
	(2) 0.177–0.250	.189	1.58	.273	.023	.778
	(3) 0.250–0.350	.231	1.92	.320	.023	.655
Yellow	(3) 0.250–0.350	.271	3.53	.596	.062	.364
	(4) 0.350–0.500	.358	2.78	.558	.062	.392
	(5) 0.500–0.707	.452	2.63	.593	.062	.366
Red	(5) 0.500–0.707	.539	2.65	.565	.096	.415
	(6) 0.707–1.00	.613	2.67	.564	.096	.415
	(7) > 1.00	.839	2.58	.546	.096	.432

TABLE 15.—*Summary of the* t, Δt, $t_{0.01}$, *and* $\bar{V}$ *data, run 2*

Mineral	Sieve class (mm)	Median fall diameter (mm)	$t_{0.01}$ (hours)	$\bar{t}$ (hours)	Δt (hours)	$\bar{V}$ (fps)
Quartz	(1) 0.125–0.177	0.152	1.85	0.310	0.017	0.664
	(2) 0.177–0.250	.204	7.37	1.55	.017	.127
	(3) 0.250–0.350	.289	7.00	.992	.017	.199
	(4) 0.350–0.500	.420	5.50	.952	.017	.208
	(5) 0.500–0.707	.541	1.97	.521	.017	.385
	(6) 0.707–1.00	.694	1.20	.401	.017	.506
Garnet	(1) 0.125–0.177	.232	15.3	8.70	.043	.0224
	(2) 0.177–0.250	.300	16.0	10.22	.043	.0191
	(3) 0.250–0.350	.405	14.4	9.84	.043	.0198
	(4) 0.350–0.500	.578	14.3	8.24	.043	.0237
	(5) 0.500–0.707	.690	14.4	7.39	.043	.0264
Monazite	(1) 0.125–0.177	.235	14.4	7.20	.061	.0272
	(2) 0.177–0.250	.305	14.6	8.35	.061	.0235
	(3) 0.250–0.350	.484	14.4	7.52	.061	.0261
	(4) 0.350–0.500	.721	14.3	8.15	.061	.0240

Curves for the quartz tracer materials of runs 1 and 2 having the centroid velocity as a function of median fall diameter are similar in shape. The curves are approximately U-shaped, with the maximum velocities occurring for the smallest particles and the minimum velocities occurring for those particles with fall diameters approximately the same as or slightly larger than the fall diameters of the natural bed-material particles comprising the largest part of the bed-material transport. The maximum centroid velocities observed were for the 0.125- to 0.177-mm sieve class of quartz tracer, and these were approximately 26 and 16 percent of the mean water velocity in runs 1 and 2, respectively.

In run 1, the centroid velocities for the large particles were only slightly larger than the minimum centroid velocity. In run 2, however, the centroid velocity for the 0.707- to 1.00-mm sieve class was about four times larger than the minimum centroid velocity and was about 76 percent of the centroid velocity for the 0.125- to 0.177-mm sieve class of quartz tracer. This large increase of the centroid velocity with fall diameter for the large particles in run 2 can be explained by the fact that the large particles project into the flow more than the small particles. Other investigators (Chang, 1939; Sundborg, 1956; Meland and Norrman, 1966) have noted and discussed the tendency for the large particles to move with the largest velocity. It is expected that the particle velocity for a specific flow condition will continue to increase with particle fall diameter until the effect of increasing surface exposed to the flow, proportional to the square of the particle diameter, is exceeded by the effect of increasing mass, proportional to the cube of the diameter. Above this size, the velocity of the particle will decrease with increasing diameter.

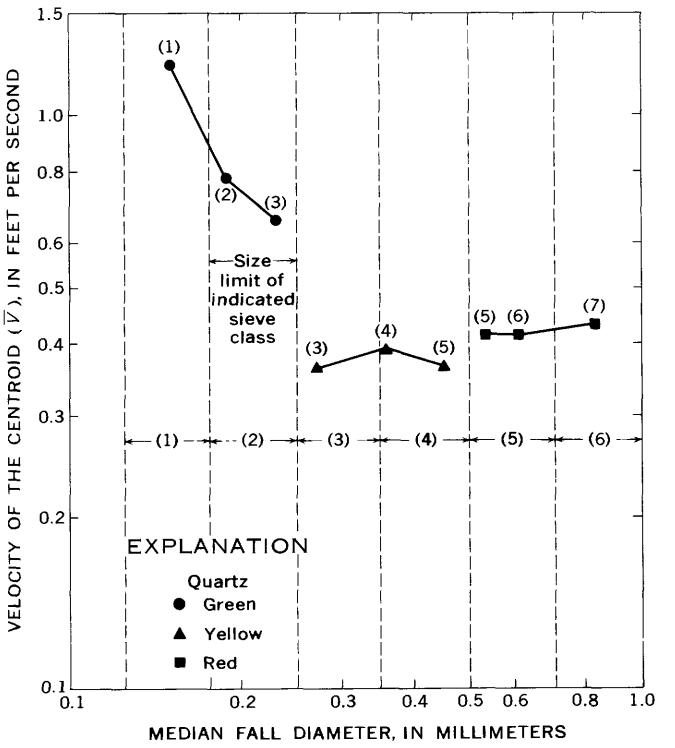

FIGURE 36.—Variation with fall diameter of the velocities of the centroids of the tracer masses, run 1. Numbers in parentheses are sieve class numbers; see tables 7 and 8.

The observation that the centroid velocities for the large red quartz particles in run 1 were only slightly larger than the minimum centroid velocity can be explained by the fact that these particles moved toward the right bank and some were trapped temporarily. This would cause the centroid velocities of the red quartz particles to be less than if these particles had moved down the center of the channel without interference.

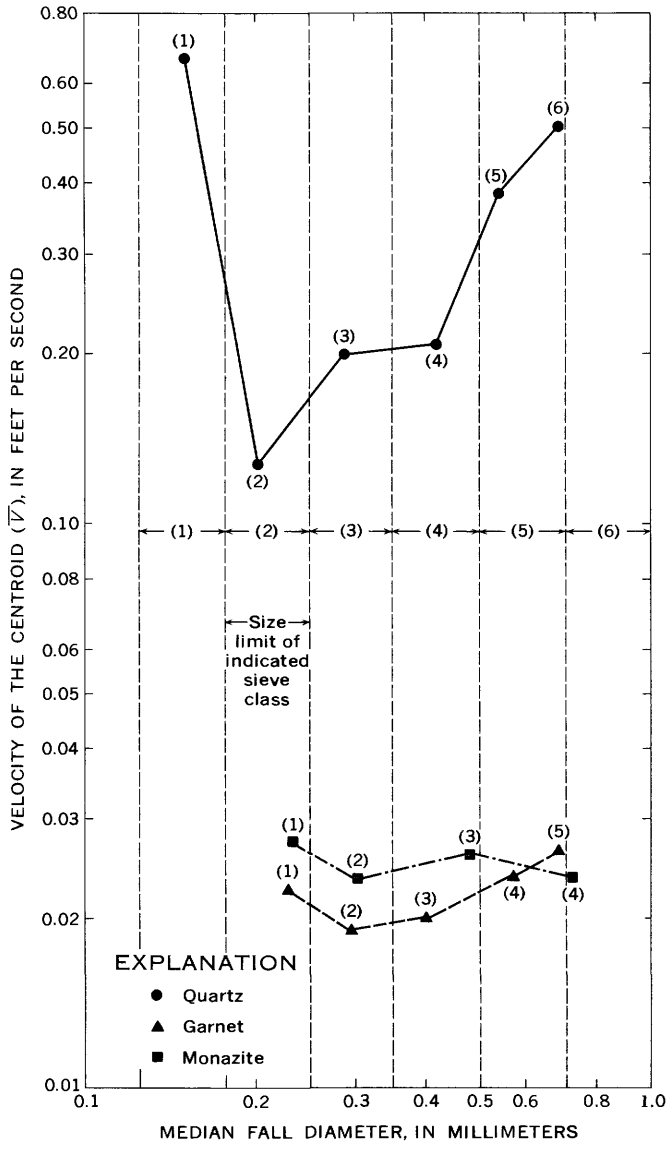

FIGURE 37.—Variation with fall diameter of the velocities of the centroids of the tracer masses, run 2. Numbers in parentheses are sieve class numbers; see tables 7 and 8.

Centroid velocities for the small particles were large in both runs because these particles apparently spent a greater proportion of the time moving as suspended material than did the natural bed-material particles composing the largest part of the bed-material transport. It is expected that the centroid velocity will continue to increase for decreasing particle fall diameter until the silt and clay size ranges are reached where the particles move with the mean water velocity.

The curve of centroid velocity versus fall diameter for the garnet was also U-shaped, but that of the monazite showed little relation to fall diameter. Also, the centroid velocities were about an order of magnitude less than the centroid velocities for the quartz. The concept of hydraulic equivalence (Rubey, 1933, Rittenhouse, 1943) suggests that particles having equal fall diameters tend to be of equivalent hydraulic value. The centroid velocities in figure 37 are plotted as a function of median fall diameter; hence, it would appear that the concept of hydraulic equivalence was not applicable to the comparison of the centroid velocities of quartz, garnet, and monazite for the high-velocity flat-bed condition.

However, if the difference between the behavior of the quartz particles and the heavy-mineral particles is attributed to the specific gravity effect, then the question may be asked as to why the denser, monazite particles moved about 20 percent faster than the garnet particles for the most of the fall-diameter range. The monazite was about 17 percent denser than the garnet, and the garnet was about 54 percent denser than the quartz. Because the difference in specific gravity between the garnet and monazite was small, the apparent anomaly may have been caused by shape differences.

None of the lead tracer particles were found in any of the "dustpan" samples at cross section *D*. The last set of samples was obtained 22 hours after injection; hence, the centroid velocity of the lead particles was something less than $700/22 \times 3600$, or 0.0088 foot per second. However, the centroid of the 0.707- to 1.00-mm sieve class of quartz tracer particles, which has a median fall diameter only slightly smaller than the median fall diameter of the 0.177- to 0.250-mm sieve class of lead (see table 1), moved through cross section *D* about 0.4 hour after injection of the fluorescent materials. This corresponds to a centroid velocity of 0.506 foot per second. As before, it would appear that the concept of hydraulic equivalence was not applicable to the comparison of the centroid velocities of quartz and lead-tracer particles of comparable fall diameter for the high-velocity flat-bed condition.

Approximately fifty 6-inch core samples were obtained over about the center third of the channel at cross sections *A*, *B*, *C*, and 15, 40, and 65 feet downstream from the injection point. These samples were obtained about 21.5 hours after the injection of the fluorescent tracer materials in run 2 and were divided into two 3-inch segments. These samples, both the top and bottom segments, contained essentially no quartz tracer particles. Two of the top segments contained an appreciable number of

garnet and monazite particles, and six top segments contained a few garnet and monazite particles. All the other segments of the core samples contained very few fluorescent particles. These results indicate that there was no general tendency for either the quartz or the heavy-mineral tracer particles to be exchanged with that part of the bed material not in transport. This is in agreement with the observation that the bed surface below the moving layer of sediment for the flat-bed condition of alluvial-channel flow is very firm.

LONGITUDINAL-DISPERSION CHARACTERISTICS OF THE TRACER MATERIALS

The longitudinal-dispersion coefficient, K_x, can be calculated from the rate of change of the variance of the concentration as a function of time curve with distance downstream (Sayre and Chang, 1968). In the fluorescent tracer experiments, meaningful data were obtained only at cross section *D* because of the rapid rate at which the tracer material moved through the study reach. Therefore, a true longitudinal-dispersion coefficient could not be calculated. However, the variance, σ_t^2, of the mean concentration as a function of time curves for the different sieve classes and specific gravities at cross section *D* was used as a measure of the longitudinal dispersion between the injection point and cross section *D*. For a valid comparison, this procedure assumes that the initial period required for the establishment of the linear variation of the variance with distance is the same for all sieve classes and specific gravities of tracer minerals.

The variance, σ_t^2, is given by

$$\sigma_t^2 = \frac{\int_0^\infty t^2 \bar{C}(t)\,dt}{\int_0^\infty \bar{C}(t)\,dt} - \bar{t}^2, \qquad (21)$$

where $\bar{t}$ is given by equation 20. The integrals were evaluated by measuring the areas under the appropriate curves with a planimeter. As in the $\bar{t}$ calculations, the $t^2\bar{C}$ versus t curves were truncated at the times at which the mean concentration decreased to 1.0 percent of the maximum mean concentration. These time values, designated $t_{0.01}$, are summarized in tables 14 and 15 for runs 1 and 2, respectively.

The variances of the curves of mean concentration at cross section *D* versus time were calculated from equation 21, and the values for the various sieve classes and specific gravities are summarized in tables 16 and 17 for runs 1 and 2, respectively. The variances are plotted as a function of the median fall diameters of the sieve classes in figures 38 and 39 for runs 1 and 2, respectively. The vertical dashed lines represent the size limits of the sieve classes, and the numbers correspond to the sieve-class numbers given in the tables.

TABLE 16.—*Summary of the σ_t^2 values of the mean concentration at cross section* D *as a function of time data, run 1*

Color	Sieve class (mm)	σ_t^2 (hours^2)
Green	(1) 0.125–0.177	0.0358
	(2) 0.177–0.250	.0455
	(3) 0.250–0.350	.0810
Yellow	(3) 0.250–0.350	.356
	(4) 0.350–0.500	.200
	(5) 0.500–0.707	.165
Red	(5) 0.500–0.707	.149
	(6) 0.707–1.00	.170
	(7) >1.00	.153

TABLE 17.—*Summary of the σ_t^2 values of the mean concentration at cross section* D *as a function of time data, run 2*

Mineral	Sieve class (mm)	σ_t^2 (hours^2)
Quartz	(1) 0.125–0.177	0.120
	(2) 0.177–0.250	3.35
	(3) 0.250–0.350	2.23
	(4) 0.350–0.500	1.70
	(5) 0.500–0.707	.0762
	(6) 0.707–1.00	.0423
Garnet	(1) 0.125–0.177	12.9
	(2) 0.177–0.250	11.6
	(3) 0.250–0.350	8.25
	(4) 0.350–0.500	7.73
	(5) 0.500–0.707	8.86
Monazite	(1) 0.125–0.177	13.0
	(2) 0.177–0.250	10.3
	(3) 0.250–0.350	11.4
	(4) 0.350–0.500	13.3

The variation of the variances with fall diameter should be approximately the inverse of the variation of the centroid velocities with fall diameter. This behavior was expected because the more rapidly a slug of tracer material of a specific size moves through the study reach, the less opportunity that slug has for dispersing in the longitudinal direction. Figures 38 and 39 show that the variation of the variance, σ_t^2, with fall diameter for the quartz tracer materials in both runs was approximately the inverse of the variation of the centroid velocities with fall diameter presented in figures 36 and 37.

The maximum σ_t^2 values occurred for particles with diameters approximately the same as or slightly larger than the diameters of the particles comprising the bulk of the natural bed material in transport. Minimum σ_t^2 values occurred for the largest and smallest particles within the fall-diameter range considered. The failure of the σ_t^2 values for the 0.707- to 1.00-mm and >1.00-mm sieve classes of red quartz to continue to decrease with increasing particle diameter (fig. 38) may be explained by the same reasoning applied to the failure of the centroid

velocities for these sieve classes to increase with fall diameter. Both the displacement of the red quartz particles toward the region of small velocities near the bank and the temporary entrapment of some of the red particles along the bank would tend to increase the variance over that expected, had the red quartz particles moved down the center of the channel.

One minor discrepancy in the inverse relation between the σ_t^2 as a function of fall diameter and $\bar{V}$ as a function of fall-diameter curves for the quartz tracer particles in run 2 is that the σ_t^2 values for the 0.500- to 0.707-mm and 0.707- to 1.00-mm sieve classes of the quartz tracer were less than σ_t^2 for the 0.125- to 0.177-mm sieve class of quartz. The centroid velocity of the 0.125- to 0.177-mm sieve class of quartz exceeded the centroid velocities for the 0.500- to 0.707-mm and 0.707- to 1.00-mm sieve classes of quartz, however.

The variances of the garnet and monazite varied with fall diameter in the same manner as the centroid velocities, as a comparison of figures 37 and 39 shows. In each instance, however, the variation of either σ_t^2 or $\bar{V}$ with fall diameter was much less for the garnet and monazite than for the quartz. The centroid velocity and the variance, σ_t^2, for the quartz tracer used in run 2 varied with fall diameter about 420 and 780 percent, respectively, from the minimum to the maximum value. The centroid velocity and the variance for the garnet varied with fall diameter about 38 and 67 percent, respectively, and these

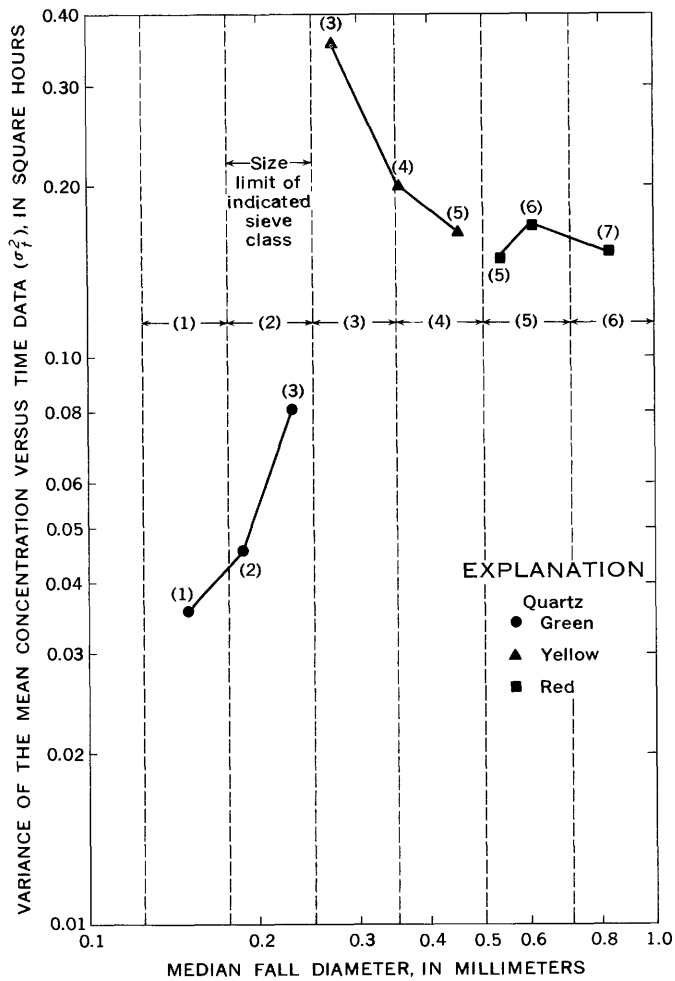

FIGURE 38.—Variation with fall diameter of the variances of the mean concentration as a function of time curves at cross section *D*, run 1. Numbers in parentheses are sieve class numbers; see tables 7 and 8.

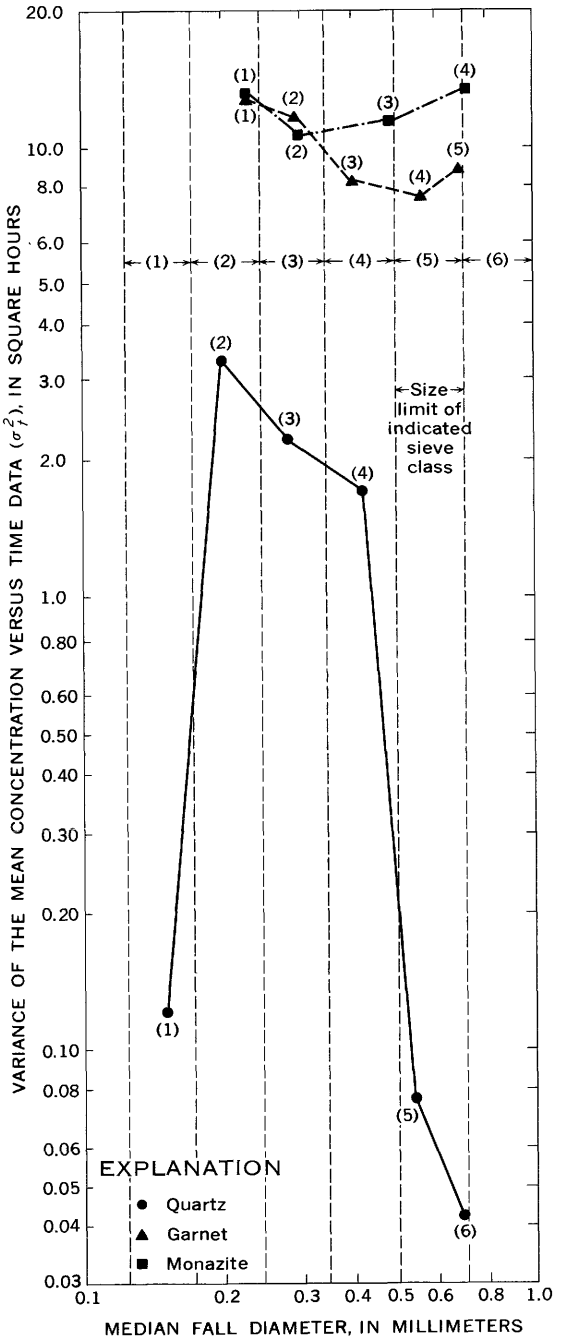

FIGURE 39.—Variation with fall diameter of the variances of the mean concentration as a function of time curves at cross section *D*, run 2. Numbers in parentheses are sieve class numbers; see tables 7 and 8.

quantities for the monazite varied with fall diameter 16 and 33 percent, respectively, from the minimum value to the maximum value. These results and the fact that the σ_t^2 values for garnet and monazite were about an order of magnitude larger than σ_t^2 for quartz particles of comparable fall diameter indicate a distinct difference in behavior between the quartz particles and the garnet and monazite particles. The differences in longitudinal-dispersion characteristics indicated in figure 39 are seen clearly in the relative mean concentration as a function of time plots, figures 33, 34, and 35. One additional difference between figures 37 and 39 is that the σ_t^2 values for garnet generally fall between the values for quartz and monazite, whereas the $\bar{V}$ values for monazite generally fall between the $\bar{V}$ values for quartz and garnet. This difference, however, probably is not significant because of the small differences between these quantities for the garnet and monazite. It is concluded that neither fall diameter nor fall diameter and specific gravity are sufficient to explain the differences in σ_t^2 for the quartz, garnet, and monazite tracers in run 2.

EVALUATION OF THE FLUORESCENT TRACER TECHNIQUE

With the experience gained in the planning and execution of the two experiments and the analysis of the results, it is possible to evaluate the application of the fluorescent tracer technique to studies of sediment movement. Four basic steps are involved in the fluorescent tracer technique. These are the preparation of the tracer materials, the injection of the tracer materials into the study reach, the sampling of the tracer masses as they move through the study reach, and the analysis of the samples.

The first step in the preparation of the tracer materials is to select the material to be coated with the fluorescent dye. At least three different sources of material may be used. The most obvious source is sediment taken from the study reach. This material has the advantage of relatively low cost, but it may have some significant disadvantages. The bed material can range widely in shape and specific gravity for a given sieve size. The use of such material makes it difficult, or impossible, to determine the effect of size alone on sediment velocity or dispersion, if considerable quantities of mica or heavy minerals are present. If one could collect and dye a sample representing the sieve-size distribution of the total sand in transport and then return it to the stream before the size distribution changed, then such a tracer should be excellent for determining sediment-transport rate. However, except under ideal circumstances, this approach is not feasible. Instead, a sample of bed material would normally be used. Such bed material does not truly represent the size, shape, or specific gravity distribution of the sediment in transport. To some extent it represents a lag deposit. The greater the difference in characteristics of bed sediment and sediment in transport, the greater will be the error in estimating the sediment-transport rate.

A second source is material from a different stream. However, such material, unless it closely matches the sediment in the stream under study, is useful mainly for reconnaissance work. Its usefulness in determining the effect of size, shape, and specific gravity on transport will depend on how uniform these characteristics are in a particular sieve size. In this study, coated material from another stream was used for reconnaissance in run 1 because it was available from a previous investigation.

A third source, and probably the best for many research studies, is a material with little variation in shape or specific gravity. Thus, one can learn how a material of known characteristics moves in a stream under particular flow conditions. Ottawa sand and other similar products are composed of clean well-rounded quartz sand with very few heavy minerals. Such sand is commercially available in large quantities at very reasonable price. In fact, total cost to buy the sand and dye can be less than 10c per pound. Because 1 pound of the fluorescent sand can "tag" 5,000 to 10,000 pounds of moving stream sand, the cost of tracer is a negligible part of the expense of a tracer experiment.

The quartz sand used in the second, and main, run of this study was Ottawa silica sand of uniform shape and specific gravity.

The problem of obtaining uniform material of specific gravity and (or) shape greatly different from quartz, but yet resembling the type of material that might be found in a stream, is a major one. Although heavy-mineral concentrates and lead shot were used in this experiment, synthetic materials whose characteristics can be closely controlled probably should be used.

The method of applying the fluorescent dye to the particles developed by Kennedy and Kouba (1970), and used in the present study with slight modification, produced a good, abrasion-resistant fluorescent coating. There was apparently no difficulty with loss of the dye coating in the stream; however, sieving of the samples resulted in some chips of dye from large particles that limited the analysis of the samples to particles larger than 0.125 mm.

The resultant coating was nonwetting, and this characteristic complicated the injection process. A detergent had to be added to the fluorescent material or the fluorescent material had to be injected as a slurry to which detergent had been added. These precautions were necessary to insure that the fluorescent particles did not clump together because of the surface effects of the coating. Further work toward the development of an abrasion-resistant fluorescent coating that is wettable is necessary.

On the other hand, there is need occasionally for fluorescent coatings that will decompose after a specific time interval so that a stream or river is not contaminated permanently with the fluorescent tracer particles. Previous work on this type of coating as well as on other types of permanent coatings has been summarized by Ingle (1966), and Teleki (1966) has presented a detailed review of the various types of fluorescent dyes and coating processes. Whatever the type of coating, however, it must be remembered that the primary requirement of any coating is that the tagged particles of a specific size behave identically with the natural sediment particles of the same size. If a range of particle sizes is considered, then the size distribution within a particular size range must approximate the distribution of natural sediment particles in this size range that are in transport. This does not necessarily mean, of course, that sediment from the stream must be the material used in the preparation of the tracers.

The injection of the fluorescent materials into the study reach must satisfy the following conditions:

1. The location of the injection point relative to the sampling point must be known accurately.
2. If an instantaneous-slug injection is used, the time required for the injection process must be negligible compared with the time scale of the sediment motion.
3. If an intermittent-slug injection is used as an approximation of the true continuous injection process, the time interval between injections should be negligible compared with the time scale of the sediment motion.
4. The injection process should disturb the natural sediment-transport process at the injection point as little as possible.

Some difficulty was experienced with the injection tube used in the present study, but it is believed that the procedure of simply dumping the fluorescent material into the channel at as high a rate as possible reasonably approximated an instantaneous point source of fluorescent material. However, because the tracer particles did move so rapidly for the high-velocity flat-bed condition, several advantages would have been gained by the use of a continuous point-source injection. For example, a better evaluation of the lateral-dispersion characteristics of the tracers would have been possible, and the calculation of the sediment-transport rates would have been simplified. Similarly the possibility of failing to sample a fast-moving slug of tracer material would have been eliminated.

Various types of injection procedures have been discussed in the literature, and these procedures range from water-soluble containers discussed by De Vries (1966) and Lean and Crickmore (1963) to the elaborate constant-injection apparatus that was used for a period of 6 weeks by Crickmore (1967). However, further work is needed in the development of injection processes.

The type of sampling required in a fluorescent tracer experiment in general depends upon the bed configuration in the study reach. If a dune bed exists, then core samples are necessary to define the spatial distribution of fluorescent material within the study reach. In the present study, the high-velocity flat-bed condition existed. Samples of the bed material moving near the bed surface were desired because large samples could be obtained rapidly at this location and because these samples should contain some of the large bed-material particles in transport. The "dustpan" sampler described previously and used in the present study appeared to be an acceptable device for obtaining these samples.

Analysis of the samples requires a determination of the number of fluorescent particles of each color in each sieve class of each sample. In the present study, the numbers of fluorescent particles were determined by a manual counting process. The manual counting process is a simple procedure, and only a minimum amount of equipment is required. Although the statistical analysis (C. F. Nordin, Jr., written commun., 1968) simplified greatly the counting process, the manual counting procedure was time consuming because the length of time any one individual could spend counting particles was limited by the tedium of the process. Automatic electronic devices for counting the number of fluorescent particles have been described by De Vries (1967) and Teleki (1967). An electronic counter has the obvious advantage of convenience and ease of sample analysis. Disadvantages are the expense and the careful calibration and maintenance of the instrument that are required to obtain accurate concentrations. If two or more different fluorescent dyes are used, care must be taken to insure that the spectra of the dyes are displaced sufficiently so the different colors can be distinguished by the instrument with the use of the proper filters.

The problem of differentiating between chips or flakes of dye from large particles and actual fluorescent particles for the small-diameter sieve classes was encountered in this study. Because of this problem, the smallest diameter sieve class considered was the 0.125- to 0.177-mm sieve class. It was impractical to attempt to distinguish visually between particles and chips in the 0.088- to 0.125-mm sieve class.

However, the 0.062- to 0.088-mm and 0.088- to 0.125-mm sieve classes often may be of importance, as they were in the present study because they contributed about 27 percent of the total sediment transport of particles larger than 0.062 mm. A way of eliminating the problem of chips and flakes in these sieve classes is to use one color of dye specifically for each of these two sieve classes. After the preparation of the fluorescent materials, the ma-

terial for each sieve class should be carefully resieved to remove all material outside the desired sieve range. Care should be taken also in the preparation of the fluorescent materials to insure that the size distributions within each sieve class of material are approximately the same as the size distributions within that sieve class of the bed material in transport.

It is concluded that the fluorescent tracer technique is a simple and sensitive experimental method for studying the movements of groups of particles either in a natural channel or in a laboratory alluvial channel. However, considerable improvement in technique in each of the four basic steps is still necessary.

SUMMARY

A fluorescent tracer technique was applied to the study of the rates of transport and dispersion of sediment particles of various sizes and specific gravities for the high-velocity flat-bed condition of alluvial-channel flow. Two runs were completed in the Rio Grande conveyance channel near Bernardo, N. Mex., and the following statements summarize the knowledge gained from these two experiments.

1. The centroid velocity of the 0.125- to 0.177-mm sieve class of sand was 1.2 fps in run 1 when the mean water velocity was 4.66 fps and 0.66 fps in run 2 when the mean water velocity was 4.05 fps. Thus, the fine sand moved about 16 to 26 percent of the mean water velocity.

2. The centroid velocity of the quartz tracer particles varied with particle size. In the size range from 0.125 to 1.0 mm, the minimum velocity occurred for a particle size slightly larger than the median diameter of the bed material (about 0.2 mm). Both the larger and the smaller particles moved faster. In run 1, the tendency of the large particles to follow the thalweg of the channel distorted the U-shaped velocity-diameter relation.

3. Garnet and monazite particles moved at velocities about an order of magnitude less than the velocities of quartz particles of equivalent fall diameter. Thus, the concept of hydraulic equivalence based on fall diameter is not applicable to sand-size particles under the conditions of this experiment.

4. At least two factors were important in producing lateral mixing of the tracer particles. These are turbulent fluctuations in the flow and the effect of the thalweg of the channel.

5. The large and heavy particles tended to follow the thalweg of the channel even though the channel was approximately straight and the flow lines at the surface appeared to follow the alinement of the channel.

6. Lateral mixing was greatest for the smallest quartz tracer particles and was approximately the same as that for a water-soluble fluorescent dye. Lateral mixing decreased with increasing size of quartz tracer in run 2 when the effect of the thalweg was minimized. The large particles mixed the least because they spent a greater proportion of the time resting on or moving along the bed surface than did the small particles.

7. Longitudinal mixing of the quartz tracer particles as related to particle size showed an approximately reciprocal relation to that observed for centroid velocity as a function of particle size; that is, the slower the sand moved, the greater was the longitudinal mixing.

8. The rapid rate of movement of the quartz tracers through the study reach made it difficult to obtain an accurate record of the passage of the tracer mass. Failure to sample the complete tracer mass will result in calculated values of the sediment-transport rate that are too large, as occurred in this study. A continuous injection of fluorescent tracer would have been preferable for the flow conditions of this study.

9. The fluorescent tracer technique has great potential as a tool for the study of movements of sediment. Further development of equipment and techniques is needed, however.

LITERATURE CITED

Chang, Y. L., 1939, Laboratory investigation of flume traction and transportation: Am. Soc. Civil Engineers Trans., v. 104, p. 1246–1313.

Crickmore, M. J., 1967, Measurement of sand transport in rivers with special reference to tracer methods: Sedimentology, v. 8, no. 3, p. 175–228.

DeVries, M., 1966, Application of luminophores in sand transport studies: Delft Hydraulics Lab. Pub. 39, 86 p., Delft, Netherlands.

——— 1967, Photometric counter for fluorescent tracers: La Houille Blanche, no. 7, p. 717–722.

Fischer, H. B., 1967, Transverse mixing in a sand-bed channel, in Geological Survey research, 1967: U.S. Geol. Survey Prof. Paper 575–D, p. D267–D272.

Gonzalez, D. D., Scott, C. H., and Culbertson, J. K., 1969, Stage-discharge characteristics of a weir in a sand-channel stream: U.S. Geol. Survey Water-Supply Paper 1898–A, 29 p.

Guy, H. P., and Norman, V. W., 1970, Field methods for measurement of fluvial sediment: U.S. Geol. Survey Techniques Water-Resources Inv., Book 3, Chap. C2, 59 p.

Harris, D. D., and Richardson, E. V., 1964, Stream gaging control structure for the Rio Grande conveyance channel near Bernardo, New Mexico: U.S. Geol. Survey Water-Supply Paper 1369–E, p. 123–154.

Hubbell, D. W., 1964, Apparatus and techniques for measuring bedload: U.S. Geol. Survey Water-Supply Paper 1748, 74 p.

Ingle, J. C., Jr., 1966, The movement of beach sand: New York, Elsevier Pub. Co., 221 p.

Kennedy, V. C., 1968, Fluorescent sand as a tracer of fluvial sediment movement: Geol. Soc. America Spec. Paper 101, p. 108–109.

Kennedy, V. C., and Kouba, D. L., 1970, Fluorescent sand as a tracer of fluvial sediment: U.S. Geol. Survey Prof. Paper 562–E, 13 p.

Lean, G. H., and Crickmore, M. J., 1963, Methods for measuring sand transport using radioactive tracers, *in* Symposium on the appli-

cation of radioisotopes in hydrology: Tokyo, Internat. Atomic Energy Agency, p. 111–131.

——— 1966, Dilution methods of measuring transport of sand from a point source: Jour. Geophys. Research, v. 71, no. 24, p. 5843–5855.

Loyacano, J. N., 1967, Fall velocity of sand particles in turbulent flume flow: Fort Collins, Colo., Colorado State Univ. Dept. Civil Eng. unpub. M.S. thesis.

Meland, N., and Norrman, J. O., 1966, Transport velocities of single particles in bed-load motion: Geog. Annaler, v. 48, ser. A, p. 165–182.

Rittenhouse, G., 1943, Transportation and deposition of heavy minerals: Geol. Soc. America Bull., v. 54, p. 1725–1780.

Rubey, W. W., 1933, The size-distribution of heavy minerals within a water-laid sandstone: Jour. Sed. Petrology, v. 3, no. 1, p. 3–29.

Sayre, W. W., and Chang, F. M., 1968, A laboratory investigation of open-channel dispersion processes for dissolved, suspended, and floating dispersants: U.S. Geol. Survey Prof. Paper 433–E, 71 p.

Sundborg, Åke, 1956, The river Klarälven—a study of fluvial processes: Geog. Annaler, v. 38, p. 127–316.

Teleki, P. G., 1966, Fluorescent sand tracers: Jour. Sed. Petrology, v. 36, no. 2, p. 468–485.

——— 1967, Automatic analysis of tracer sand: Jour. Sed. Petrology, v. 37, no. 3, p. 749–759.

U.S. Inter-Agency Committee on Water Resources, 1941, Laboratory investigations of suspended sediment samplers, *in* A study of methods used in measurement and analysis of sediment loads in streams: Washington, U.S. Govt. Printing Office, Rept. 5, 99 p.

——— 1957a, The development and calibration of the visual-accumulation tube, *in* A study of methods used in measurement and analysis of sediment loads in streams: Washington, U.S. Govt. Printing Office, Rept. 11, 109 p.

——— 1957b, Some fundamentals of particle size analysis, *in* A study of methods used in measurement and analysis of sediment loads in streams: Washington, U.S. Govt. Printing Office, Rept. 12, 55 p.

APPENDIXES

APPENDIX A—DISCUSSION OF THE WASHING EFFECT

Because of the flow through the "dustpan" sampler during the collection of the sample, some of the fines may have been preferentially washed from the sample. This effect is not of concern if the tracer particles of a specific sieve diameter behave exactly as nontagged particles of the same diameter, as is assumed to be true for the quartz tracer particles. For the garnet and monazite, however, the natural bed material in a specific sieve class would be of a smaller median fall diameter than that of the garnet or monazite in the same sieve class because of the specific gravity difference. Thus, if the washing effect were related to fall diameter, the concentrations of the garnet and monazite would be affected. The purpose of this appendix is to discuss briefly some observations concerning the washing effect. These observations are based primarily on the size distributions of various types of samples collected in runs 1 and 2.

The median diameter, d_{50}, and the gradation, σ, for the size distributions of various types of samples obtained in runs 1 and 2 are presented in table 18. The median diameter, d_{50}, is defined as the diameter for which 50 percent of the sediment by weight is finer. The gradation, σ, is defined as $\frac{1}{2}(d_{84}/d_{50}+d_{50}/d_{16})$, where d_{84} and d_{16} are, respectively, the diameters for which 84 and 16 percent of the sediment by weight are finer.

TABLE 18.—*Comparison of the median diameters and the gradations of the size distributions of selected "dustpan," core, and depth-integrated samples*

Type of sample	Run	Time	Method of analysis	Cross section	Lateral position (feet from right bank)	d_{50} (mm)	σ
Depth-integrated	1	1326	Sieve	Weir	[1]	0.168	1.60
Do	2	1015	do	do	[1]	.164	1.57
Do	1	1542	VA tube	do	[1]	.176	1.54
Do	2	1604	do	do	[1]	.170	1.48
6-inch core	2	1655	Sieve	*B*	35	.185	1.46
"Dustpan"	2	1701	do	do	35	.251	1.28
Do	2	1638	do	do	35	.245	1.27
Do	2	1552	do	do	35	.258	1.27
6-inch core	2	1620	do	*D*[2]	37	.172	1.45
"Dustpan"	2	1605	do	*D*	36	.270	1.33
Do	2	1623	do	do	36	.280	1.34
Do	2	1634	do	do	36	.283	1.36
Core, top 3 in	2	[3]0830	do	*A*	36	.193	1.44
Core, bottom 3 in	2	do[3]	do	do	36	.201	1.46
Core, top 3 in	2	[3]0815	do	*B*	35	.208	1.38
Core, bottom 3 in	2	do[3]	do	do	35	.202	1.52
Core, top 3 in	2	[3]0845	do	*C*	35	.206	1.47
Core, bottom 3 in	2	do[3]	do	do	35	.184	1.51

[1] Composite over channel width.
[2] 50 feet upstream of *D*.
[3] Dec. 15.

At the centerline of cross section *B*, the median sieve diameter of a 6-inch core sample was 0.185 mm and the gradation, σ, was 1.46. The mean median diameter of three "dustpan" samples obtained at the same point at about the same time was 0.251 mm, and the mean gradation was 1.27. Similar results were obtained at cross section *D*. A comparison of the median diameters of the "dustpan" samples with the median diameters of the depth-integrated samples and the top and bottom 3-inch segments of the core samples showed that the median diameters of the "dustpan" samples were about 25 to 40 percent larger than the median diameters of the other samples. Also the gradations of the "dustpan" samples were less than the gradations of the other samples, indicating more uniform size distributions. These observations would be expected if some of the fine material had been washed from the "dustpan" samples.

However, other factors could contribute to the observation that the "dustpan" samples contained coarser material than did the other types of samples. As was discussed previously, it was found in the fluorescent tracer experiments that particles larger than the median size of material in the bed moved faster than the median-size particles did. Thus, the material in the "dustpan" would tend to become enriched with the larger particles. Also, the fact that the "dustpan" samples were obtained on the bed surface emphasized the coarser material.

The results presented in table 18 show that the median diameters and gradations for "dustpan" samples obtained at different times at the same position are essentially identical. However, there is a slight difference between the results at cross sections *B* and *D*. Because the calculations, described previously, of the quantities $\bar{V}$, t, σ_t^2, $\bar{z}$, and σ_z^2 involve ratios of concentration integrals, the effect of the washing depends on how much the washing varies with time and position at cross section *D*.

The d_{16}, d_{50}, d_{84}, and σ values for sieve-size distributions for "dustpan" samples obtained at cross section *D* at lateral positions of 18, 30, 42, and 54 feet for times near the beginning, the middle, and the end of run 2 are tabulated in table 19 to show the variation of the size distributions with time and position.

The results presented in table 19 show that d_{16} varies little with either time or position, d_{50} shows increased variation, and d_{84} shows the greatest variation with time and position. The mean values of d_{84} and σ for cross section *D* vary little with time; however, these quantities at a specific position do vary appreciably with time. Also, the d_{84} values for the sampling positions in the right-hand

part of the channel ($z=18$ and $z=30$) are, with one exception, larger than the d_{84} values for $z=42$ and $z=54$. This means that the samples from the right-hand part of the channel contained more coarse material than the samples from the left-hand part of the channel. This observation is in agreement, as was discussed previously, with the observed behavior of the large quartz tracer particles.

To summarize this discussion of the washing effect, the results in table 18 show that the median diameters of the "dustpan" samples are larger than the median diameters of other types of samples. This could be the result of washing of the fines from the "dustpan" sampler or the several factors that tend to increase the numbers of large particles in the "dustpan" samples. The results in table 19 suggest that if washing of the fines is occurring, then the effect is essentially uniform with respect to time and position at cross section *D*.

TABLE 19.—*Comparison of the* d_{16}, d_{50}, d_{84}, *and* σ *values for selected "dustpan" samples at cross section* D, *run 2*

Approximate time	Particle diameter	Diameter (mm) or gradation at				
		$z=18$	$z=30$	$z=42$	$z=54$	Mean
1015	d_{16}	0.225	0.214	0.210	0.220	0.217
	d_{50}	.311	.300	.291	.283	.296
	d_{84}	.424	.441	.407	.352	.406
	σ	1.37	1.44	1.39	1.26	1.36
1700	d_{16}	.199	.213	.190	.223	.206
	d_{50}	.281	.307	.253	.304	.286
	d_{84}	.450	.467	.327	.418	.416
	σ	1.50	1.48	1.31	1.36	1.41
2400	d_{16}	.212	.223	.201	.240	.219
	d_{50}	.289	.329	.262	.323	.301
	d_{84}	.393	.498	.323	.422	.409
	σ	1.36	1.50	1.26	1.33	1.36
Mean	d_{16}	.212	.217	.200	.228	
	d_{50}	.294	.312	.269	.303	
	d_{84}	.422	.469	.352	.397	
	σ	1.41	1.47	1.32	1.32	

APPENDIX B—DETERMINATION OF THE WEIGHTING FACTORS

The weighting factors, $w(z)$, defined by equation 9 were determined from a set of depth-integrated samples obtained at the weir. A set of samples obtained near the beginning of each run was used in the determination of the $w(z)$ values because most of the quartz tracer moved through the measurement section during the early part of each run. Both the water discharge and the sediment concentration at each vertical were necessary in the computation of the weighting factors. The procedure was as follows.

The sediment concentration, $C^*(z)$, for 5-foot intervals from $z=5$ feet to $z=70$ feet was determined from the depth-integrated samples. The asterisk is added to differentiate the standard sediment concentration, expressed as milligrams of sediment per liter of water-sediment mixture, from the fluorescent tracer concentration. The sampling transit rate was relatively uniform at all verticals; therefore, the distribution of water weights in the samples across the weir was the same as the distribution of water discharge across the weir. The water-discharge distribution was represented by T_z where

$$T_z=\frac{\text{net weight at vertical } z}{\text{sum of the net weights}}. \tag{B-1}$$

The weight of the sand was not subtracted from the net weights of the depth-integrated samples because the sand weight was less than 0.5 percent of the total weight at each vertical.

The incremental water discharge at each vertical, $q(z)$, was calculated from

$$q(z)=T_zQ, \tag{B-2}$$

where Q is the measured total water discharge.

The incremental sediment-transport rate, $q_s(z)$, was calculated from

$$q_s(z)=\frac{\gamma}{10^6}q(z)C^*(z), \tag{B-3}$$

where γ is the specific weight of the water-sediment mixture. The mean unit sediment-transport rate, $\bar{q}_s(z)$, was obtained from

$$\bar{q}_s(z)=\sum_{z=5}^{z=70}\left(\frac{\gamma}{10^6}\right)\frac{q(z)C^*(z)}{14}, \tag{B-4}$$

where 14 is the total number of verticals at 5-foot intervals between $z=5$ feet and $z=70$ feet. The weighting factor, $w(z)$, is given by

$$w(z)=\frac{q_s(z)}{\bar{q}_s}=\frac{\frac{\gamma}{10^6}q(z)C^*(z)}{\sum_{z=5}^{z=70}\left(\frac{\gamma}{10^6}\right)\frac{q(z)C^*(z)}{14}}=\frac{q(z)C^*(z)}{\overline{q(z)C^*(z)}}. \tag{B-5}$$

Two additional assumptions were necessary in the application of the weighting factors obtained from equation B–5 to data obtained at cross section *D*. First, it was assumed that the variation of the weighting factor with lateral position was the same at cross section *D* as at the weir; second, it was assumed that the weighting factor at a given lateral position applied to all size classes of material. The shift of the large particles toward the right bank suggests that the second assumption was not exactly true for all sizes; however, the contribution of the large sizes to the total sediment-transport rate was insignificant.

The weighting factors obtained from the depth-integrated samples for runs 1 and 2 are presented in figure 40. The distribution of the weighting factors across the channel was similar for the two runs.

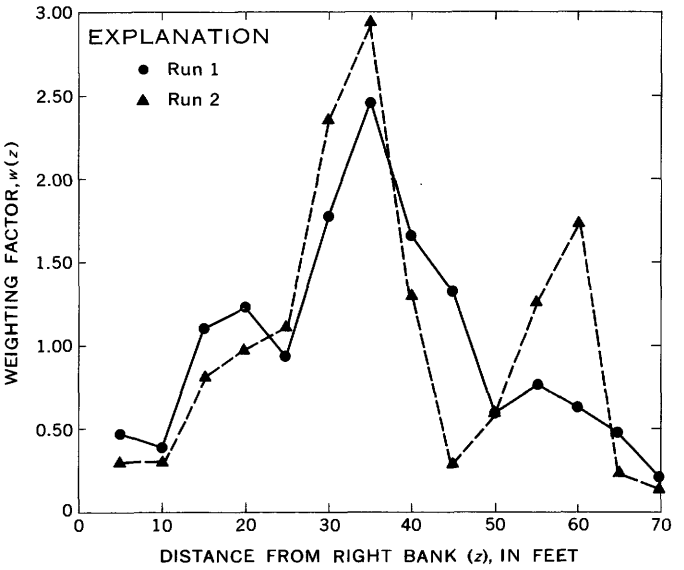

FIGURE 40.—Variation with lateral position of the sediment-transport weighting factors, runs 1 and 2.

APPENDIX C—CALCULATION OF THE SEDIMENT-TRANSPORT RATES FROM THE DEPTH-INTEGRATED SAMPLES AT THE WEIR

Because the depth-integrated samples from the weir were small, the samples generally were not sieved into size classes; and because these samples were not sieved, only the total number of fluorescent particles of each color was obtained for each sample. Thus, two assumptions were necessary to permit the calculation of the sediment-transport rates from the numbers of fluorescent particles in the depth-integrated samples. These assumptions and the development of the equation for the calculation of the sediment-transport rate are discussed in the following paragraphs.

First, it was assumed that the fluorescent particles were sampled at the weir in the same proportion at which the particles were injected. For example, in run 1 the number of green quartz particles injected was 23.0×10^8, 27.9×10^8, and 12.0×10^8 for the 0.125- to 0.177-mm, 0.177- to 0.250-mm, and 0.250- to 0.350-mm sieve classes, respectively. Therefore, it was assumed that 36.6 percent of the green particles in any sample were from the 0.125- to 0.177-mm sieve class, 44.3 percent were from the 0.177- to 0.250-mm sieve class, and 19.1 percent were from the 0.250- to 0.350-mm sieve class. This assumption should be valid if all of the sediment is suspended by the weir and if the depth-integrated sampler functions properly; that is, each size of sediment is sampled in direct proportion to the amount of that size in transport. A problem exists with the fluorescent tracers, however, because the instantaneous type of injection was used. The fastest-moving particles would be sampled first, and the slowest would be sampled last. This problem was not too great in run 1, where, as was discussed previously, the variation of centroid velocity for the sieve classes within a specific color of tracer was not large. In run 2, however, quartz particles of all sizes were coated one color, and, as was discussed previously, the fastest moving particles were the largest and the smallest particles. Thus, it is expected that the quartz tracer particles sampled first were predominately the large and the small particles and that those sampled last were the medium-sized quartz tracer particles. As a result, some deviations from this assumption might occur in run 2.

Second, it was assumed that the sieve-size distribution of the depth-integrated samples at the weir did not change with time. If this assumption is valid, then size distributions determined for one sample in each run could be used for all of the depth-integrated samples. Figure 41 shows the sieve-size distributions of two depth-integrated samples, one from each run, obtained at the weir; and figure 42 shows the visual-accumulation-tube size distributions of two other depth-integrated samples, one from each run, obtained at the weir. The sieve-size distributions of the two depth-integrated samples presented in figure 41 are essentially identical, even though the time interval between the samples was about 21 hours. Also, the visual-accumulation-tube size distributions presented in figure 42 are similar for two other samples obtained about 24 hours apart. These distributions differ slightly from the sieve-size distributions, particularly at the large diameter

end of the distributions. This difference was not considered significant, however. On the basis of these size distributions, therefore, the second assumption was considered to be valid. The sieve-size distributions presented in figure 41 were used in the calculations in preference to the visual-accumulation-tube distributions presented in figure 42 because the size distributions of the fluorescent tracer materials were determined by sieve analysis.

If the sediment-transport rate is assumed to be independent of time, then the equation for the calculation of the sediment-transport rate from the fluorescent tracer concentrations of the depth-integrated samples has the form

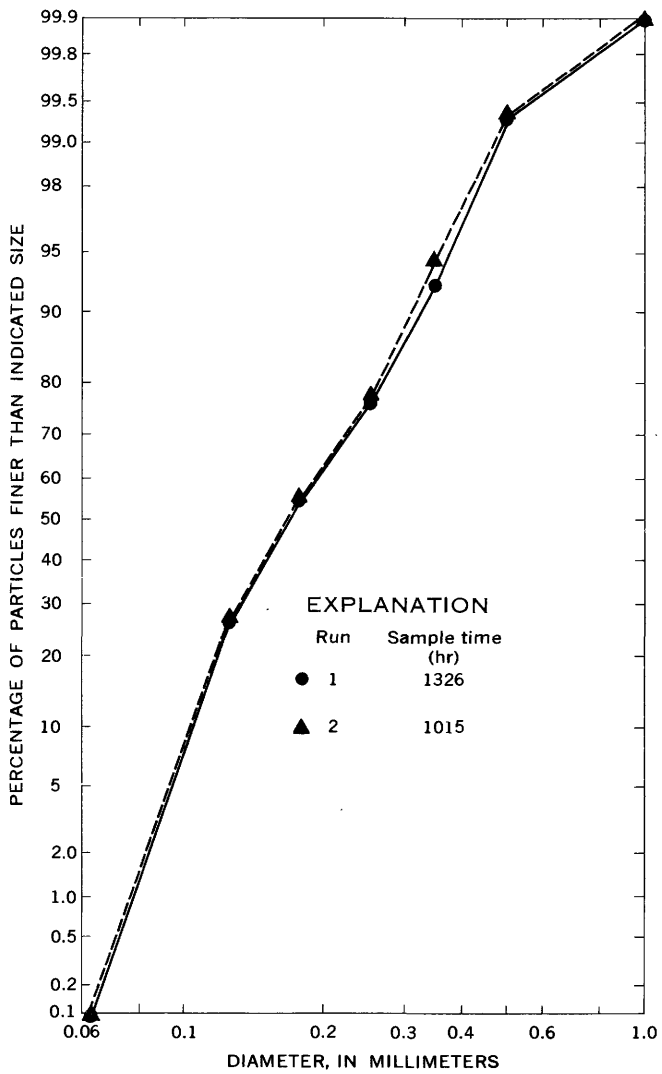

FIGURE 41.—Sieve-size distributions of two depth-integrated samples obtained at the weir.

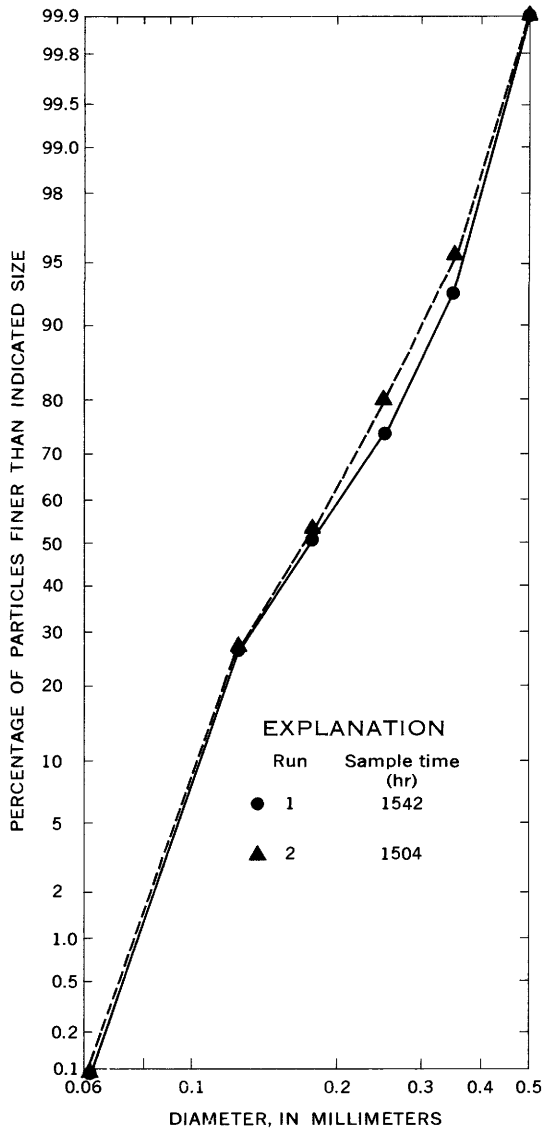

FIGURE 42.—Visual-accumulation-tube size distributions of two depth-integrated samples obtained at the weir.

tracer injected, W, has been replaced by N, the number of fluorescent particles of a specific color injected, second, the concentration, C, as grams of fluorescent material per gram of sediment, has been replaced by C', the concentration as number of fluorescent particles per gram of sediment; third, the integration across the channel width has been accomplished by the averaging effect of compositing a set of samples taken across the weir; hence, the transport rate, Q_s, is the total transport rate for the cross section, and the concentration is a mean concentration, indicated by the overbar, for the cross section.

If $n(t)$ is the total number of fluorescent particles of a specific color in a sample at time t and if $W(t)$ is the

total weight of sediment in the sample, then A', the integral in equation C–1, can be written

$$A' = \int_0^\infty \frac{n(t)}{W(t)}\, dt. \tag{C–2}$$

With the two assumptions discussed previously, equation C–2 can be written for a specific size class i, or

$$A_i' = \int_0^\infty \frac{n(t)\,\frac{N_i}{N}}{W(t)p_i}\, dt, \tag{C–3}$$

where p_i is the fraction of the total weight of sediment in the sample that is in size class i, and N_i is the total number of fluorescent particles of size class i of a specific color injected at the beginning of the experiment. The quantity N_i/N is a constant for a specific experiment, and p_i is independent of time because of the second assumption. Therefore

$$A_i' = \frac{N_i}{Np_i} \int_0^\infty \frac{n(t)}{W(t)}\, dt. \tag{C–4}$$

By comparing equations C–4 and C–2, it follows that

$$A_i' = \frac{N_i}{Np_i} A'. \tag{C–5}$$

If equation C–1 is written for size class i, the result is

$$N_i = Q_{s_i} A_i', \tag{C–6}$$

where

$$A_i' = \int_0^\infty \bar{C}_i'(t)\, dt. \tag{C–7}$$

By combining equations C–6 and C–5 and rearranging, it follows that

$$Q_{s_i} = \frac{Np_i}{A'}. \tag{C–8}$$

Equation C–8 is equation 11, which was used to calculate the sediment-transport rates for the different sieve classes from the numbers of fluorescent particles of each color in the depth-integrated samples. Because of the two assumptions, only one integral evaluation was necessary for each color of tracer particle.

U. S. GOVERNMENT PRINTING OFFICE : 1971 OL - 405-770